CONF-960267--

DK9601561 NEI-DK--2424

INTERNATIONAL ENERGY AGENCY

Implementing Agreement for Co-operation in the Research and Development of Wind Turbine Systems ANNEX XI

IEA Joint Action

Wind Turbine Fatigue

4th Symposium

SEP 03 1996
OSTI

Stuttgart, February 1-2, 1996

Organized by : DLR, Institute of Structures and Design, Stuttgart

Scientific Coordination :

B. Maribo Pedersen
Dept. of Fluid Mechanics
Technical University of Denmark

MASTER

DISTRIBUTION OF THIS DOCUMENT IS UNLIMITED

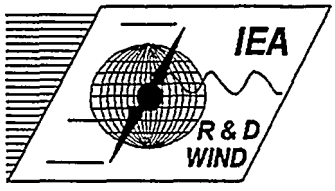

INTERNATIONAL ENERGY AGENCY

Implementing Agreement for Co-operation in the Research and Development of Wind Turbine Systems ANNEX XI

IEA Joint Action

Wind Turbine Fatigue

4th Symposium

Stuttgart, February 1-2, 1996

Organized by : DLR, Institute of Structures and Design, Stuttgart

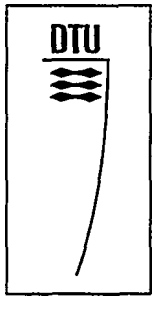

Scientific Coordination :

B. Maribo Pedersen
Dept. of Fluid Mechanics
Technical University of Denmark

ISSN 0590-8809

DISCLAIMER

Portions of this document may be illegible in electronic image products. Images are produced from the best available original document.

CONTENTS

page

MARKUS REES 1
Comparison between simplified Load Spectra in accordance with Germanische Lloyd Guidelines, and Load Spectra derived from Time Domain Simulations

K. ARGYRIADIS 7
Comparison of some European Regulations

GUNNER LARSEN, KENNETH THOMSEN 17
A simple approximative procedure for taking into account low cycle fatigue loads

A.F.RIDDLE, L.L.FRERIS, J.M.R.GRAHAM 29
Effect of control activity on blade fatigue damage rate for a small horizontal axis wind turbine

N.W.M. BISHOP 41
Fatigue of wind turbines in the frequency domain

HOLGER SÖKER 47
Rainflow Counting revisited

HERBERT J. SUTHERLAND 55
Damage estimates for European and U.S. sites using the U.S. high-cycle fatigue data base

G.A.LOWE, D.J.RICHARDSON 63
Fatigue testing of a carbon fibre composite wind turbine blade with associated material characterisation

J.R.LOWE 69
The carbon fibre market and uses for composite wind blades

D.R.V. van DELFT, G.D. de WINKEL, P.A.JOOSSE 75
Fatigue behaviour of fibreglass wind turbine blade material under variable amplitude loading

CHR.W.KENSCHE 81
Which slope for Gl-Ep fatigue curve?

PETER JOOSSE 87
EN-WISPER: Research overview and consequences

D.R.V. van DELFT 91
Testing of rotor blades

PETER JOOSSE, BERNARD BULDER 97
Is there a future for material fatigue research?

LIST OF PARTICIPANTS 103

COMPARISON BETWEEN SIMPLIFIED LOAD SPECTRA IN ACCORDANCE WITH GERMANISCHE LLOYD GUIDELINES, AND LOAD SPECTRA DERIVED FROM TIME DOMAIN SIMULATIONS

Markus Rees

aerodyn Energiesysteme GmbH
Provianthausstr. 9, D-24768 Rendsburg, Germany, Tel: ++49 - 4331 - 12750, Fax: ++49 - 4331 - 127555

ABSTRACT

The Germanische Lloyd guideline allows calculations of load spectra in two fundamentally different ways. In the case of the so-called "simplified load spectra" the maximum amplitude of fluctuation of a load component is formed as ±75% of the average value of the purely aerodynamic loads of this component at rated wind conditions, together with an overlay of mass-related loads.
The second method allowed in the GL guideline is the calculation of load spectra from simulation results in the time domain. For a number of average wind speeds the time-dependent characteristics of the load components are calculated taking account of the natural spatial turbulence of the wind. These are converted into load spectra using the rainflow method.
In a parametric study the load spectra are calculated according to both methods and compared. The calculations are performed for turbines with rated powers of 100 kW to 2000 kW, with two and three blades, and also for stall-controlled and pitch-controlled turbines. The calculated load spectra are compared with each by means of 1 P fatigue equivalent load spectra.
The influence of individual parameters is presented, as is the validity of the simplified load spectra.

INTRODUCTION

With the increasing size of turbines, the fatigue loads are becoming ever more important in the dimensioning of individual components. For this reason, particular attention has been paid in the development of the MW class generation to the most accurate and realistic calculation of fatigue loads that is possible. In the preparations for type certification of these wind energy converters, fatigue loads, on the manufacturer's own initiative are usually no longer calculated according to the simplified method. This is because earlier findings have already indicated that the loads anticipated for some components lie significantly above those calculated using the simplified method. Since the economic success of a wind energy converter is very much dependent upon the achievement of the projected in-service life of 20 years, an underestimation of the fatigue loads and the damage thereby resulting to the turbine would be a considerable disadvantage to the operating authority in question.
These new results have led Germanische Lloyd to reduce the applicability of the simplified load spectra to turbines with rotor diameters of up to 46 m and three blades. Since the 7th July 1995 the simplified load spectra are no longer permissible for any other wind energy converters for type certification achievement.
The question must now be asked, whether this more or less arbitrarily set boundary is justified, or whether a significant discrepancy with the load spectra from simulation calculations has not already been established for the smaller turbines. To answer this, load spectra are calculated for a number of turbines using the two methods. The results are compared by means of 1 P equivalent load spectra.

CALCULATION METHODS

As already indicated, the average value of the purely aerodynamic load, together with the amplitude of fluctuation of the purely mass-related load, over one revolution at the rated wind speed, form the basis of the calculation of simplified load spectra according to the GL guidelines /1/. From the average value of the aerodynamic load a trapezoidal load spectra is produced, whose maximum amplitude of fluctuation is derived as 1.5 times the average value. The maximum number of load cycles N_{max} is calculated from the rotational speed and the in-service life of the turbine. The number of load cycles at the knee of the load spectrum is set as $N_{max}/1000$. A single-level spectrum of mass-related forces is overlaid on this trapezoidal spectrum of aerodynamic forces. The number of load cycles N_{mas} is set as $x_{mas}*N_{max}$. The factor x_{max} is calculated from the rotational speed and the real in-service life for the used type class. This is the only influence of the type class in the calculation of the simplified load spectrum. The resultant load spectrum is presented in Figure 1. The turbine's control system remains neglected to a large extent in the calculation of the simplified load spectra. Using this method, for example, it is not possible to distinguish between stall-controlled and pitch-controlled turbines.

In the second method simulations are executed in the time domain for a number of average wind speeds. Wind turbulence is taken into account in the simulations in the form of a three-dimensional turbulence field. The turbulent wind velocity fields are calculated according to the method of Jan and Shinozuka /2/. The same turbulence fields are used for all the simulations. The circular fields have a diameter of 90 m and contain a mesh of 11 by 20 points. The turbulence load spectra used and the coherence function were selected in accordance with IEC 1400-1. However, in contrast to the IEC guidelines, a constant turbulence intensity of I = 0.2 was formulated. This constant turbulence intensity is required by the GL guidelines. In the simulations a constant deviation of wind direction from the horizontal of 10° and a sinusoidal deviation of wind direction from the vertical of ±30° with an average value of 10° are assumed. All simulations are carried out over a time period of 600 s.

For the calculation of the time history of the load components an ideal rigid mechanical model is used. The use of an aeroelastic computer model is dispensed with, since the effort required for the large number of calculations would be too high. For turbines in the MW range, however, comparative calculations have already been performed with this ideal rigid model and aeroelastic computer models. For a turbine with sound dynamic behaviour, the agreement between the results was so good that the program used here appears to be entirely suitable for the parametric study that has been undertaken. In individual cases, however, significant discrepancies can occur between the results, so the data presented here should only be used for relative comparison with the simplified load spectra.
The time history of the loads for the various wind speeds thus produced are converted into load spectra with the aid of the rainflow method. The load spectra for the individual wind speeds are weighted according to their frequency for an in-service life of 20 years and summated. All load spectra presented are applicable for type class 1 as defined by IEC 1400-1.

The comparison between the results is carried out using the 1P equivalent single-level load spectra (1P load spectrum). The calculation of the 1P load spectrum is performed using the equation /3/

$$S_{1P} = \sqrt[m]{\frac{\sum_i S_i^m * n_i}{n_{ref}}}$$

With

S_{1P}: range of the 1P fatigue equivalent load spectrum
S_i: range of load cycle i
n_i: number of load cycles
n_{ref}: reference number of load cycles
m: S/N-curve parameter

All the 1P spectra presented have been calculated using the reference number of load cycles $n_{ref} = 2*10^6$ and an constant S/N curve parameter m = 4.

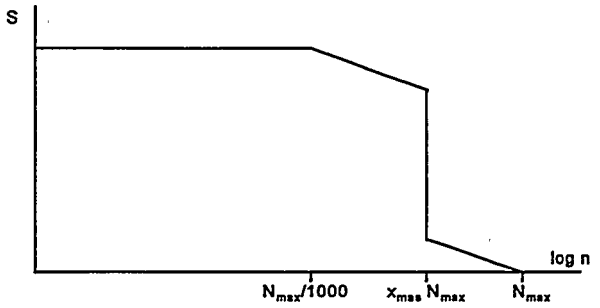

Figure 1: Simplified load spectrum

TURBINE PARAMETERS USED

A family of rotor blades has been developed for the three-bladed, stall-controlled turbines investigated. The blades of all the turbines have similar geometries and use the same aerodynamic profiles. Figure 2 shows the configuration of this rotor blade family. Both the location of the maximum blade chord and the positioning of the aerodynamic profiles are functions of the rotor diameter in question. All turbines investigated have two levels of rotational speed. The technical data for the individual turbines are listed in Table 1.
Profiles from the NACA 63 series with 35%, 18% and 12% relative thickness have been used. The positioning of the profiles is displayed in Figure 2. The masses of the blades, up to the 2000-80 blade, have been selected so that they lay as close as possible to the weight of blades that already exist. The mass distribution of a stall-controlled blade designed by ***aerodyn*** served as a reference for all the turbines. The mass distribution of the other blades was scaled so that the desired blade weight was achieved.
In the same manner, a family of rotor blades was developed for the two-bladed turbines investigated. These differ from those of the three-bladed turbines only in respect of differing rotor rotational speeds and a different blade chord distribution. The data for the two-bladed turbines are listed in Table 2.

Table 1: Technical data for the 3-bladed stall-controlled turbines

name	power [kW]	blade mass [kg]	diam. [m]	rotational velocities [rpm]	t_i [m]	t_a [m]	d [m]
100-20	100	220	20	38.7 / 58.1	0.75	0.2	0.5
300-33	300	827	33	23.5 / 35.2	1.4	0.35	0.85
600-43	600	1740	43	18 / 27	2.0	0.55	1.05
800-50	800	2650	50	15.5 / 23.2	2.35	0.65	1.25
1100-60	1100	4373	60	12.9 / 19.4	2.7	0.72	1.5
1500-70	1500	6330	70	11.1 / 16.6	3.1	0.85	1.75
2000-80	2000	9350	80	9.7 / 14.5	3.6	1.0	2.0

Table 2:Technical data for the 2-bladed stall controlled turbines

name	power [kW]	blade mass [kg]	diam. [m]	rotational velocities [rpm]	t_i [m]	t_a [m]	d [m]
100-20	100	220	20	42.6 / 63.9	0.85	0.21	0.58
300-33	300	827	33	25.8 / 38.7	1.6	0.38	1.0
600-43	600	1740	43	19.8 / 29.7	2.28	0.6	1.16
800-50	800	2650	50	17.0 / 25.5	2.68	0.7	1.42
1100-60	1100	4373	60	14.3 / 21.4	3.1	0.8	1.7
1500-70	1500	6330	70	12.2 / 18.2	3.5	0.93	2.0
2000-80	2000	9350	80	10.6 / 15.9	4.1	1.12	2.3

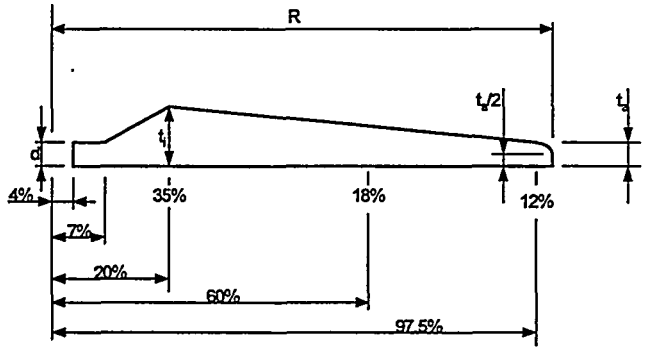

Figure 2: Blade geometrie

SIMULATION RESULTS

Discussion of the results is presented in terms of those load components relevant for dimensioning of individual components. These are detailed as follows:

- flapping moment at the blade root $M_{y\text{-}B}$
- edgewise moment at the blade root $M_{z\text{-}B}$
- pitching moment at the R-point $M_{y\text{-}R}$
- yawing moment at the R-point $M_{x\text{-}R}$
- tower top thrust force $F_{z\text{-}T}$
- tower top pitching moment $M_{y\text{-}T}$
- tower top torsional moment $M_{x\text{-}T}$

Point R is located at the connection between the hub and the drive train and point T is located at the connection between the machine bed and the tower. The coordinate systems R and T aré fixed coordinate systems. The coordinate system B is rotating with the blade root.

Results for the three-bladed, stall-controlled turbines are presented in Figure 3 for the load components referred to above. Here the discrepancies are presented between the 1P spectra derived from simulation calculations (ΔS_{sim}) and the 1P spectra derived from simplified expressions (ΔS_{simpl}). It can be seen that moments $M_{x\text{-}R}$, $M_{y\text{-}R}$ and $M_{x\text{-}T}$, in particular, display large discrepancies when compared with the simplified load spectra. The discrepancy is greatest for the small turbines and decreases with movement to the large turbines. This is in gross contradiction to the limitation devised by Germanische Lloyd, that accepts the simplified load spectra for turbines with rotor diameters up to 46 m.

Since these load components are mainly dominated by aerodynamic forces the reason for these discrepancies could be the increasing low-pass behaviour of the blade. With increasing rotor diameter the blade take the mean of local turbulences much better.

The blade root edge bending moment $M_{z\text{-}B}$ is reproduced very well by the simplified load spectra, since it is mainly dominated by mass-related terms.

Significantly lower loads are produced using the simulated load spectra for the tower top thrust force $F_{z\text{-}T}$, for all the turbines investigated. Since the tower thrust force in most cases defines the tower dimensions, the simulated load spectra offer in this instance clear advantages over the simplified load spectra. There are also significant discrepancies between the spectra for the load components not shown here, such that the validity of the simplified load spectra assumed by GL for turbines with rotor diameters less than 46 m cannot be confirmed.

In addition, the 1P spectra for the two-bladed turbines are now brought into the comparison. The 1P spectra are presented in Figure 4 for the load components referred to above. It can be seen that, with the exception of $M_{z\text{-}B}$ and $F_{z\text{-}T}$, the simulated spectra lay above the simplified spectra. The greatest discrepancies are once again produced in the case of $M_{x\text{-}R}$, $M_{x\text{-}T}$ and $M_{y\text{-}T}$. Moreover, contrary tendencies between the simulated and simplified spectra can be discerned where these components are concerned. Whereas with the simulated spectra the loads on the two-bladed turbine lie above those on the three-bladed turbine, this is reversed in the case of the simplified spectra. One reason for the higher loads of the two-bladed turbines could be that the three-bladed turbines take the mean of the local turbulences much better then the two-bladed turbines. For the two-bladed turbines the probability is higher that the gusts are influencing only one blade then for the three-bladed turbines. These asymetric loads lead to higher moments at the rotor shaft and the tower top.

For a further comparison, the spectra for stall and pitch power regulation are compared using the example of the 1100-60 three-bladed turbine. The 1P spectra for both turbines are shown in Figure 5. In these Figure is only one simplified 1P spectrum for the pitch- and the stall-controlled turbine because the power control method cannot be taken into account with the simplified method. This is another big disadvantage of the simplified load spectrum. The simple PI-controller used in the simulations is not very well optimized. Therefor the results will be slightly different with an better controller.
It can be seen that the blade root bending moments deviate only insignificantly from each other. Both the moments at the R-point and the tower top forces and moments are uniformly higher for the pitch-controlled turbine. In the case of the fatigue loads the pitch-controlled turbines are unfavourable whereas in the case of extreme loads they have significant advantages. The overall judgement including all relevant aspects of these two power control methods has to be done for each new turbine.

CONCLUSIONS

On the basis of the comparisons conducted, significant weaknesses of the simplified load spectra have become visible. For the important load components they reproduce the real loading pattern either only very unsatisfactorily, or not at all, for all the sizes of turbines investigated. The validity of the simplified load spectra for three-bladed turbines with rotor diameters of less than 46 m cannot be confirmed. The discrepancies between the simplified spectra and the simulated spectra are higher for smaller turbines. Since extrem loads often define the dimensions of small wind turbines ther is not necessary a fatigue problem because of the higher fatigue loads for these turbines.
In the comparison between two-bladed and three-bladed turbines significantly higher fatigue loads have been observed for some load components for the two-bladed turbines. Since two-bladed turbines have also no significant advantages in the case of the extreme loads they lead to higher loads than three-bladed turbines. The decisive factor for an overall assessment is of course not only the loads but also the price/performance ratio which could be better for the two-bladed turbine.
The comparison between stall-controlled and pitch-controlled turbines, using the example of the three-bladed 1100-60 turbine, showed equal or higher fatigue loads for the pitch-controlled turbine. It should be noted again that these results depend on the controller used in the simulations. An overall assessment is very difficult since pitch-controlled turbines have significantly advantages in the case of the extreme loads and has to be done again for each turbine.

REFERENCES

/1/ Germanischer Lloyd
Richtlinie für die Zertifizierung von Windkraftanlagen
GL-Hamburg, Selbstverlag des GL
März 1993 mit Ergänzungen März 1994

/2/ Shinozuka, M., Jan, C. M.
Digital Simulation of Random Processes and its Applications"
Journal of Sound and Vibration
Vol. 25, 1972, S. 111 - 128

/3/ E. Haibach
Betriebsfestigkeit
VDI-Verlag, Düsseldorf 1989

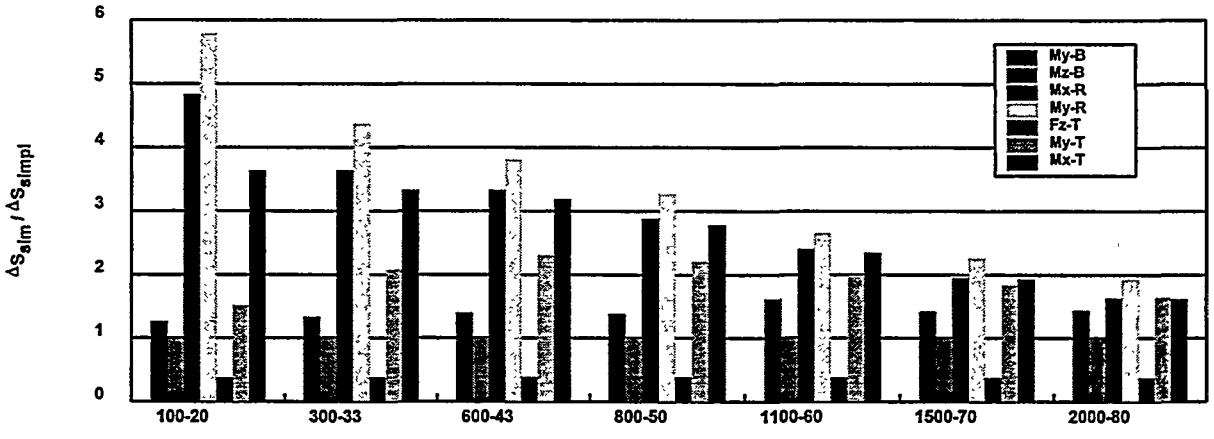

Figure 3: Non-dimensional 1P fatigue equivalent load spectra of three-bladed stall-controlled turbines

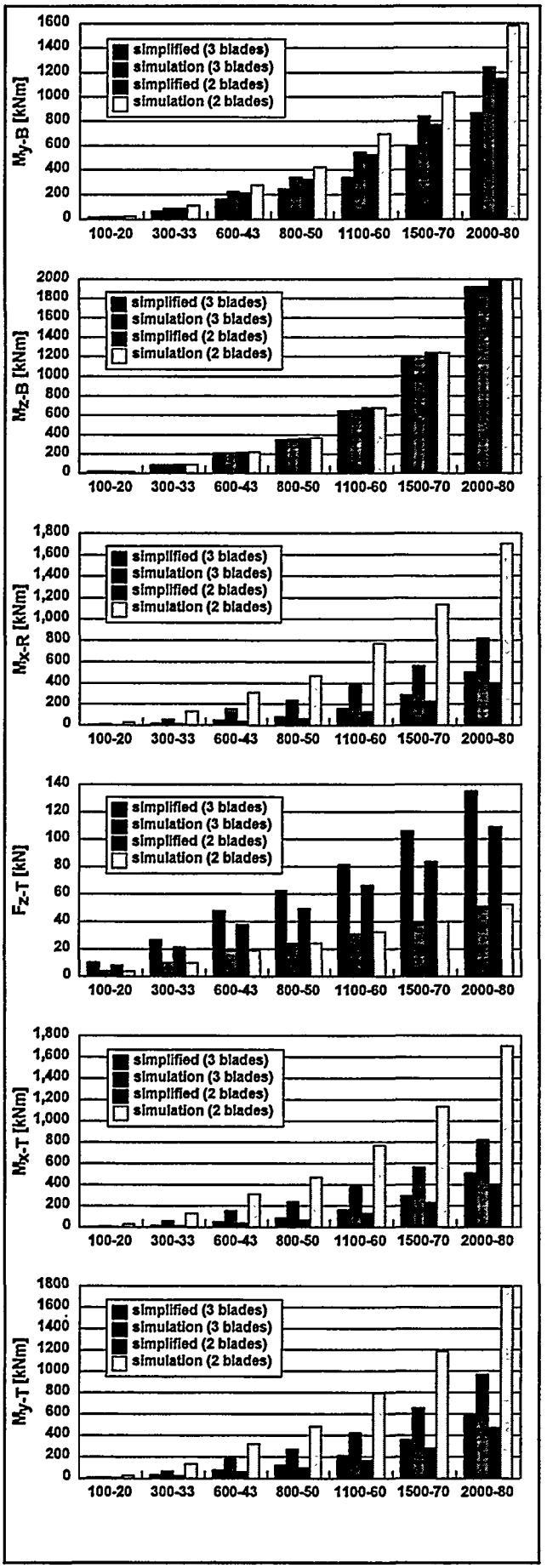

Figure 4: 1P spectra of two- and three-bladed turbines

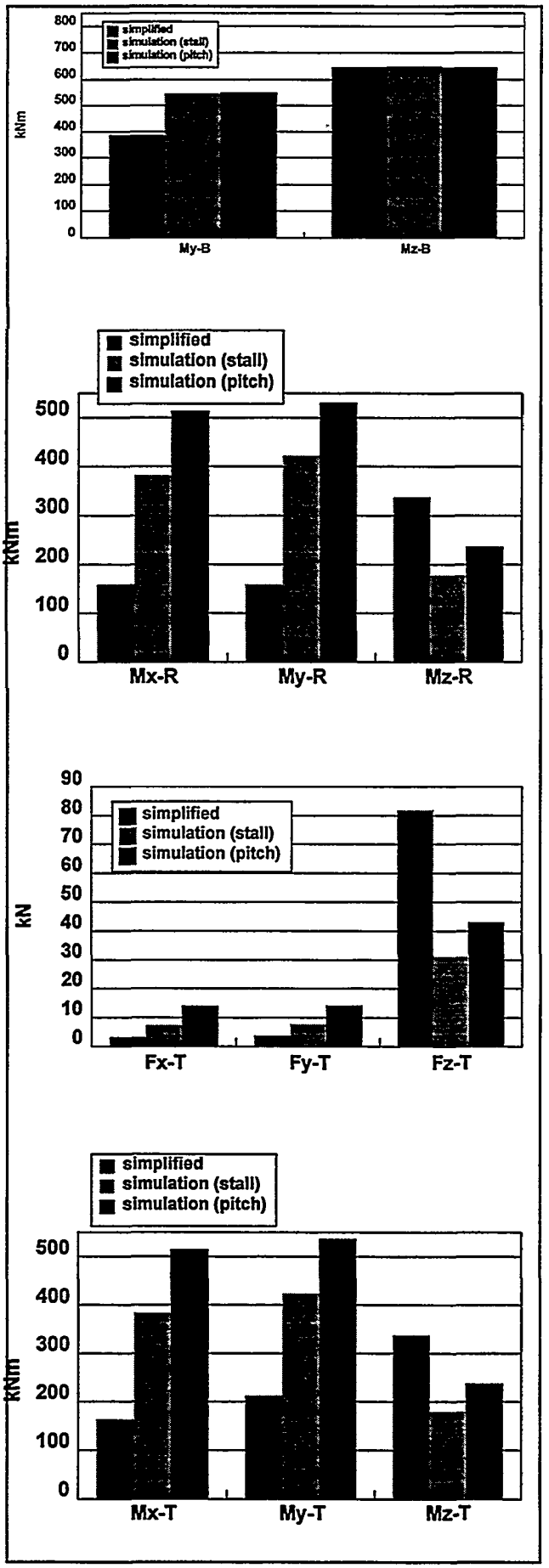

Figure 5: 1P spectra of two- and three-bladed stall-controlled turbines

Comparison of some European Regulations

K. Argyriadis, Germanischer Lloyd, Vorsetzen 32, D-20459 Hamburg

1 General

Fatigue calculations are an essential part in certification of a wind turbine. Manufacturers have to fulfil recommendations of several different regulations throughout Europe with the result that the design has often to be altered to satisfy them.

In general three national (D/GL, NL, DK) [1], [2], [3], [4], [5], and two international (GL,IEC) [1],[6] regulations are in use, with the IEC standard getting more importance with wind energy deploying to more in regions with no yet clearly defined national standards (India, Spain). The German DIBt and the GL regulations differ in mean windspeed sligtly. This has little impact on fatigue calculations, and can be negleted.

To overcome implications in wind tubine design GL and others made comparisons of the different standards in the past [7], [8]. These concentrated mainly on load definition and applied safety factors, omitting the influence of different methods for damage accumulation. This was aknowledged recently and fatigue calculation is introduced in comparisons [9], [10].

Germanischer Lloyd made calculations for wind tubines they are certifying and in one case we compared the resulting damages for different regulations and classes on a 600 kW , three bladed, stall regulated wind turbine. Hub height is 50 m and rotor diameter ca. 43 m. For the calculation of the loads simulations of timeseries ($t = 600\,s$) for 8 classes between cut-in ($5\,m/s$) and cut-out ($25\,m/s$) windspeeds with turbulent wind have been performed. The turbulence model is the IEC one. For simplicity and saving of computation time (factor 2-3) the simulations have been performed for a non flexible machine. We believe this is not an essential error, in this case, as the machine behaves similar in all cases.

The damage is not directly compared but, the "load reserve factor". The principal parameters influencing the loads are shown in table 1.

Regulation	GL			NEN 6069/2	DS 472				IEC 1400-1		
Class	1	2	3		1	2	3	4	1	2	3
$v_M[m/s]$	10.0	8.5	7.5	9.62	8.34	7.03	6.5	5.4	10.0	8.5	7.5
A	2			2.336	1.9				2		
I	0.2			0.166	0.092	0.117	0.145	0.196	0.17*		
α	0.16								0.2		
$z_0[m]$				0.25	0.001	0.01	0.05	0.3			
γ_F	1.0			1.0	1.0				1.0		

Table 1: Principal parameters for load calculation, Hub height 50m

with:

- v_M Mean wind speed
- A Weibull exponent
- I Turbulence intensity (* average value)
- α Exponent of wind slope
- z_0 Roughness length
- γ_F Load safety factor

In the following three critical locations of the turbine are examinated: Blade (glassfibre reinforced polyester), machine (cast steel), tower (welded steel).

2 Blade

For the damage calculation a section near the root of a polyester blade has been chosen. Two different cases, edgewise and flapwise loadings are considered, without interaction.

In contrary to the GL [1] and NEN [3] regulations the IEC standard [6] gives no reference to methods used for damage accumulation. Only the material safety factor (γ_m) according to IEC is to be larger 1.25 for non fail-safe parts of the turbine. Reference is made to national standards where these exist. For GRP materials a safety factor of 1.25 is insufficient, therefore the GL and NEN methods will be used.

The Danish standards rely heavily on blade tests [4], [5]. For calculations the DS 472 recommends a material safety factor of $\gamma_m = 1.7$, for normal safety class and refers to DS 412, 445 and 456 [11], [12], [13]. In these standards it is defined how material properties have to be calculated from specimen tests, but there is no evidence how, for normal safety class, a fatigue calculation for GRP has to be done and how mean stress is incorporated in the calculation.

The GL and NEN Regulations determine both the damage accumulation with the "Goodman" relation, although they have differences in the application of safety factors. The Goodman relation as defined in NEN 6096/2 is:

$$N = \left(\frac{\frac{UTS+|UCS|}{2\gamma_m} - |\sigma_m - \frac{UTS-|UCS|}{2\gamma_m}|}{\sigma_a}\right)^k$$

with:

N	allowable number of cycles at the stress range σ_a
k	Woehler exponent
σ_m	mean stress
σ_a	stress range (double amplitude)
γ_m	material safety factor
UTS	ultimate tensile strength
UCS	ultimate compression strength

Ultimate stresses are determined for 95% survival probability and a 95% confidence level.

Deviating from this formula in accordance with the GL-Regulation the safety factors for static loading have to be applied on the mean stress, leading to a factor $\gamma_{m,static}/\gamma_{m,dynamic} = 1.5$.

For comparison the damages for the IEC and DS 472 loadcases is calculated by using the NEN formulation and the corresponding material factors. The ultimate tensile and compress strengths were for all cases taken as $510\,N/mm^2$ and $350\,N/mm^2$ respectively. The governing factors and exponents are shown in table 2, the resulting load reserve factors in table 3 and figures 1 or 2.

safety factor	GL	NEN 6096/2	Danish Criteria	IEC 1400-1
γ_m	$C1 * C2 * C3 * C4 * C5$ $C1 = 1.35$(general) $C2 = 1.0\ N^{1/k}$ $C3 = 1.1$ (temperature) $C4 = 1.0 - 1.2$(fibre dir.) $C5 = 1.0$or1.1 (tempered)	$C1 * C2 * C3$ $C1 = 1.25$(moist) $C2 = 1.0 - 1.2$(fibre dir.) $C3 = 1.2$(general)	1.7	> 1.25
γ_{SD}	1.0	1.35	1.0	1.0
$\gamma_m \gamma_{SD}$	$1.485 \cdots 1.96$	$2.025 \cdots 2.43$	1.7	
exponent k	polyester 9 epoxy 10	10	10	
example γ_m	$1.35 * 1.1 =$ 1.485	$1.25 * 1.2$ 1.5	1.7	ref. GL/NEN/DS
k	9	10	10	9/10

Table 2: GRP material factors end Woehler exponents, polyester Blade

Regulation	Class	Edgewise	Flapwise
GL	1	1.0	1.0
GL	2	1.023	1.073
GL	3	1.043	1.156
NEN		0.903	0.98
DS	1	1.109	1.745
DS	2	1.135	1.669
DS	3	1.144	1.471
DS	4	1.153	1.24
IEC/GL	1	1.004	1.145
IEC/NEN	1	1.219	1.255
IEC/DS	1	1.074	1.13
IEC/GL	2	1.027	1.221
IEC/NEN	2	1.239	1.335
IEC/DS	2	1.097	1.202

Table 3: Load reserve factors, polyester GRP blade

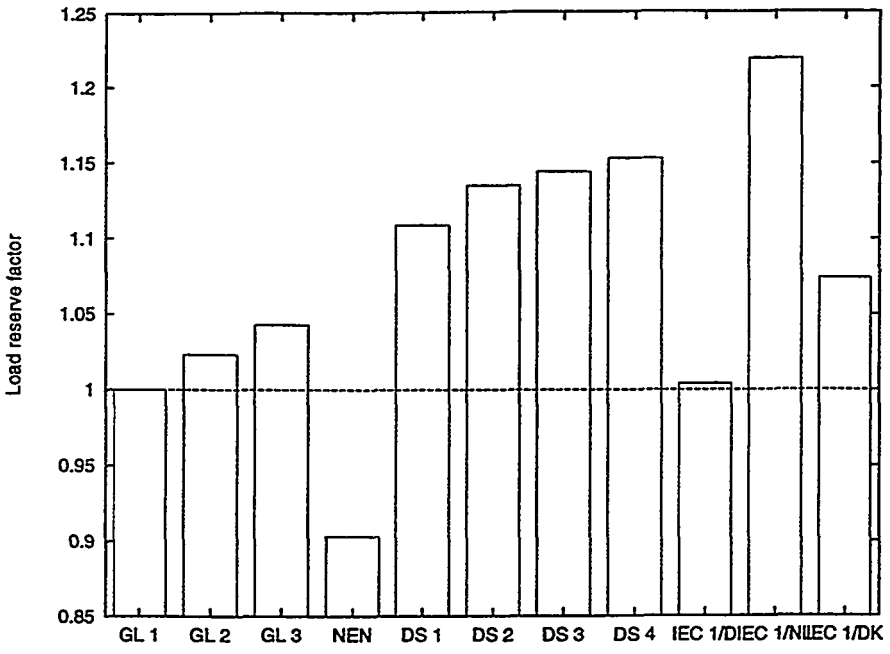

Figure 1: Load reserve factor, edgewise load

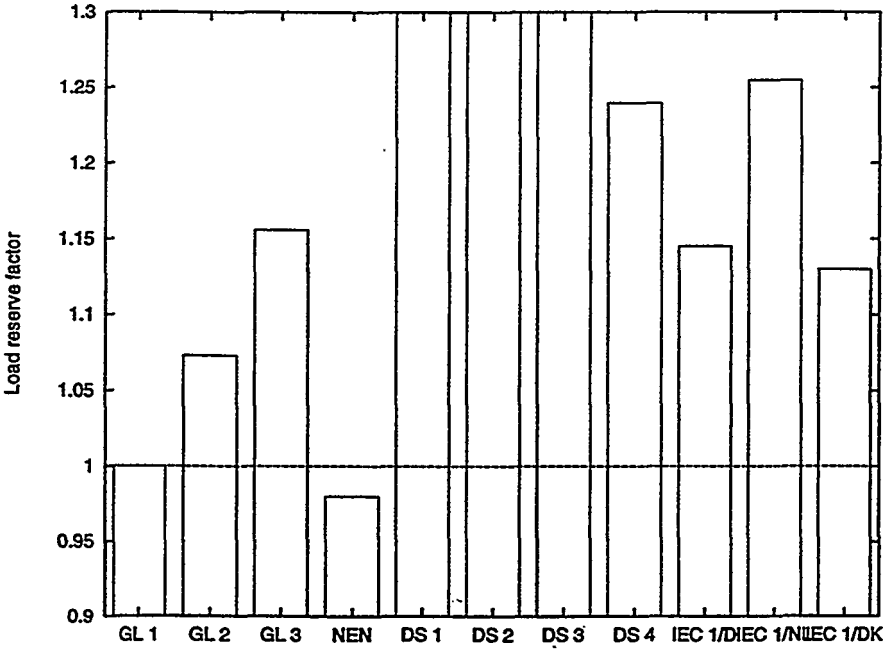

Figure 2: Load reserve factor, flapwise load

3 Machine

Often there is no method indicated in the regulations on how to analyse the different machine components. For castings i.e. a Woehler curve dependend on material, geometry and load shall be detrmined. Normaly, the designer would use the Finite Element Method to calculate stresses, find out the hot spots and calculate the equivalent stresses using an generaly accepted method like the ASME-Code [14]. The influence of notches can taken into account by application of stress concentration factors [15] or directly in the Woehler curve. The construction of a synthetic curve is described in [16].

In the regulations governing wind turbine design there is no special method mentioned for evaluating a Woehler curve for castings, reference is given to DIN-standards on cast steel (DIN 1693, part 2). A typical synthetic Woehler curve for GGG.40 cast iron is shown in figure 3. To the ori-

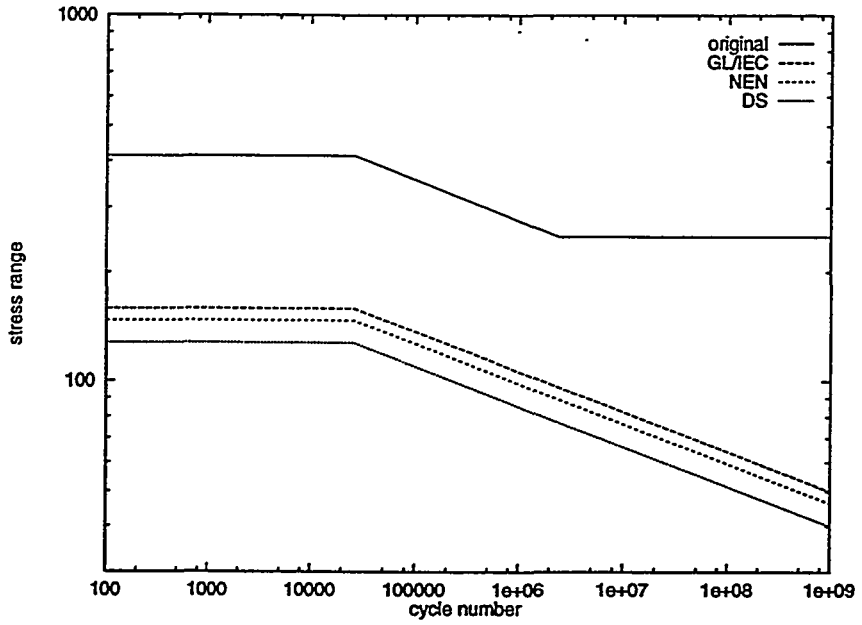

Figure 3: Synthetic Woehler curve for GGG 40

ginal curve factors to account for survivability 97.7%, main stress influence, thickness and surface quality have to be applied. According to GL-regulation these factors are:

Survival level 97.7%	S_{pu}	=	2/3
Mean stress (R)	S_R	=	0.85 for $R > 0$
Thickness	S_t	=	$(\frac{t}{25})^{-0.15}$ for $t > 25mm$
Surface	S_d	=	0.85^{j-1} (normal level $j = 3$)

Another alternation is that for GL the curve has no cut-off. For the comparison it was decided to calculate the damage for all cases with the GL-defined curve and apply the required material safety factors and the component dependend factors to correct the curves (table 4).

Regulation	GL	NEN	DS	IEC
$\gamma_m \gamma_{SD}$	1.25	1.35	1.56	1.25

Table 4: Material safety factors for machine components

The component dependent factors chosen are:

$$S_{pu} \cdot S_R \cdot S_t \cdot S_d = 2/3 \cdot 1.0 \cdot 1.0 \cdot 0.722 = 0.481$$

When the safety factors are applied the Woehler curves shown in figure 3 are produced.
Supposing that only the tilting moment at the hub contributes to damage the following load reserve factors are calculated, table 5, figure 4.

Regulation	Class	lrf
GL	1	1.0
GL	2	1.137
GL	3	1.433
NEN		1.195
DS	1	1.850
DS	2	2.075
DS	3	1.778
DS	4	1.189
IEC	1	1.192
IEC	2	1.387
IEC	3	1.551

Table 5: Load reserve factor for GGG.40 machine component

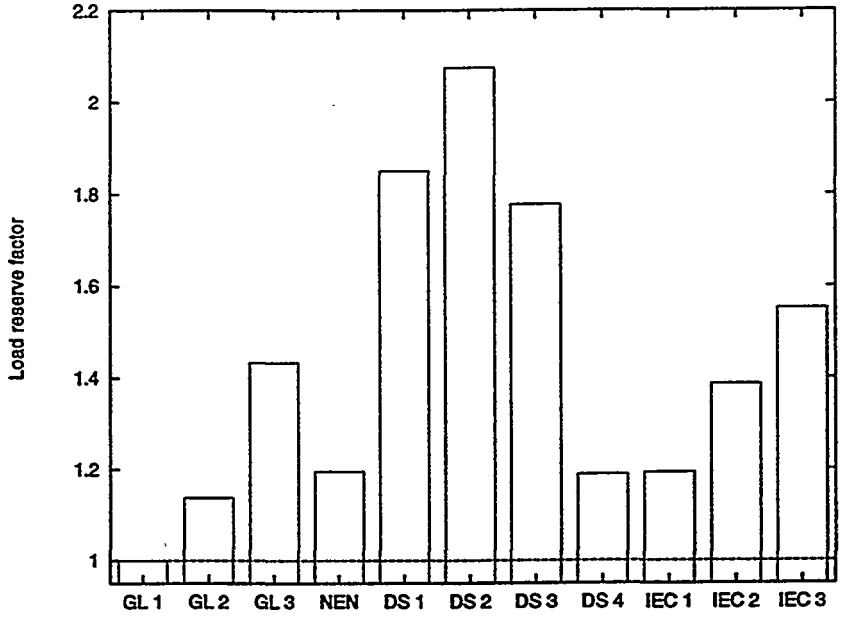

Figure 4: Load reserve factor machine component, GGG.40

4 Tower

The calculation of tower fatigue for a welded steel structure is defined in all standards analysed. The loads are mainly thrust dominated, the resulting material factors are shown in table 6. It has

Regulation	GL (*)	NEN	DS	IEC
$\gamma_m \gamma_{SD}$	1.1	1.35	1.56	1.25

Table 6: Material safety factors for the tower

to be mentioned that the GL regulation recommends a sasety factor of 1.25 for welded connections (see * in table 6).

In GL, NEN and IEC regulations the detail category is defined in accordance to Eurocode 3 [17]. Differences are found in the description of Woehler curves, mainly in the position of cut-off points. In Denmark DS 412 applies, in which not only the category but also the curves, the exponent and the method differ. While for Eurocode the criterium for selecting the gradient is the stress $\Delta\sigma_D$, for the Danish standard it is the resulting load cycle number.

For a typical tubular tower the flange at the root could i.e. fit to category 71 to Eurocode 3 and curve f for DS 412, when normal welding quality and control are assumed. The corresponding curves are shown in figures 5 or 6.

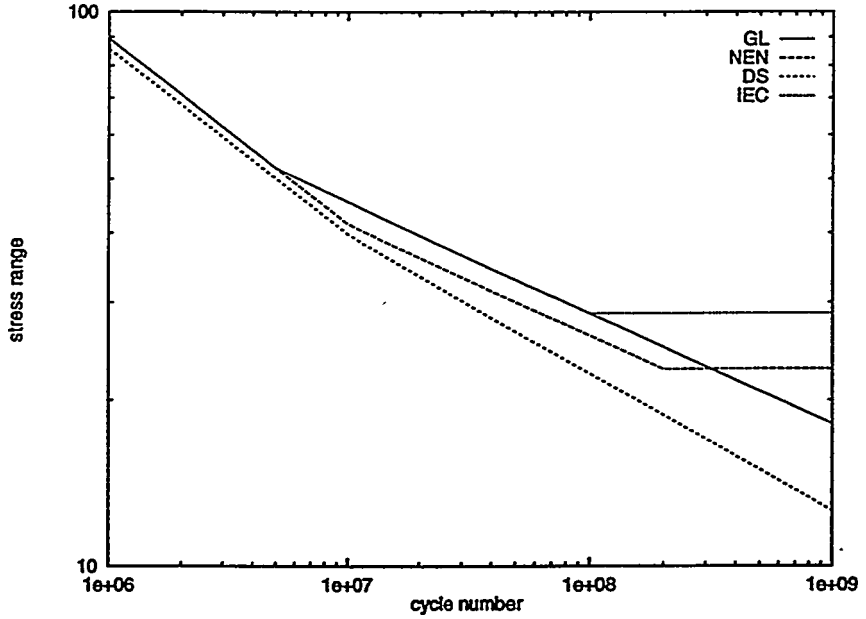

Figure 5: Woehler curves, welded steel

The resulting reserve factors are shown in table 7 and figure 7.

5 Conclusion

There is a clear difference between the safety levels of the various regulations. This difference varies not only with the regulation applied, but also from component to component or according to the material of the wind turbine. The NEN 6096/2 shows the greatest amount of damage at

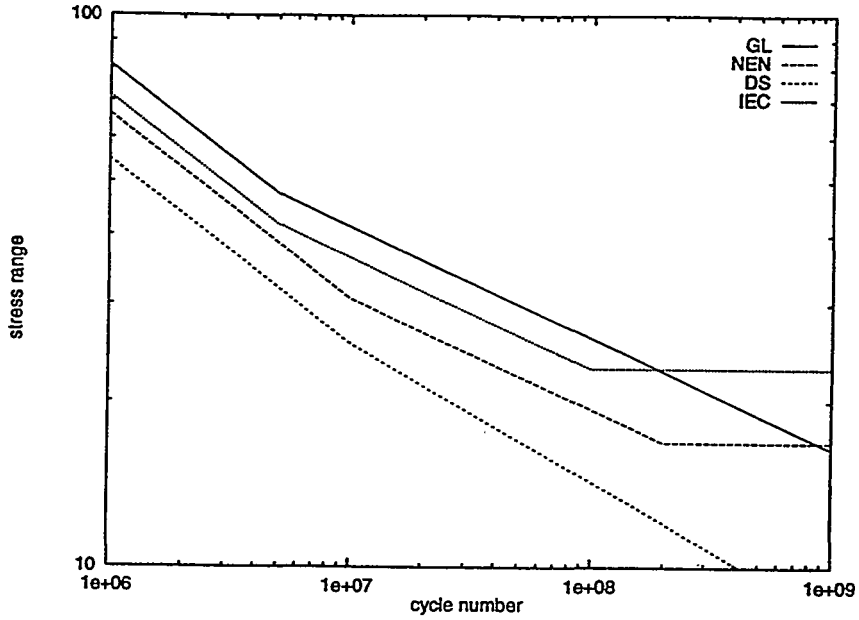

Figure 6: Woehler curves including safety factor, welded steel

Regulation	Class	lrf
GL	1	1.0
GL	2	1.038
GL	3	1.079
NEN		0.937
DS	1	1.567
DS	2	1.266
DS	3	1.085
DS	4	0.877
IEC	1	0.983
IEC	2	1.009
IEC	3	1.039
GL $\gamma_m = 1.25$	1	0.880
GL $\gamma_m = 1.25$	2	0.913
GL $\gamma_m = 1.25$	3	0.950

Table 7: Load reserve factor, tower root

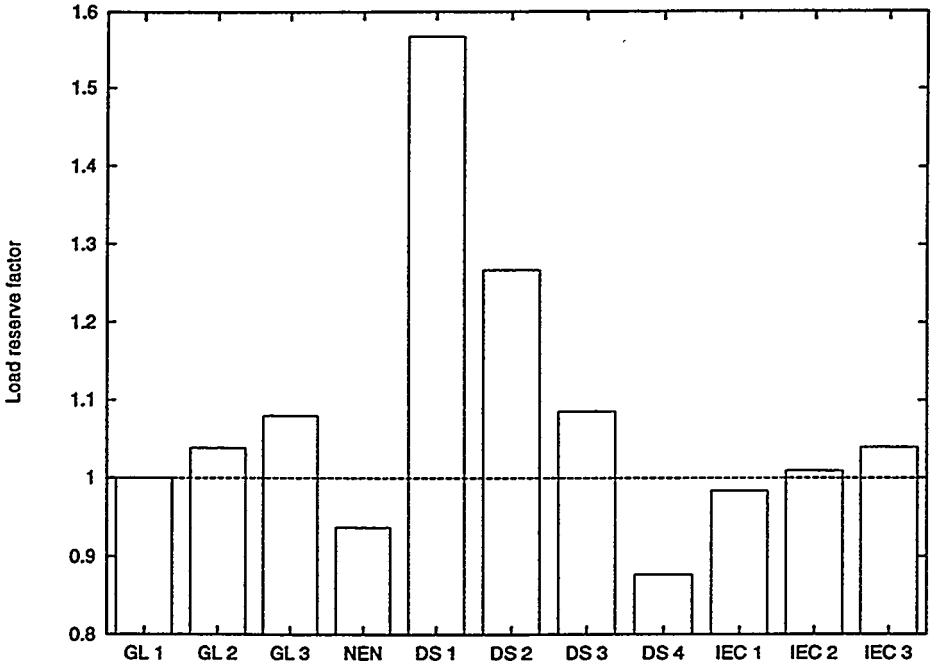

Figure 7: Load reserve factor, tower root

the blade, mainly due to the high load safety factor of 1.35. The GL regulation gives in Class 1 the highest loads, due to the high turbulence, the highest damage for a component of the machine loaded by a tilt moment. The high material factor of the Danish standard results in the highest damage at the tower root for class 4. The high differences in turbulence in the Danish code result in high differences in fatigue, where the differences in the GL and IEC codes are minimal. A formulation with different turbulences for the wind classes, as in discussion for the revision of the IEC regulation, seems usefull.

Several other combinations could lead to results with different ranking, but in general the same tendencies, dependent of material, design and regulation. Size and principle of the turbine can change the rankings, as some parameters are dimension dependend (turbulence is height dependend for NEN and DS) and some force components can significantly be influenced by turbine control (pitch, variable speed, teeter). For MW-sized machines the difference can become even more serious as the rotor diameter gets larger than the integral length scales of horizontal and vertical direction i.e. the partial gusts are not correlated. Another factor is the uncertainity of the theory used and possible deviations between programs used. These are sometimes larger than the differences between the load reserve factors calculated here [18].

References

[1] GERMANISCHER LLOYD: **Regulation for the Certification of Wind Energy Conversion Systems**, Hamburg 1993

[2] DEUTSCHES INSTITUT FÜR BAUTECHNIK: **Richtlinie für Windkraftanlagen**, Berlin, Juni 1993

[3] STAM W.J.: **Regulations for the Type–Certification of Wind Turbines: Technical Criteria**, NEN 6069/2, ECN-R–94-005, February 1994

[4] DANISH STANDARD DS 472: **Loads and Safety of Wind Turbine Construction**, 1st Edition, Copenhagen, May 1992

[5] NATIONAL ENGINEERING LABORATORY: **Recommendation in Compliance with Requirement 1, Technical Basis for the Type Approval and Certification of Wind Turbines in Denmark**, July 1992

[6] IEC 1400-1: **Wind Turbine Generator Systems**, 1st Edition, 1994

[7] C.J. CHRISTENSEN, P. HJULER JENSEN: **EFP-92 Sikkerhedssystemer vor Vindmoller, Bilag 1: IEC Normforslag: Sammenligning med DS–472**, Risø-I-687(DA)(Bilag1), Roskilde, June 1993

[8] K. ARGYRIADIS, C. NATH, J.D. SCHNEIDER: **European Type Approval for Wind Turbines**, Proceedings of the 5th European Wind Energy Association Conference, Thessaloniki, October 1994

[9] F. VAN HULLE, H. WIERSMA, D. WINKELAAR: **Comparison of wind turbine structural design according to Dutch Standard and Draft IEC TC88 Standard**, IEA Topical Expert Meeting, Risø, Denmark, April 1993

[10] W.J.A. WIERSMA-VAN SCHENDEL ET AL: **Interpretation of Document of IEC-TC88: Safety of Wind Turbine generator Systems**, Intron report No. 94056, Houten, Netherlands, Aug. May 1994

[11] DANISH STANDARD DS 412: **Structural use of steel**, 2nd Edition, Copenhagen, April 1983

[12] DANISH STANDARD DS 445: **gelcoat og topcoat på konstruktioner af glasfiberarmeret polyester** 1st Edition, Copenhagen, Sept. 1980

[13] DANISH STANDARD DS 456: **konstruktioner af glasfiberarmeret umaettet polyester**, 1st Edition, Copenhagen, April 1985

[14] ASME BOILER & PRESSURE VESSEL CODE, SECTION III, DIVISION 1 -SUBSECTION NB , 1995

[15] C. PETERSEN: **Stahlbau**, 3rd Edition, Vieweg, 1993

[16] H. GUDEHUS: **Leitfaden für eine Betriebsfestigkeitsrechnung**, 2nd Edition, Verlag Stahleisen, Düsseldorf, 1985

[17] EUROCODE 3, ABSCHNITT 9: **Grenzzustand der Betriebsfestigkeit (Ermüdung)**, Stahlbau-Verlagsgeselschaft mbH, Köln

[18] H.J. VAN GROL, B.H. BULDER ET AL: **Reference procedure to establish fatigue stresses for large size wind turbines**, ECN-C–94-013, Petten, Feb. 1994

IEA–Symposium on Wind Turbine Fatigue

Stuttgart February 1–2, 1996

A simple approximative procedure for taking into account low cycle fatigue loads.

Gunner Larsen and Kenneth Thomsen

Risø National Laboratory, Roskilde, Denmark
January 1996

1 Introduction

In this paper a simple approximative algorithm for taking into account low cycle fatigue loads is presented.

Traditionally, the fatigue life consumption of a wind turbine is estimated by considering a number of (independant) load cases and performing a rainflow counting analysis on each of those. These results are then subsequently synthesized into a total load spectrum by performing a weighed sum of the number of individual load case ranges. The fatigue life consumption is thus obtained by applying the Palmgren–Miner rule on the total load spectrum.

However, due to the assumption of isolated basic load cases, the above procedure fail to represent the low–frequency contributions related to the transition between those load cases. The procedure to be described in the following aims at taking the fatigue contribution, related to the transitions between the defined load cases, into account in an approximative manner.

2 Definitions

Definition 1 : For each of the wind turbine classes I – IV and S in the IEC1400–1 document, *a reference year is* introduced as a representative meteorological year with respect to 10–minutes mean wind speed values.

The Weibull distribution is known to describe the distribution of the mean wind speed values with good approximation. The Weibull distribution is defined by only two parametres – a shape parameter and a scale parameter[1].

For the wind turbine classes I – IV, the IEC–standard prescribes the use of a Rayleigh distribution for the mean wind description. However, the Rayleigh distribution is a special case of the Weibull distribution, as the Weibull distribution degenerate to a Rayleigh distribution if the shape parameter 2 and the scale parameter $\frac{2}{\sqrt{\pi}}\bar{U}_a (\approx 1.128\bar{U}_a)$, where $\bar{U}_a$ denotes the annual mean wind speed, are applied.

For the wind turbine class S, it is legitimate to use different shape– and scale parameters. Usually, for annual mean wind speeds larger than roughly 6 m/s (which is of the same order of magnitude as the cut–in wind speed for most wind turbines), the shape parameter takes values in the interval 1.5 to 2.5. As we intend to approximate the effect of low–frequency wind speed variations on the fatigue consumption, a low value of the shape parameter will be conservative[2] as more probalitity is placed in the tails of the distribution in this situation. Consequently a *default shape parameter value* of 1.5 is recommended as a probably conservative

[1]The probability density function describing the Weibull distribution is mathematically expressed as

$$f(\bar{U}) = \frac{k}{A}\left(\frac{\bar{U}}{A}\right)^{k-1} \exp\left(-\left(\frac{\bar{U}}{A}\right)^{k}\right),$$

where $f(\bar{U})$ is the frequency of occurence of mean wind speed $\bar{U}$, k is a shape parameter, and A is a scale parameter.

[2]For $k > 1$, the function has a single maximum up to which it increases monotonically, and after which it decreases monotonically. When k decreases in the interval described by $4.33 > k > 1$, the Weibull function tends to "broaden" thus given rise to increasing variability. This is also seen directly from the analytical expression for the mean square (m.s.) of the function, given by

$$m.s. = A^2\Gamma\left(1+\frac{2}{k}\right),$$

where $\Gamma(\cdot)$ denotes the gamma function.

value for the reference year with respect to low cycle fatigue consumption. As for the scale parameter, the value (assuming $k = 1.5$) resulting in the design annual mean wind speed, characteristic for the particular S–class application, must been selected. The scale parameter is thus in this case obtained from

$$A = \frac{\bar{U}_a}{\Gamma\left(\frac{5}{3}\right)}, \tag{2.1}$$

where $\Gamma(\cdot)$ denotes the gamma function.

3 Synthetic time series

The basic idea is to supplement the total load spectrum, as evaluated based on a number of isolated basic load cases, with a low–frequency contribution obtained from a synthetic load series.

To create a particular synthetic load series, the reference meteorological mean wind speed year, related to the relevant wind turbine class, is utilized. The algorithm has the following steps:

- The 52560 10–minutes mean wind speed values, constituting the reference year, are ordered chronological as illustrated in the figure below.

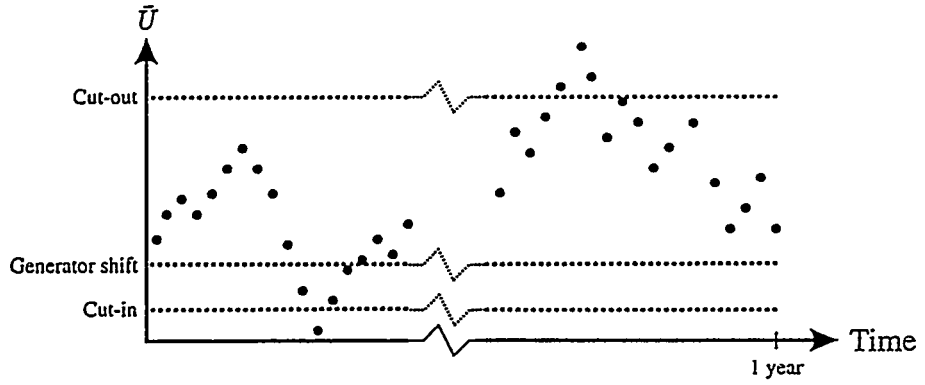

Figure 1. 10–minutes mean wind values related to the reference year.

It is here implicitly *assumed* that one year of 10–minutes mean wind velocities constitute a statistical significant basis for the low cycle load fatigue evaluation.

- The relevant structural response, related to the load cases defined in the IEC1400–1 document, are established by means of aeroelastic simulations and/or by measurements. Note, that some of the (production) load cases may require more that one 10–minutes time series (typically between 3 and 6), primarely due to the demand for sufficient statistical significance of the low–frequency turbulence contribution to the fatigue life consumption (related to an isolated load case).
- For each of the load case time series, the global maximum and minimum values are identified, extracted and saved in the order they appear. Note, that load cases in this respect include normal procuction load cases, start/stop situations, shift between generators, stand still loads at high wind speeds, stand still loads at low wind speeds, etc.. For the production load case no. i (in this case consisting of 6 10–minutes time series), the procedure is illustrated in the figure below.

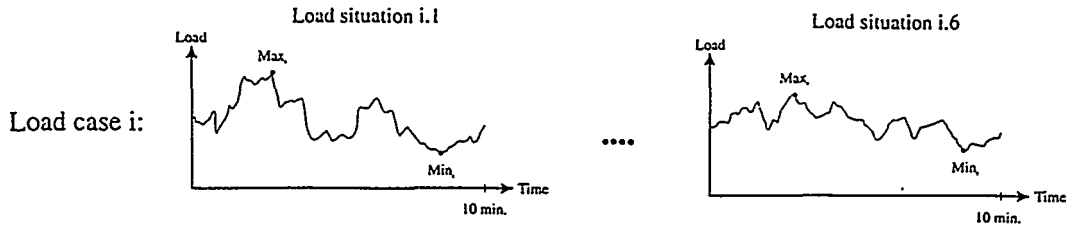

Figure 2. Identification of global extremes of 6 elementary load situations related to production load case no. i.

- The mean wind values contained in the reference year is now examined successively, starting with the first 10–minutes mean value. For each mean velocity value, the relevant load case[3] is identified and it is furthermore examined whether the transition from the previous to the present load case give rise to sublementary transient load cases (start/stop, shift between generators, etc.). Having identified the relevant involved load situations, the corresponding extremum values are transferred to the synthetic structural response time series in the order they appear.
  In case a load case is described by more than one 10–minutes series (as f. ex. the one illustrated in Fig. 2 above), a cyclic procedure is adopted as the first series is used first time the particular load case appear, the second series is used the second time the particular load case appear, etc.. When the last time series related to the particular load case has been utilized, the first time series related to the same load case is applied next time the particular load case appears.

- Considering all the 10–minutes mean wind speed values belonging to the reference year in the above described manner, a systetic low–frequency structural response time series is constructed. The final result is illustrated in the figure below, where N denotes the total number of load cases considered, in the above described sence, during the reference year.

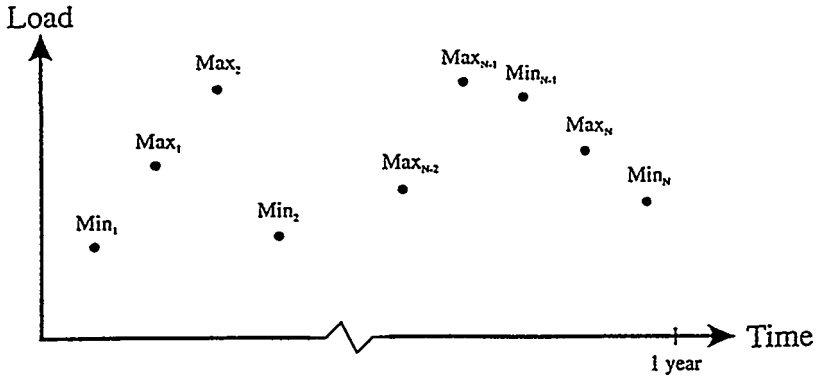

Figure 3. Resulting load time series describing the low–frequency load content.

[3]As for the production load cases, the production wind interval is subdivided into a number bin intervals, typically with a width of 2 m/s. Each load case, belonging to a particular bin, is then described by *one* load case representative for the entire bin interval. This representative load case is often taken as being related to the mean wind speed in the bin interval.

4 Modified total load spectrum

Performing a rainflow analysis on the synthetic load response time series, constructed along the lines described above, results in the desired approximation of the low–frequency contribution to the load spectrum. The result can be added directly to the total load spectrum obtained in the traditionel manner, and a modified total load spectrum emerges which in an approximative manner treat the low–[4] as well as the high frequency load cycles experienced in the life time of the wind turbine.

5 Demonstration example

In order to evaluate the influence, primarily on the load spectrum but also on the fatigue evaluation, from taking the low frequency fluctuations into account, an example has been analysed. The reference year of 10–minutes mean wind speed values has (rather arbitrary) been selected as a monitored series from 1995 originating from the Great Belt Experiment, conducted on the island Sprogø in the middle of the Great Belt between the islands Zealand and Funen in Denmark.

The wind data refer to a position 70 m above average sea level. In order to obtain values corresponding to the hub level of the selected wind turbine (Micon M1500–750kW/150kW), the mean wind speed profile is *assumed* to follow the potential law

$$\bar{U}(z) = \bar{U}(z_{ref}) \left(\frac{z}{z_{ref}} \right)^{0.14} , \tag{5.1}$$

where $\bar{U}(z)$ denotes the mean wind speed at hight z above average sea level. The value at hub level is thus expressed as :

$$\bar{U}(40m) = \bar{U}(70m) \left(\frac{40m}{70m} \right)^{0.14} . \tag{5.2}$$

The time series of the mean wind speed corresponding to a position 40 m above average sea level is presented in Fig. 4 below. Note, the distinct season variation with high wind speeds in the winter period, and lower wind speeds in the summer period.

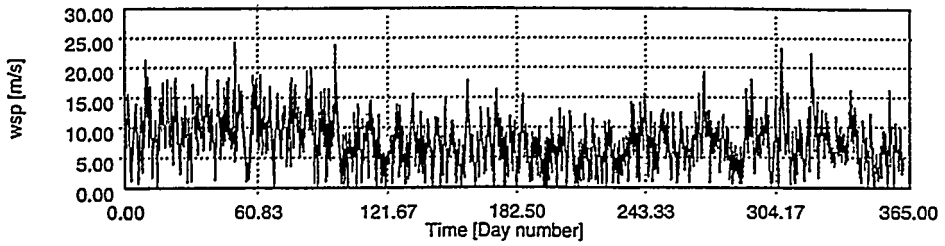

Figure 4. One year of 10–minutes mean wind velocity values at level 40 m.

[4] In case a particular material is not sensible to low–frequency fatigue contributions, this must be taken care of in the fatigue evaluation model. Hence, in this situation, the Palmgren–Miner approximation must either be modified or substituted by an other model. A more heuristic approach is to apply a high–pass filter, with appropriate filter characteristics, on the synthetic load response time series before performing the rainflow analysis, and then subsequently apply the traditional Palmgren–Miner approximation on the filtered result. However, the last procedure has the draw back that it is necessary to produce a "wrong" load spectrum in order to obtain a satisfactory description of the fatigue consumption.

A propability distribution, describing the occurence of a particular mean wind speed value, has been estimated based on a binning of the above time series. A Weibull distribution has been fitted to the result by a maximum likeness procedure, and the result is given in Fig. 5 below. The Weibull parameters corresponding to the fit were A = 8.8 m/s and k = 2.31, and as seen a convincing agreement between measured and estimated values is obtained.

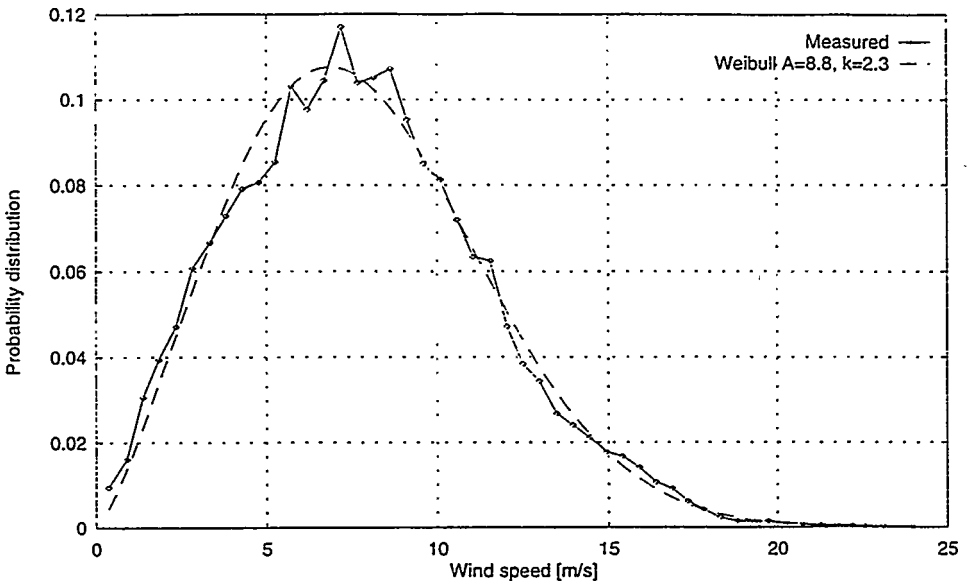

Figure 5. Measured and estimated probability density function of average mean wind speed.

The wind turbine selected for the example is, as mentioned above, the Micon M1500–750kW/150kW turbine equipped with LM19.1 blades. For this turbine, the cut–in wind speed is 3 m/s and the cut–out wind speed is 25 m/s. Load cases related to the flap moment at the rotor radius 1.5 m, referring to both production and transient situations (start/stop), have been simulated with an aeroelastic model. The load cases related to stand–still situations has been neglected in the present study, but could equally well have been included.

For the production load cases, the production wind interval [3 m/s;25 m/s] is subdivided into 11 bin intervals with a width of 2 m/s. The turbulence intensity is assumed equal to 17%, in accordance with the specifications in the IEC1400–1 document, and zero yaw error was furthermore presumed. Thus, the mean wind interval [3 m/s;5 m/s] is characterized by a simulation with the mean wind speed 4 m/s, the mean wind interval [5 m/s;7 m/s] is characterized by a simulation with the mean wind speed 6 m/s, and so forth.

Three transient load situations have been evaluated corresponding to a start at the cut–in wind speed, a start at the cut–out wind speed, and to a stop at the cut out wind speed. The load situation corresponding to a stop at the cut–in wind speed introduces very modest loads, and is assumed resonably well described by the load case corresponding to the start at the cut–in wind speed.

The main characteristics of the simulated flap moments is summarized in Table 1, where $\bar{U}$ denotes the mean wind speed related to a particular simulation, and T the corresponding length of the simulation.

As described above, the extreme values, related to the selected load cases, must

Load case type	$\bar{U}$ [m/s]	T [s]	Mean [kNm]	Rms [kNm]	Min. [kNm]	Max. [kNm]	Max.-Min. [kNm]
production	4	300	109.6	19.25	36.73	164.8	128.0
production	6	300	167.9	31.03	48.28	253.1	204.8
production	8	300	231.0	39.81	69.43	337.9	268.5
production	10	300	282.3	41.24	94.37	408.8	314.4
production	12	300	313.4	39.20	117.6	449.3	331.7
production	14	300	330.9	38.79	140.3	484.8	344.5
production	16	300	343.5	40.37	162.6	512.5	349.9
production	18	300	355.8	43.12	183.3	545.4	362.1
production	20	300	369.5	46.91	197.4	565.0	367.6
production	22	300	385.4	51.67	192.7	600.9	408.3
production	24	300	403.3	57.30	193.4	636.7	443.3
start; cut–in	3	100	64.34	52.19	10.99	218.9	208.0
start; cut–out	25	100	225.1	92.92	14.17	468.2	454.0
stop; cut–out	25	30	314.8	122.2	40.29	711.5	671.2

Table 1. Main characteristics of the flap moment simulated at $R = 1.5$ m.

be transferred to the synthetic structural response time series in the order they appear[5]. However, for the production load cases the same seed–value (in the turbulence simulation) was used for all simulations, resulting in only a scaling of the turbulence and thus obviously the same sequencing of the minimum– and the maximum structural loads. In order to compensate for that, a random selection of the sequencing of these extrema was performed. The resulting low–frequency synthetic time series, related to the flap moment at R = 1.5 m, is shown on Fig. 6 below.

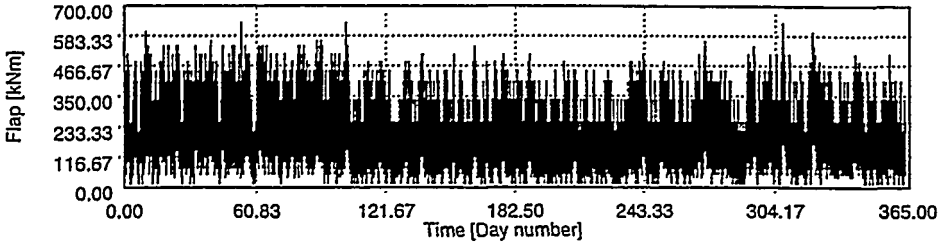

Figure 6. Synthetic time series containing the low–frequency contributions to the flap moment at $R = 1.5$ m.

Based on the above 11 production load cases, a traditional load spectrum is is established by considering the load cases as being independant, performing a rainflow counting analysis on each of those, and then subsequently add the results as a weighed sum of number of occurences related to individual load ranges. The weight parameters are the probalitities attached to the particular load cases, determined from the estimated Weibull distribution presented in Fig. 5 (A = 8.8 m/s ,k = 2.31), multiplied by the number of 10 minutes sequences contained within a

[5]For the present purpose (rainflow analysis), a frequency analysis of the synthetic time series is of no relevance, and therefore the load values have been transferred to the synthetic series with equidistant time separations rather than the true time separations.

year.

The low–frequency contibution originating from the transitions between the considered load cases, as based on the measured reference year, is taken into account by performing a rainflow counting analysis on the low–frequency synthetic time series presented in Fig. 6 and subsequently add the result directly to the traditional load spectrum described above. The resulting traditional– and total load spectrum are presented in Fig. 7 below.

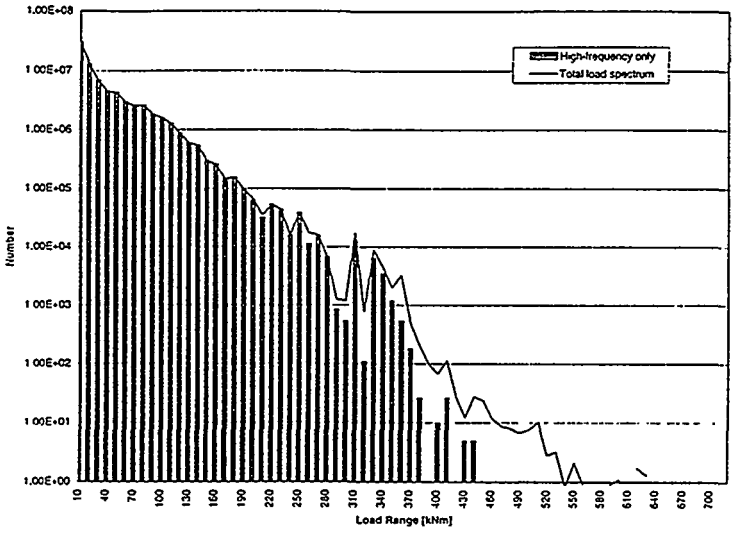

Figure 7. Traditional– and total one year load spectrum for the flap moment at $R = 1.5$ m.

In Fig. 8 below, the similar results are displayed in terms of accumulated load spectra, where the the number of cycles related to a load range expresses the number of load ranges *larger* than the particuler load range.

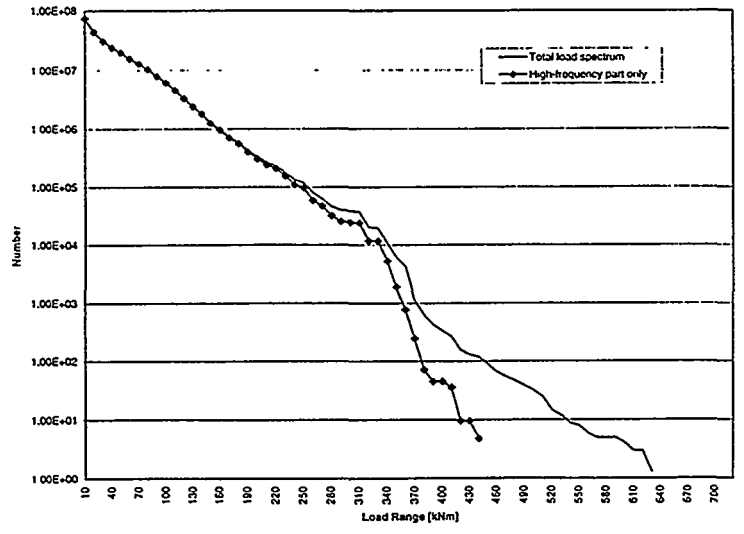

Figure 8. Traditional– and total accumulated one year load spectrum for the flap moment at $R = 1.5$ m.

Comparing the traditional– and the total load spectrum, it appears that the parts related to moderate range sizes are very similar, whereas the parts associated with large load ranges differ considerable.

In order to quantify the impact of including the low–frequence contribution in the load spectrum in terms of fatigue life consumption, equivalent load ranges (based on an equivalent number of load ranges equal to 10^6) are established by applying the Palmgren–Miner rule both on the traditional load spectrum and on the total load spectrum. In order to cover a broad range of materials, the Wöhler exponents m = 3, m = 7, and m = 12 were (arbitrary) selected. The results appear from Table 2 below.

m	Traditional load spectrum	Total load spectrum	Ratio
3	277.67 kNm	280.84 kNm	1.01
7	221.01 kNm	230.27 kNm	1.04
12	245.87 kNm	264.72 kNm	1.08

Table 2. Equivalent load ranges based on traditional– and total load spectra for various Wöhler exponents.

From Table 2 the damage ratios, corresponding to the listed ratios of equivalent loads, are determined to 1.03, 1.33, and 2.43, respectively.

The relative importance of the load ranges in terms of fatigue life time consumption is illustrated on Fig. 9, Fig. 10, and Fig. 11 for different values of the Wöhler exponent. Each of the figures show the relative life time consumption of a particular load range compared to the total fatigue life time consumption related to the specific load spectrum.

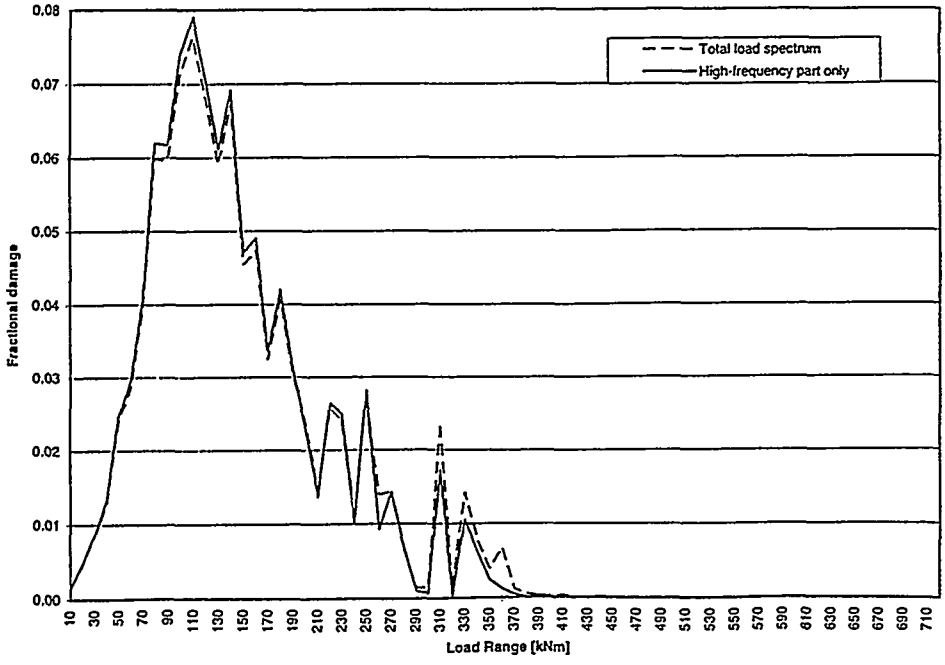

Figure 9. Relative fatigue life time consumption for the traditional– and the total load spectrum for m = 3.

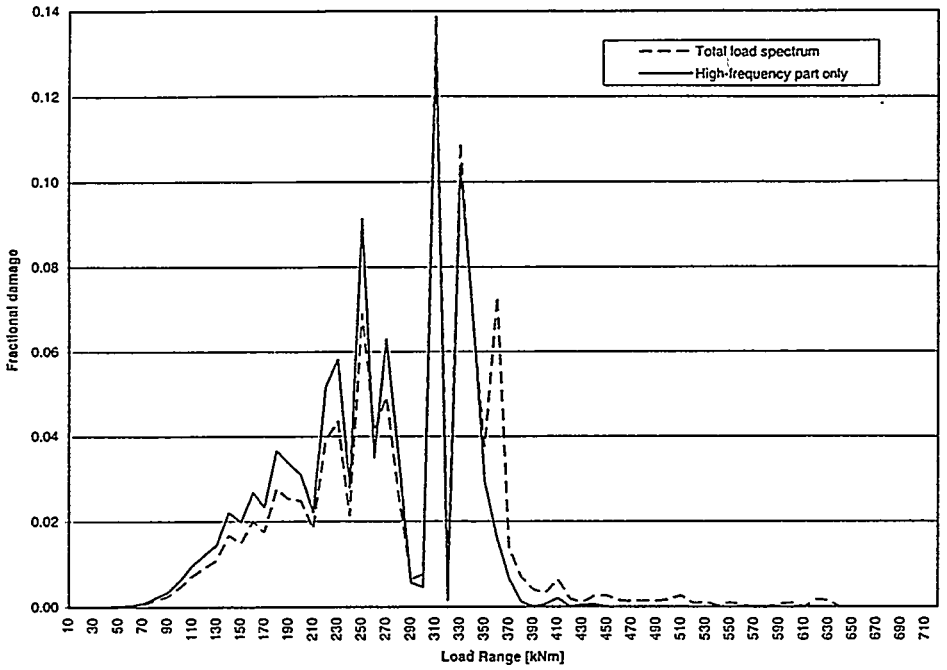

Figure 10. Relative fatigue life time consumption for the traditional– and the total load spectrum for m = 7.

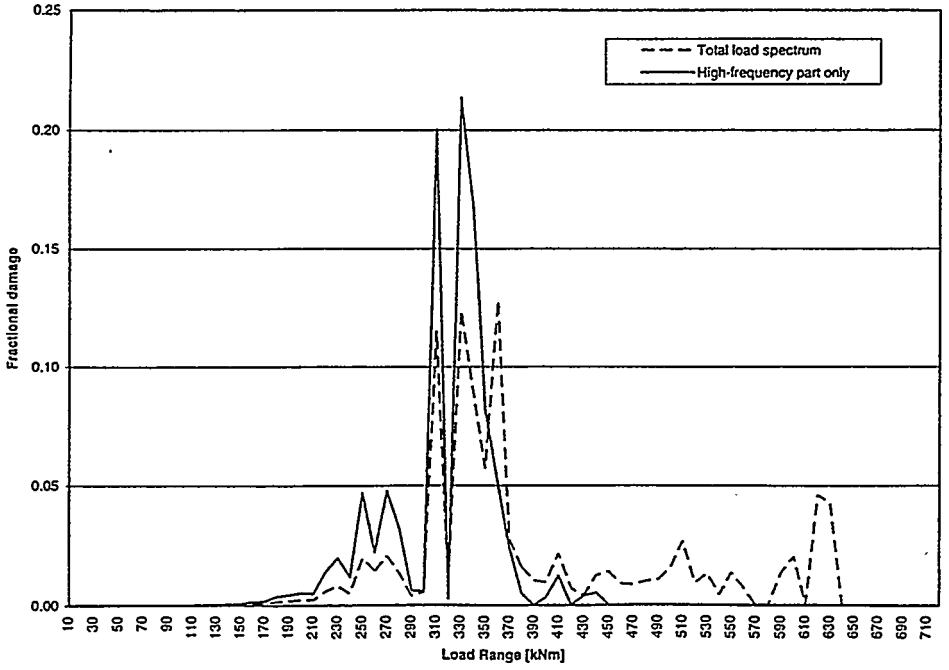

Figure 11. Relative fatigue life time consumption for the traditional– and the total load spectrum for m = 12.

As mentioned above, the main difference between the traditional– and the total load spectrum is attached to a relative limited number of relative large load ranges. On this background, it is not surpricing that the most noticeable difference in curves describing the relative life time consumption is obtained for large values of the Wöhler exponent.

6 Conclusion

A framework for an approximative inclusion of low–frequency contributions, originating from the transition between the basic load cases in the duty cycle description, has been established. The algorithm allows for inclusion of both contributions associated with transient load cases and production load cases. The method has been applied to a demonstration example consisting of simulated load events associated with the flap moment on a wind turbine during a one year period. The low–frequency contribution is shown to add a limited number of relative large load ranges to the traditional load spectrum. In terms of equivalent moments, the low–frequency part account for of the order of magnitude 10%/1% for relative large/small Wöhler exponents, corresponding to a reduction in the lifetime of the order of magnitude 60%/3%.

4th IEA SYMPOSIUM ON WIND TURBINE FATIGUE - DLR Stuttgart, 1&2 Feb 1996

Effect Of Control Activity on Blade Fatigue Damage Rate for a Small Horizontal Axis Wind Turbine.

Dr. A.F. Riddle, Dr L.L. Freris, Prof. JMR. Graham. Imperial College, London, U.K.

1.0 Overview

An experiment into the effect of control activity on blade fatigue damage rate for a 5 kW, two bladed, teetered HAWT has been performed. It has been shown that control activity influences the distribution of strain in the blade but that in a high rotorspeed, high cycle fatigue regime this has little influence on damage rate.
The experiment was conducted on a small test turbine by implementing variable speed stall, pitch and yaw control strategies and measuring blade flapwise strain response at root and midspan locations. A full description of the investigation is provided in [1].

2.0 Experimental Set-up

The Imperial College Wind Turbine (ICWT) is a small, stand alone, variable speed test horizontal axis wind turbine. It was developed at Imperial College and is located at the Wind Test Site at Rutherford Appleton Laboratory. The turbine consists of a 6.5 m diameter, two bladed, teetered, GRP rotor connected through a parallel shaft gearbox to a 7.5 kW field controllable DC machine acting as a generator. The turbine is loaded electrically using a bank of resistors rated at 10 kW.
Dynamic control of ICWT is implemented in software using a 16 MHz 386 personal computer. Algorithms are coded in QBasic and apply single input single output fuzzy based logic. Pitch and yaw control activity are applied through 12 V DC actuators and generator field voltage is regulated through a rectified, chopped 415 V AC supply. See [2] for further details of the electrical and control systems.
For the purpose of the experiment, ICWT is operated in three variable speed strategies. At below rated windspeed, all strategies implement a constant tipspeed ratio policy. This is achieved through generator field voltage excitation. In above rated operation all strategies implement a constant power policy. In stall regulated operation power is maintained passively through field regulation of rotorspeed and setpoints of 16 rad/s and 14 rad/s are implemented. In pitch and yaw regulated operation power is regulated through blade pitch angle or rotor yaw angle variation. In these strategies rotorspeed is maintained nominally constant at 16 rad/s through an outer speed control loop. Rated windspeed is 8.5 m/s in all strategies.

3.0 Measurement and Post Processing of Blade Strain Data

The blades mounted on ICWT are supplied by Aerpak. They are manufactured in GRP using approximately a 55% E-glass fibre to 45% polyester resin ratio by weight. Their Young's Modulus is estimated to be 25 GN/m^2 and in the vicinity of the gauges fibre lay-up is approximately unidirectional.
For the purpose of fatigue measurement, one blade is equipped with fully active strain bridges at root and midspan locations. The bridges are mounted in the flapwise plane, along the blade quarterchord in the case of the centre gauge, and on the blade flange in the case of the root gauge. Edgewise bridges are not mounted at either location because of slipring limitations.
Strain data is collected using interrupt transfer to a second 16 MHz 386 personal computer. Blade strain information is measured at 60 Hz to comply with [3], and control and environmental parameters are measured at 6 Hz. Campaigns of five minutes duration are collected in view of the high cycle accumulation rate.
For the purpose of fatigue calculations, measured strain time histories are rainflow counted and summed according to Miner's Rule across a suitable blade life surface in the mean range plane. For this calculation a Goodman Transformation is applied and blade ϵN data is taken from [4] at an R ratio of -1. In root strain calculations approximate mean edgewise and spanwise strains are added back to flapwise strain time histories to account for centrifugal and blade inplane shear forces. This is done using 6 Hz measurements of rotorspeed and shaft torque respectively. Modal vibration in the edgewise signal is clearly absent using this approximation and the net effect of the transformation is to scale mean strain condition and add some low frequency rotor acceleration cycles. Torque cycles are also added but these are small and represent rotor averaged values. These corrections are not applied for centre strain calculations because the aerodynamic and inertial load

distributions about the blade midspan are unknown. Shear strains arising from pitching moments are neglected in all calculations as are blade edgewise gravity strains.

4.0 Experimental Results

In total fourteen campaigns have been selected for analysis. Six of these are in stall regulated operation and four are in each of pitch and yaw regulated operation. Two of the stall regulation campaigns take place at reduced rotorspeed.

4.1 Time Histories Example operating campaigns in above rated operation are shown for each strategy in Figure 1. Windspeed is roughly 10 m/s in all cases and Turbulence Intensity is about 14%.
In stall regulated operation, mean strain response is highly stochastic. In low speed operation, rotorspeed variance is moderate and strain response is well correlated with windspeed. In high speed operation, strain response remains well correlated with windspeed but, since rotorspeed variance reduces, it becomes more narrow band. In pitch and yaw regulated operation mean strain response is more deterministic. Low frequency high amplitude load cycles appear due to pitching, yawing and speed cycling activity. In these strategies the correlation between mean strain response and windspeed is low whilst the correlation between mean strain response, pitch angle, yaw angle and rotorspeed is high. In all strategies mean strain response lies in the range 500 to 700 $\mu\varepsilon$. This is a factor of around 30 below the Ultimate Tensile Strain of the blade. Variations in mean strain condition between strategies are attributed to differing mean windspeeds and rotorspeeds as well as to pitch and yaw control activity. The quality of dynamic control of ICWT is generally quite poor in all strategies. This is primarily due to an inadequate control system response time for the given edgewise inertia of the rotor. The low power output in all strategies is thought to be due to the aeroelastic behaviour of the rotor in high speed operation (see section 4.2).

4.2 Auto Power Spectral Density functions Auto Power Spectral Density (APSD) functions of blade root and centre gauge signals in example high speed stall and pitch regulation campaigns are shown in Figure 2. In both campaigns the spectral peaks in the root correspond to rotorspeed harmonic excitation at 1P and 2P, blade 1st flapwise mode response at 7.5 Hz and blade 1st and 2nd edgewise mode responses at 11.5 Hz and 23.0 Hz respectively. The 2nd flapwise mode is absent in the root gauge signals but appears in corresponding centre strain signals at 15 Hz. Flapwise response in the 2nd mode is removed at the hub by the action of the teeter hinge.
The amplitudes of spectral peaks are similar in the two strategies. The main differences in spectra occur in the low frequency range where background pitch regulated response is higher. This is due to blade pitching and rotorspeed cycling activity. Pitching activity also appears to attenuate the 2P rotorspeed harmonic.
In both strategies, the 1st flapwise mode response is large in relation to rotorspeed harmonic response. Over the operating range of the rotor, dynamic magnification of this mode increases rapidly with rotorspeed. This is a consequence of mounting stiff blades, designed for three bladed operation, on a higher speed two bladed rotor. The theoretical dynamic magnification factor of the first flapwise mode to 1P and 2P disturbances is shown as a function of rotorspeed and damping ratio in Figure 3. The damping ratio of the mode is estimated to be about 0.25 from its half power bandwidth in Figure 2. The large amount of dynamic vibration predicted by this curve goes some way to explaining the low power output of the turbine in all strategies.

4.3 Rainflow Cycle Distributions Rainflow cycle distributions for example campaigns in each strategy are shown in Figure 4. At first glance there are distinct differences in rainflow cycle distributions between strategies. High speed stall regulated operation generates a sharp, narrow band distribution, whilst pitch and yaw regulated operation generate broader band distributions. This broadening effect reflects rotorspeed cycling effects as well the thrust variations introduced by pitching and yawing activity. As rotorspeed is reduced in stall regulated operation, the distribution of cycles becomes more broadband. This reflects a loss of aerodynamic damping, larger rotorspeed variance and greater modal excitation caused by resonant vibration of the tower structure. In all strategies, rainflow distributions at centre locations are similar but more narrow in band than corresponding root distributions. This reflects an increased ratio of inertial to aerodynamic response at the root with respect to the centre.
In Figure 5, the rainflow distributions of Figure 4 are plotted in two dimensions. Differences between cycle distributions of mean strain are clearly visible as are similarities between cycle distributions of ranges. The differences between cycle distributions of means are attributed to pitching, yawing and speed cycling activity and the similarities in cycle distributions of ranges are attributed to the similar amplitudes of 1P, 2P and 1st flapwise mode cycles in each strategy.

In Figure 6 2D cycle distributions for successive campaigns in pitch regulated operation are shown. This figure indicates a high degree of repeatability of the experiment. The degree of repeatability is similarly high in other strategies.

4.4 Projected lifetimes to Failure In Figures 7, 8 and 9 projected lifetimes at root and centre locations are plotted against strategy number, mean rotorspeed and cycles accumulated respectively. Projected lifetimes are calculated as reciprocal functions of fractional damage.
Differences in projected lifetimes between campaigns are generally small (Figure 7). Lifetime is slightly higher in pitch regulated operation because of the lower mean strain condition experienced, but lifetime in yaw regulated operation is no lower than in stall regulated operation. This indicates that control activity has little influence on damage rate. Differences in projected lifetimes with rotorspeed (Figure 8) are large but show no significant correlation. This reflects the proportionately high accumulation rate of 1st flapwise mode cycles in all campaigns and the varying dynamic magnification of 1P and 2P harmonics with rotorspeed. Correlation is better at the centre gauge location because 1st flapwise modal response is less significant there. Differences in projected lifetimes with cycles accumulated (Figure 9) are large and show a reasonably strong correlation. Again correlation is better at the centre gauge location but, in this case, this reflects smaller differences in strain condition at the midspan than at the root. The reduction in projected lifetime in yaw regulated operation is thought to result from a higher mean strain condition in that strategy. The reduction is greatest at the root because the change in mean strain condition with respect to other strategies is greatest there. The reduction in projected lifetime in low speed stall regulated operation is thought to be due to reduced aerodynamic damping and increased tower structural resonance at that rotorspeed. The relative increase in life with respect to other strategies at the centre gauge reflects improved damping at the outboard section of the blade and a lower 1st flapwise modal response.
The ratio of projected lifetimes at root and centre locations is shown in Table 1. In all campaigns there is a 15% to 20% higher lifetime expectation at the root gauge than at the centre gauge. This is attributed to the removal of 2nd flapwise mode root cycles by the teeter hinge. The ratio of cycles accumulated at the root to cycles accumulated at the centre can be inferred from Figure 9. In all campaigns there is a corresponding 15% to 20% lower cycle count at the root gauge than at the centre gauge.

5.0 Discussion
5.1 Materials Viewpoint An extrapolated lower 95% confidence ϵN curve [4] for unidirectional glass polyester laminate at an R ratio of -1 is shown in Figure 10. The approximate strain condition of the blade in the experiment is marked on the figure and indicates that approximately 10^{12} cycles can be accumulated before fatigue failure is likely to occur.
In Figure 11 a 95% confidence range strain surface in the cycles to failure - mean strain plane is shown. For constant range strain, there is an inverse relationship between allowable cycles to failure and mean strain condition. The slope of this relationship is approximately linear and is independent of the allowable number of cycles to failure. For a given mean strain condition on the other hand, the rate of change of range strain with life increases exponentially with increasing range strain. This is a consequence of the use of a Log-Log ϵN relationship and is seen more clearly in the contour plot of Figure 12. For a given design cycle lifetime therefore, a higher mean strain condition will reduce the allowable range strain variation for a given variation in lifetime. Put another way, in more highly utilised rotors, given variations between load spectra in different control strategies will magnify variations in fractional damage rates.
Another way of interpreting this is to consider the Goodman Diagram (see for example [4]). In high mean, low range strain conditions (ie at high R ratios) the rate of change of lifetime with range strain variations is high, whereas in low mean, high range strain conditions (ie at low R ratios) the rate of change of lifetime with range strain variations is low. For a given R ratio of operation, a higher degree of utilisation (ie a higher mean strain condition) reduces the sensitivity of lifetime to range strain variations. Conversely for a given degree of utilisation, higher R ratio operation increases the sensitivity of lifetime to range strain variations. Finally for a given range strain variation, a higher utilisation factor increases the sensitivity of lifetime to range strain variation. The implication of all of this is that, for a given range strain variation, lifetime can be extended by low utilisation of the rotor and high R ratio operation. Furthermore, in this operating scenario, the effect of differing range strain conditions on lifetime variations can be suppressed. The R ratio of operation of the ICWT blade in the mean range plane is marked in Figure 13. In the condition of the experiment it has a value of about 0.8. In the Goodman Diagram, this represents a line at 12.5 degrees to the horizontal. ICWT's position on this line is defined by the rotor utilisation factor which is approximately 1/30th of the Ultimate Tensile Strain of the blade.

5.2 Implications For Larger Rotors In large rotors the controller crossover frequency is of the same order as the blade passing frequency. Consequently the relative damaging effect of control cycles with respect to rotorspeed harmonic and modal response cycles will increase. Indeed in highly active pitch regulated machines, control activity may ultimately constitute the dominant blade damaging mechanism.
In power control mode, pitch regulated rotors can be expected to induce higher damage rates in the blades than stall regulated rotors. As well as introducing control cyclics, pitching activity will amplify incident turbulence loads that are otherwise damped out in stall regulated rotors by the stalling process (ie by operation around the neck of the blade lift curve). Since pitching response time constants are invariably too long to counteract higher frequency components of the incident turbulence energy, pitching activity cannot even be expected to reduce stochastic loading significantly. Finally, although mean flapwise loads are higher in stall regulated rotors, the rate of change of mean load with windspeed is higher in pitch regulated rotors. In terms of fatigue it is, of course, the rate of change of loads that is most important. Having said this, the expected benefits of stall regulated rotors may be outweighed, in deep stall conditions, by increased rotor modal excitation. Indeed with regards to blade fatigue, the main benefit of pitch regulated rotors in extreme windspeeds lies in their ability to preserve aerodynamic damping and hence modal stability of the rotor. In general the influence of modal excitation on overall damage rate can be largely suppressed by appropriate blade design. Softer rotor design will reduce the accumulation rate of modal vibration cycles (and potentially their magnification also) but will amplify aerodynamic disturbances to the blade through larger tip deflections. For variable speed designs, the need to avoid structural resonances will significantly limit the useful operating ranges of rotors.

6.0 Conclusions

An experiment into the damaging effect of control activity on rotor blades has been performed. The experiment has identified distinct differences in the rainflow cycle distributions in different dynamic control strategies. However, the rotor in question has suffered significant vibration in the first flapwise mode and, in view of high accumulation rate of rotorspeed harmonic cycles, the effect of control activity on damage rate has been found to be small. Although the experiment was based on a small dataset, a high degree of experimental repeatability has been observed. This has added confidence to the findings of the paper.
In larger designs it is anticipated that control activity will play a more significant role in blade damage accumulation rate and pitch regulated operation can be expected to induce a higher fatigue penalty in the rotor blades than stall regulated operation. Finally in teetered rotor designs, the removal of first flapwise mode vibration at the root may reduce damage rates at inboard sections of the blade with respect to outboard sections.

7.0 Acknowledgements

This research project was co funded by EPSRC and WEG Ltd under a CASE Ph.D. studentship at Imperial College. ICWT was constructed in the Department of Electrical Engineering at Imperial College with design assistance from WEG Ltd and was operated at Rutherford Appleton Laboratory with the kind permission of the Energy Research Unit. Electrical and control aspects of the project were implemented by M.T. Iqbal as part of his research studentship at Imperial College.
The author would like to thank National Wind Power for financing attendance of the Symposium.

8.0 References

[1] Riddle, A.F., 1995, 'An Investigation into Energy Capture And Fatigue Implications of Wind Turbine Control Policies'. Ph.D. Thesis, University of London, 1995.
[2] Iqbal, M.T., 1994, 'Dynamic Control Strategies for Fixed and Variable Speed Wind Turbines'. Ph.D. Thesis, University of London, 1994.
[3] International Energy Agency (IEA), 1990, Recommended Practices for Wind Turbine Testing and Evaluation. Prt. 3. Fatigue Loads 2nd Ed.
[4] De Smet, B.J. & Bach, P.W., 1994, 'Database FACT, Fatigue of Composites for Wind Turbines' ECN report no ECN C 94 045.

FDBA58 Pitch regulation of power.

FFBA70 Yaw regulation of power.

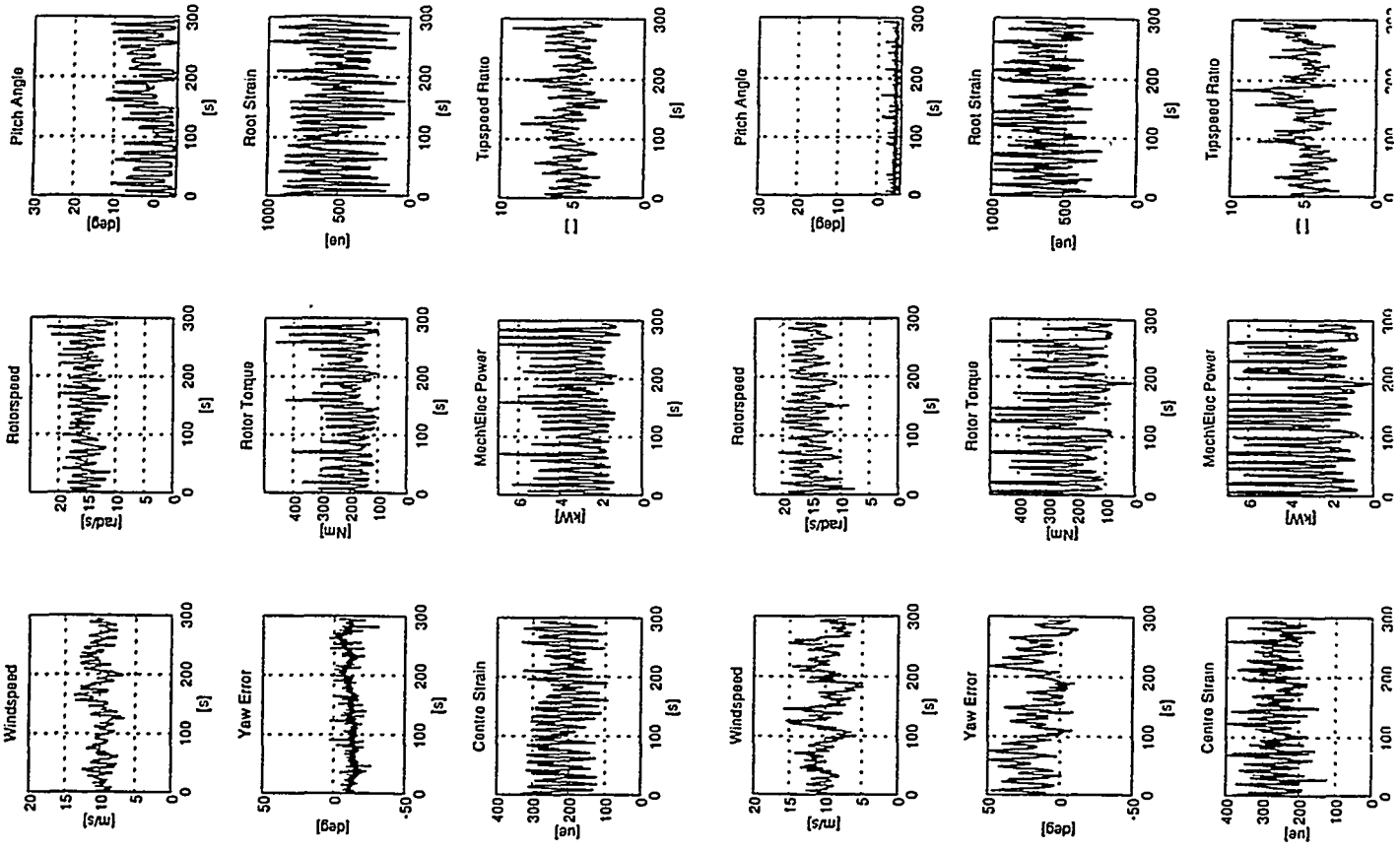

FABA40 Field regulation of speed.

FABA51 Field regulation of speed.

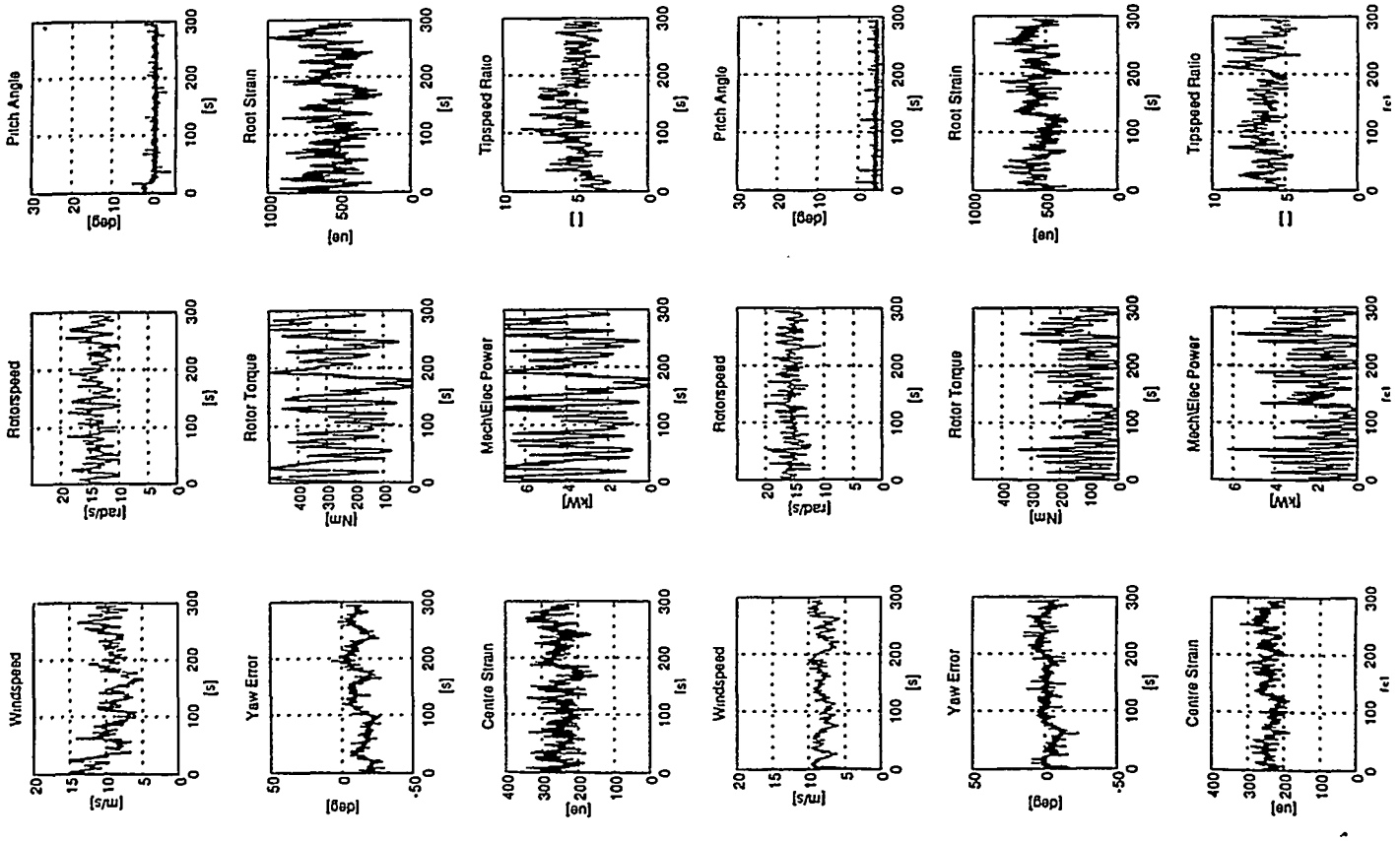

Figure 1 Campaign Time Histories In Each Strategy.

FABA51 Field regulation of speed.

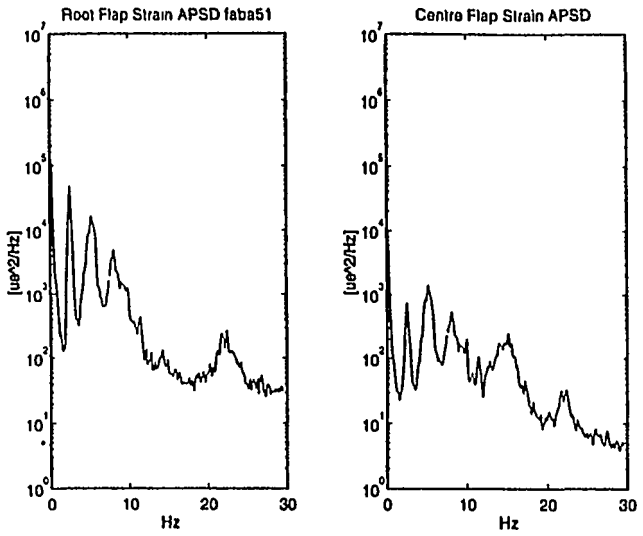

FDBA58 Pitch regulation of power.

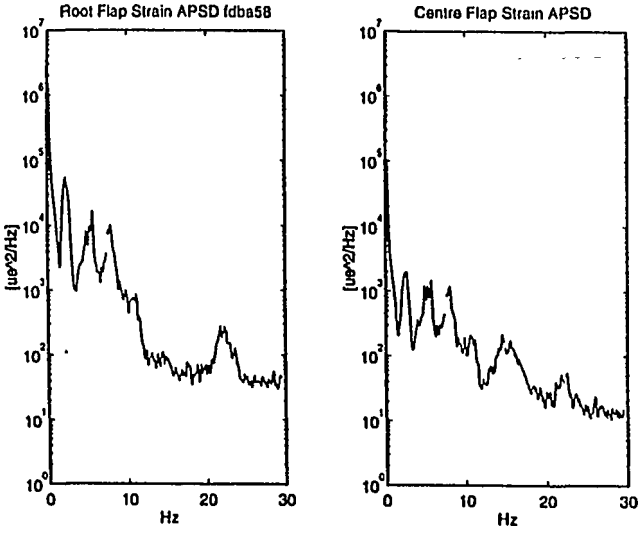

Figure 2 Root and Centre Gauge Spectra for Stall and Pitch Regulated Operation.

Magnification in Response to 1P Excitation (ζ=0.2,0.4,0.6,0.8,1.0).

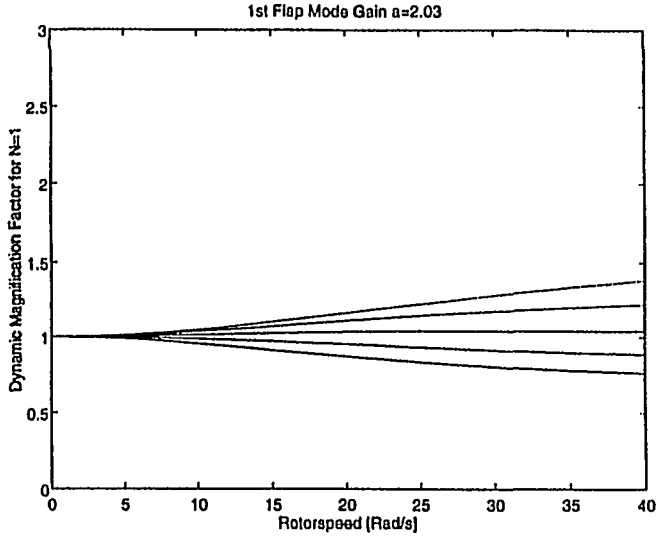

Magnification in Response to 2P Excitation (ζ=0.2,0.4,0.6,0.8,1.0).

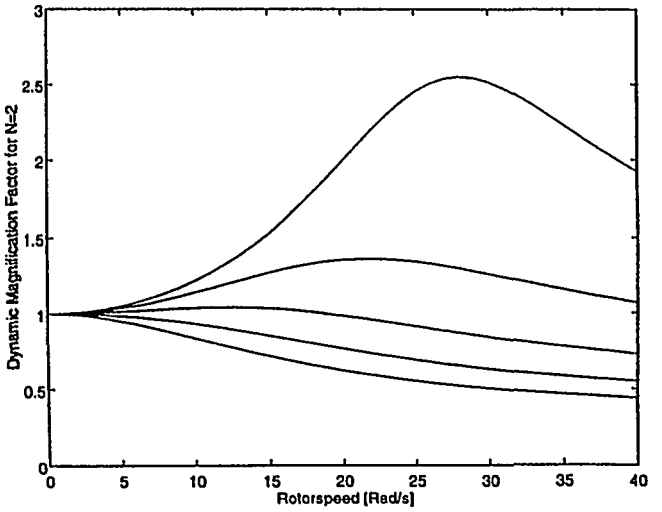

Figure 3 First Flapwise Modal Response to 1P and 2P Excitation.

FABA40 Field regulation of speed.

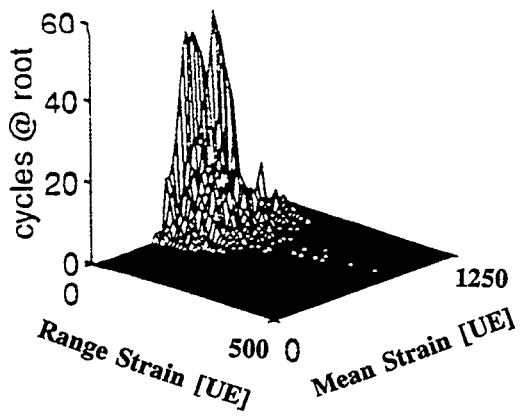

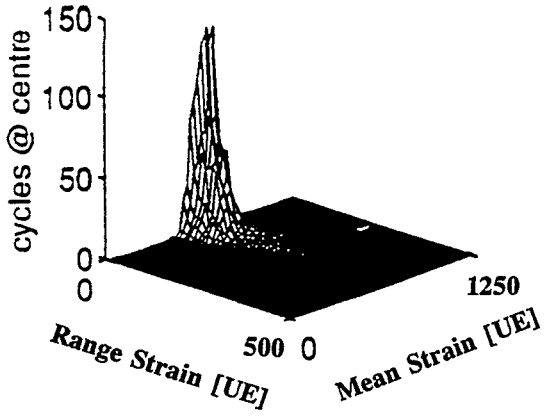

FABA51 Field regulation of speed.

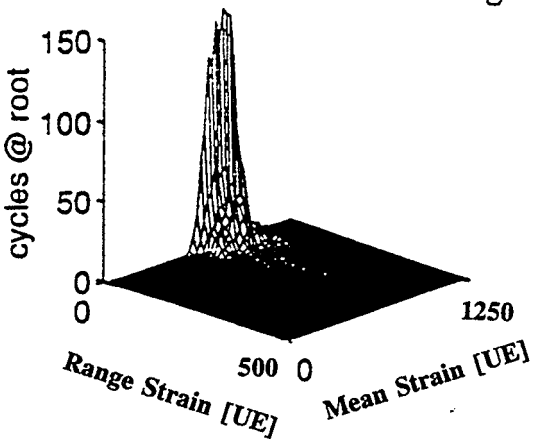

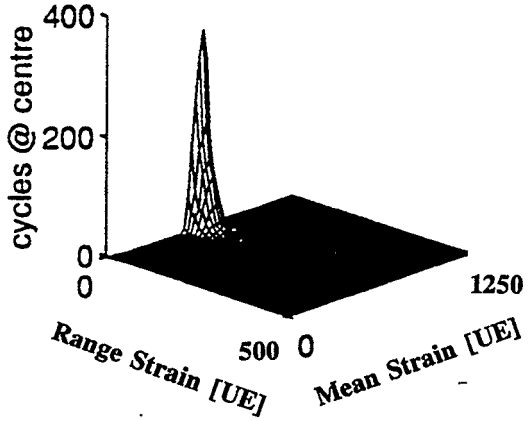

FDBA58 Pitch regulation of power.

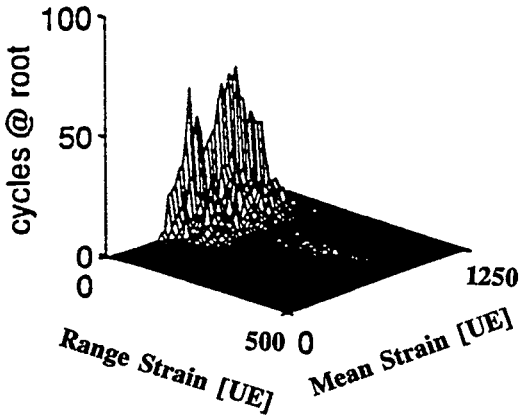

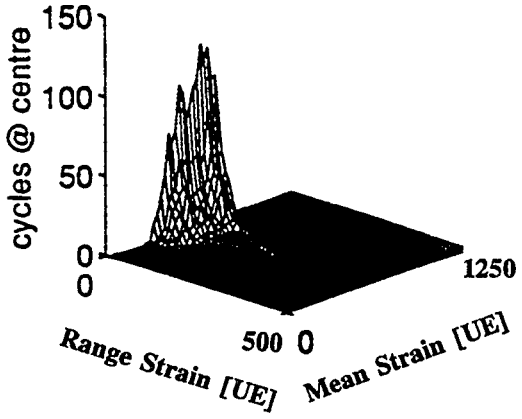

FFBA70 Yaw regulation of power.

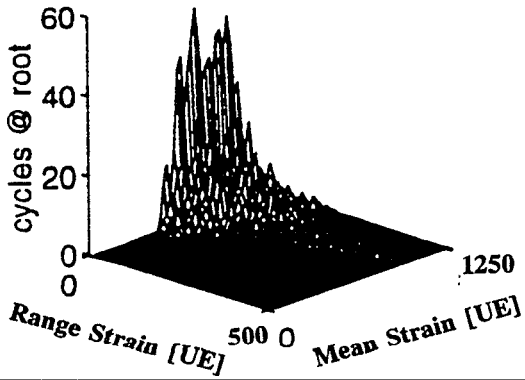

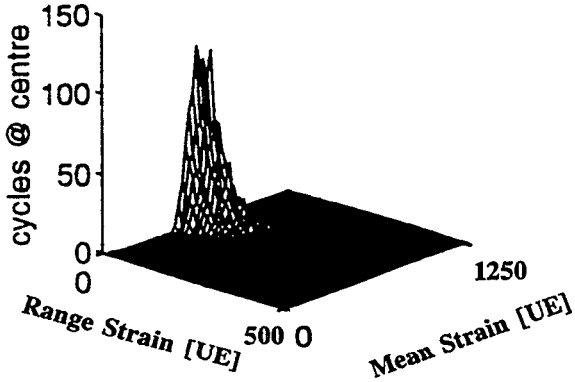

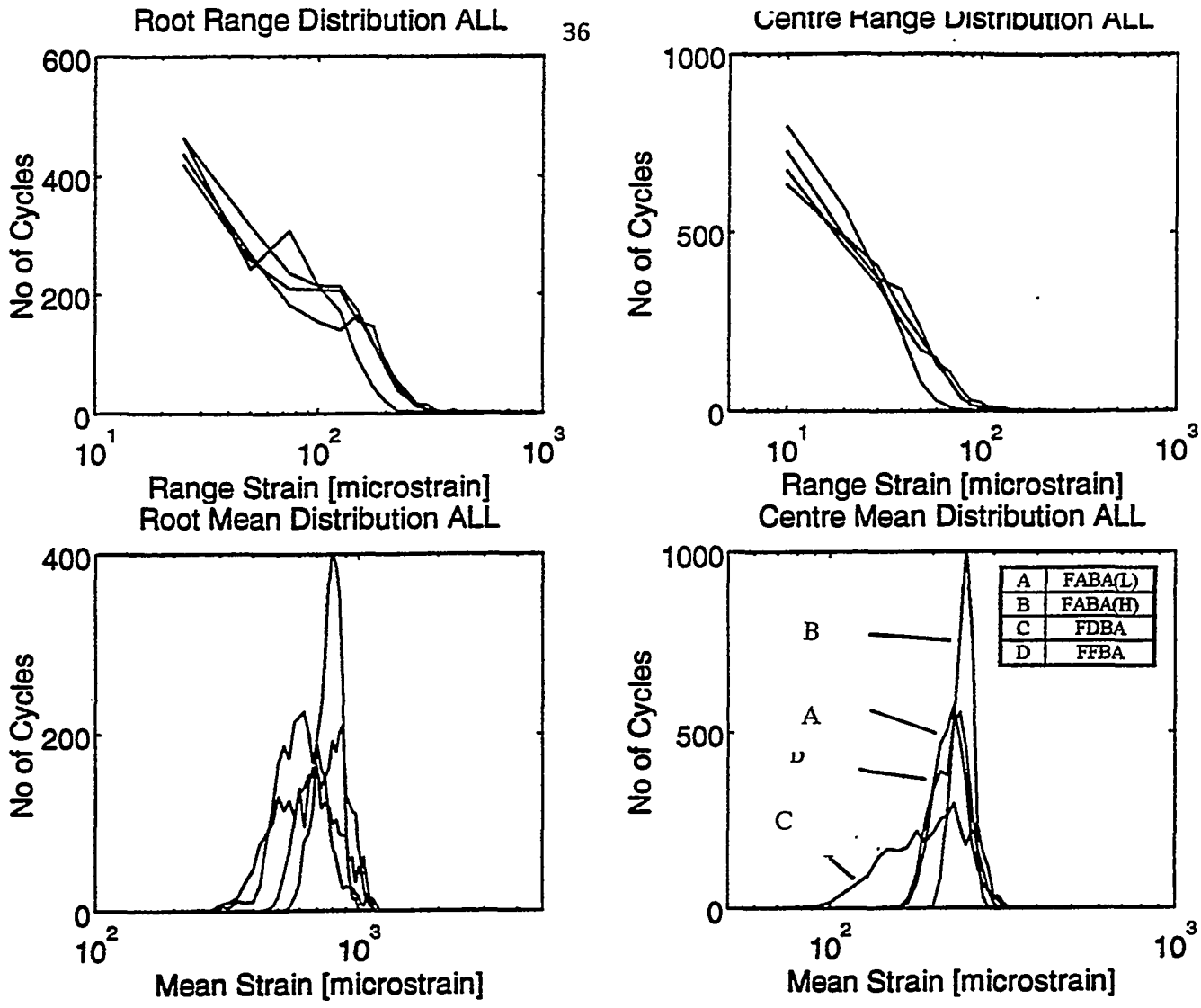

Figure 5 Comparison of Root and Centre Gauge 2D Rainflow Spectra in Different Strategies.

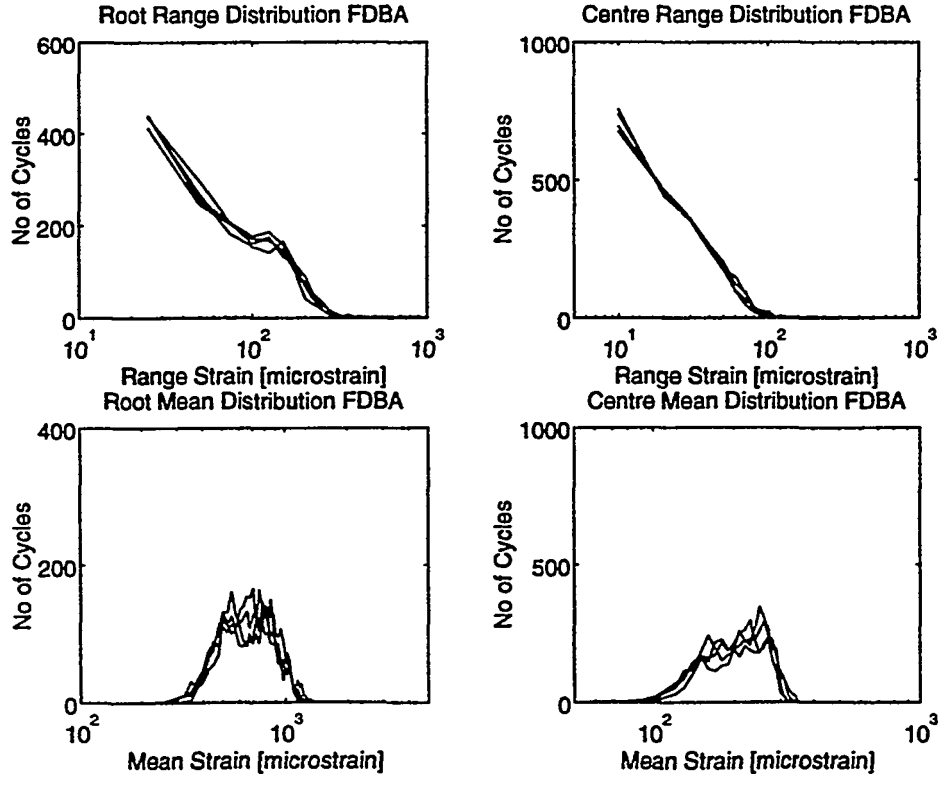

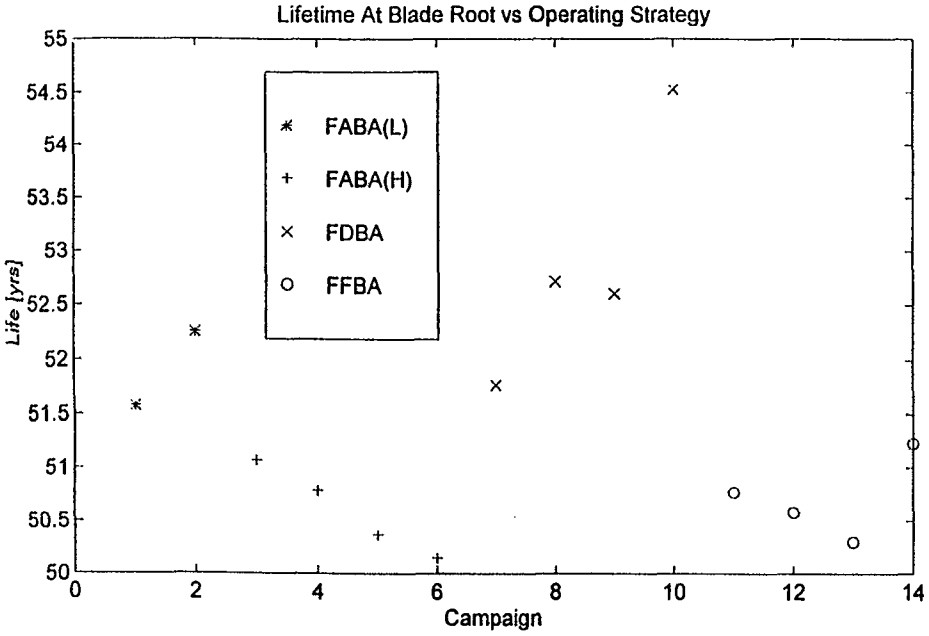

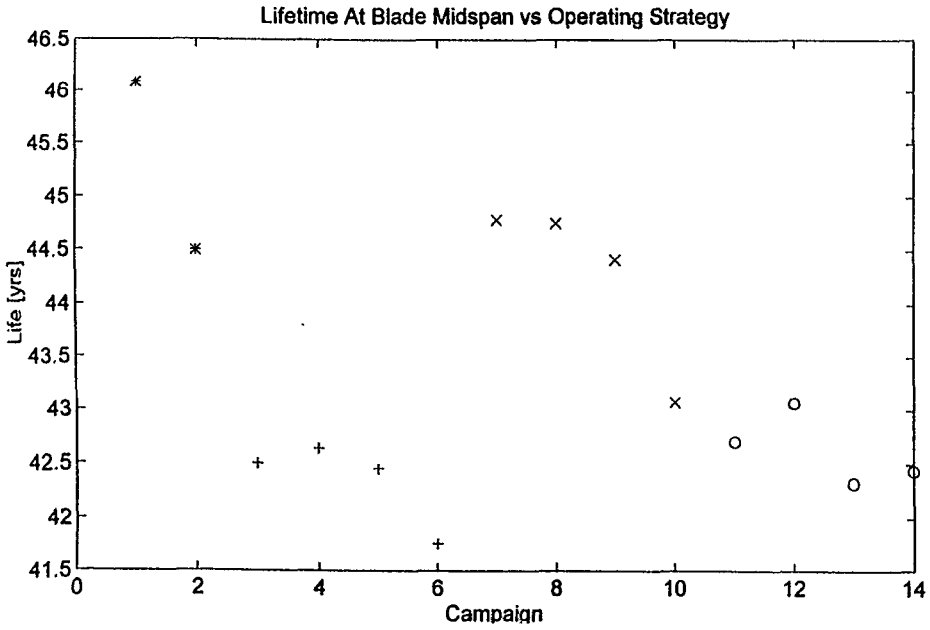

Figure 7 Projected Lifetimes In Different Strategies.

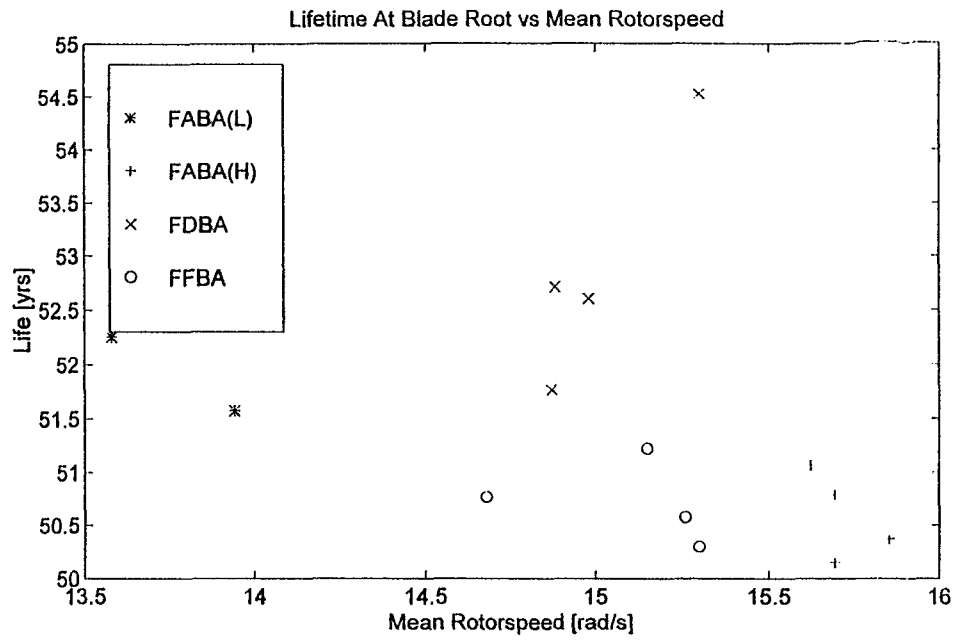

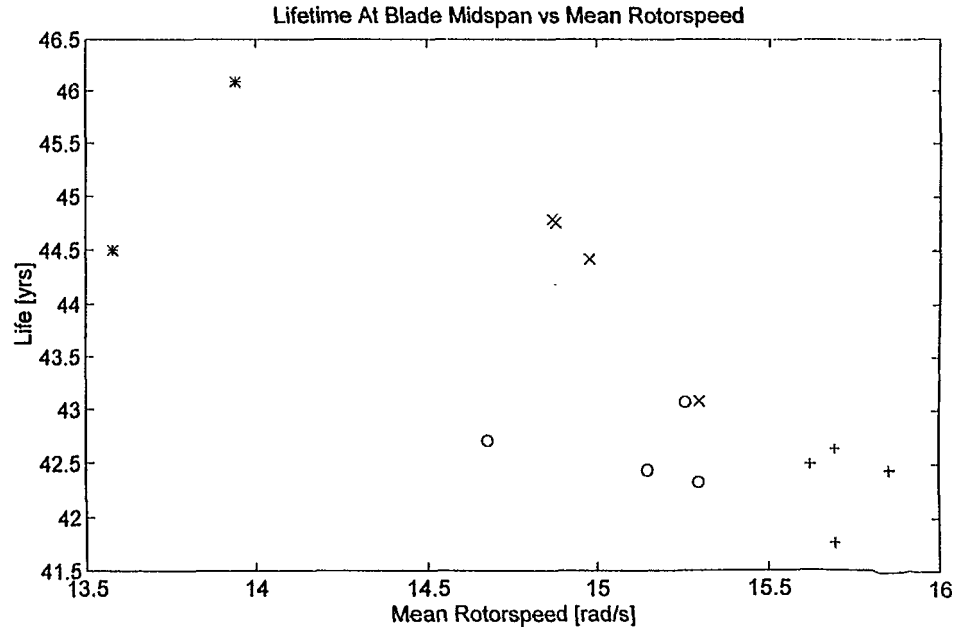

Figure 8 Influence of Mean Rotorspeed on Projected Lifetime.

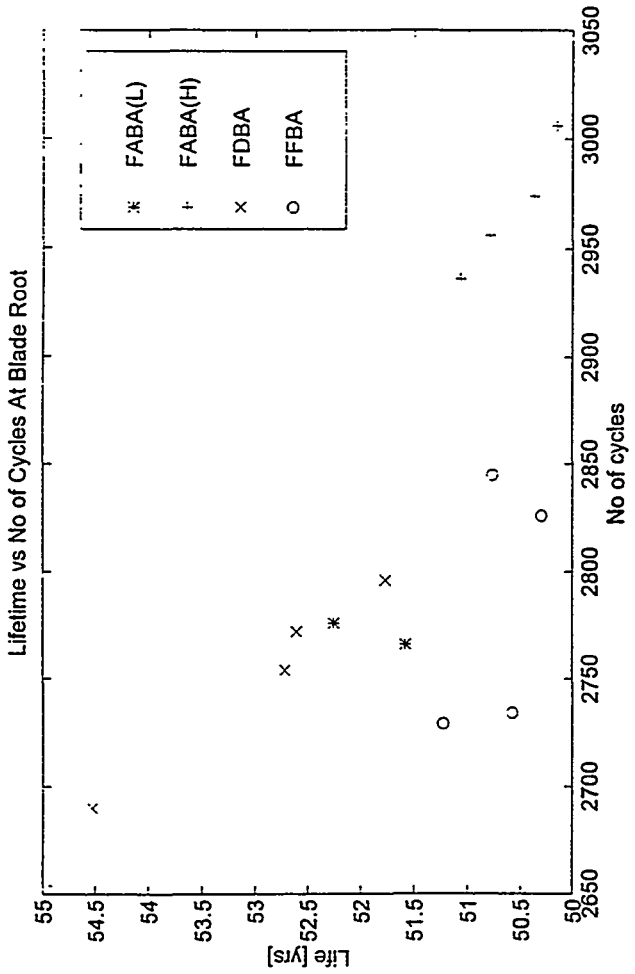

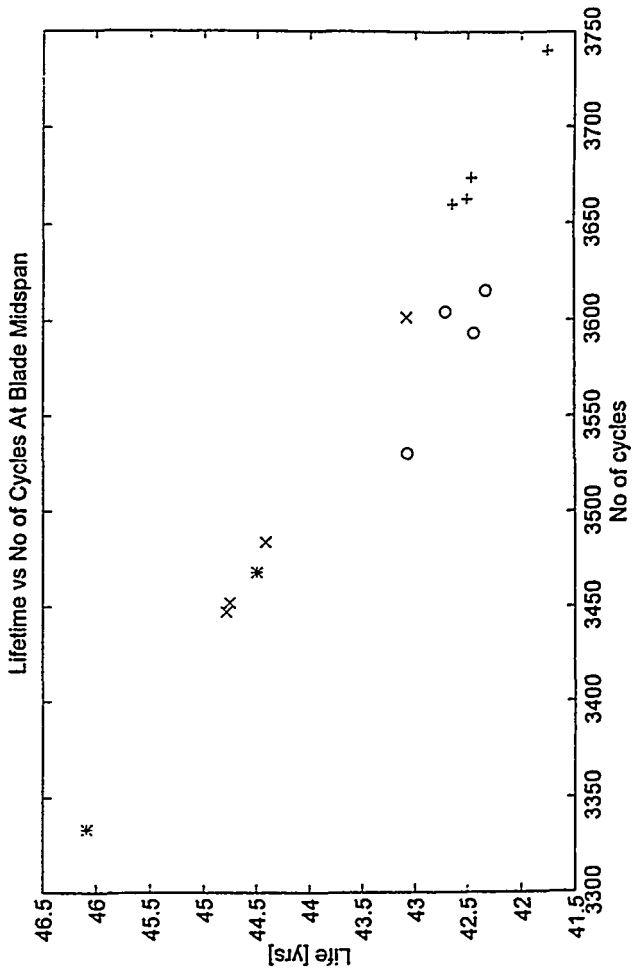

Campaign Name	Run ID	Mean Windspeed [m/s]	Mean Rotorspeed [rad/s]	Life at Root [yr]	Life at Centre [yr]	Lives Ratio [ ]
FABA40(L)	1	9.38	13.94	51.58	46.09	1.12
FABA42(L)	2	7.64	13.58	52.26	44.50	1.17
FABA51(H)	3	8.07	15.62	51.07	42.50	1.20
FABA52(H)	4	8.80	15.69	50.79	42.64	1.19
FABA57(H)	5	8.65	15.86	50.37	42.46	1.19
FABA60(H)	6	7.59	15.69	50.15	41.76	1.20
FDBA51	7	10.78	14.87	51.77	44.79	1.16
FDBA54	8	10.92	14.88	52.72	44.76	1.18
FDBA56	9	10.16	14.98	52.61	44.42	1.18
FDBA58	10	10.01	15.30	54.53	43.08	1.27
FFBA58	11	10.28	14.68	50.77	42.71	1.19
FFBA68	12	9.19	15.26	50.58	43.07	1.17
FFBA69	13	9.64	15.30	50.30	42.33	1.19
FFBA70	14	9.99	15.15	51.23	42.44	1.21

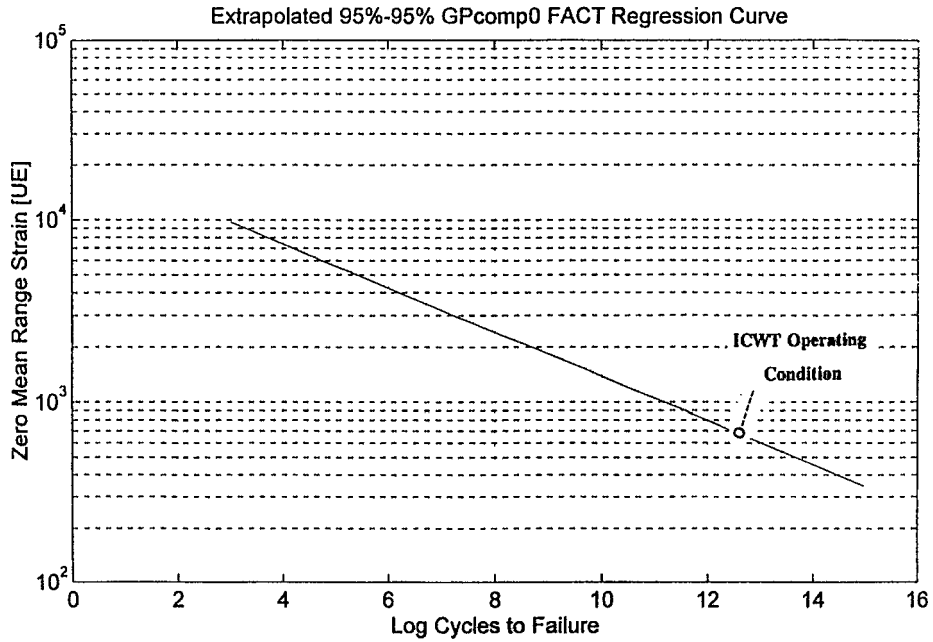

Figure 10 95%-95% Confidence εN Curve for Unidirectional Glass Polyester laminate at R=-1 (taken from [4]).

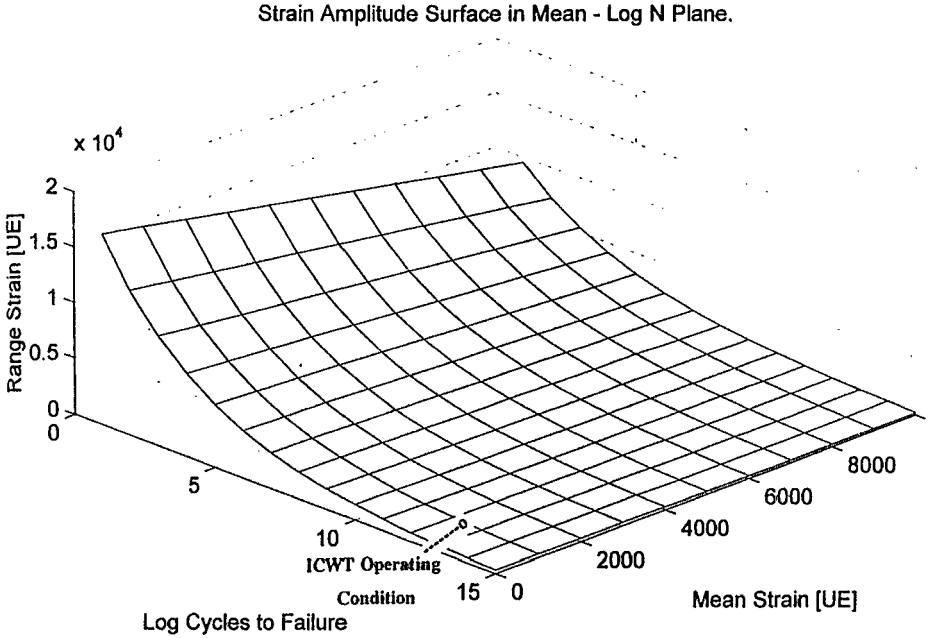

Figure 11 95%-95% Confidence Strain Amplitude Surface As Function of Allowable Cycles and Mean Strain Condition.

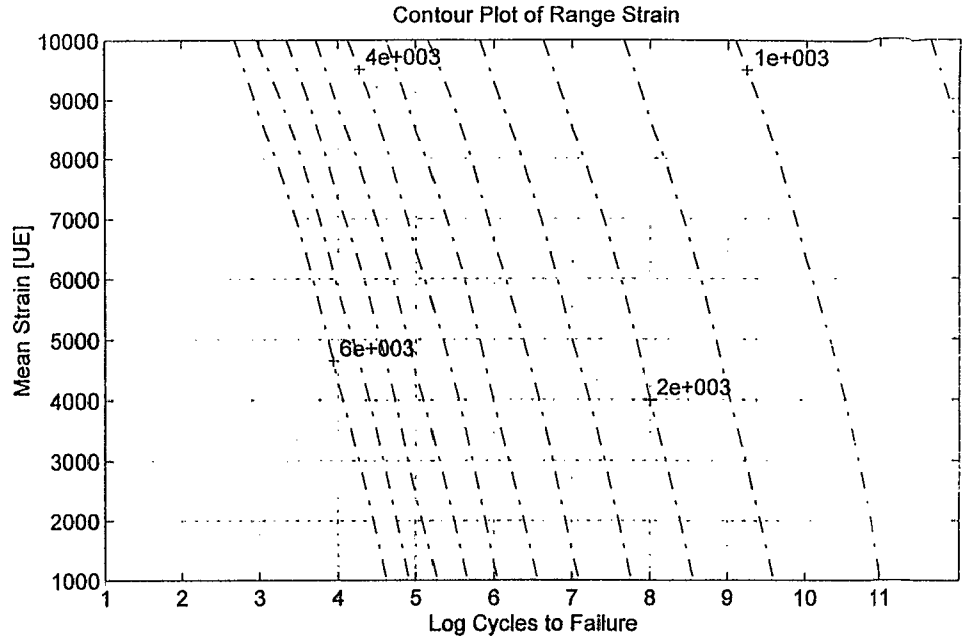

Figure 12. Contour Plot of Strain Amplitude Surface.

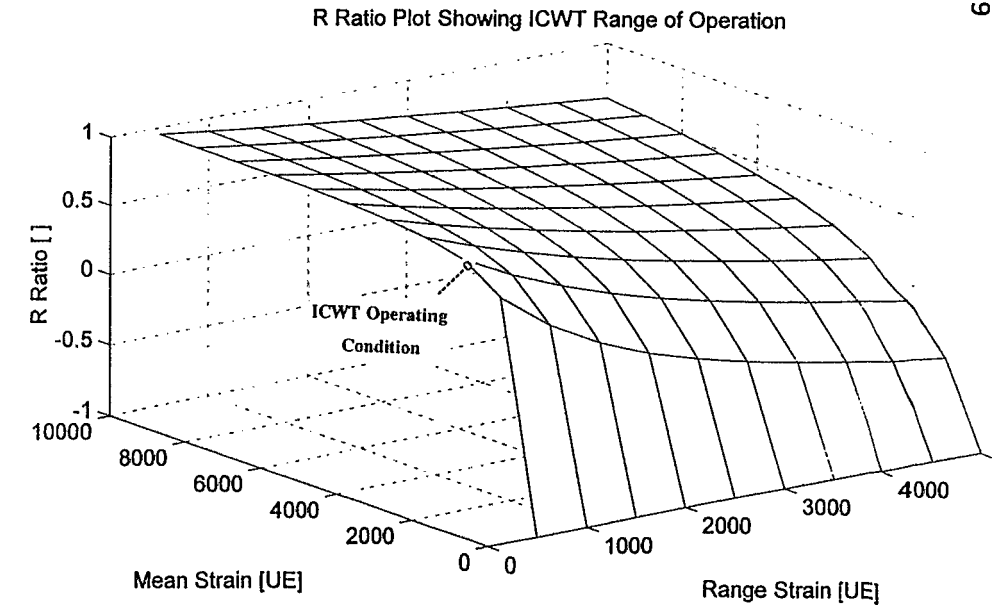

Figure 13. R Ratio of Operation of Blade in the Experiment.

Fatigue of Wind Turbines in the Frequency Domain

Dr NWM Bishop - University College London

Introduction

Fatigue damage is traditionally determined from time signals of loading, usually in the form of stress or strain. However, there are three design scenarios when a spectral form of loading is more appropriate. In this case the loading is defined in terms of its magnitude at different frequencies in the form of a Power Spectral Density (PSD) plot.

Firstly, the ***measurement engineer*** recording responses from in-service components or structures may be interested in PSD's because they are a very efficient way of defining a random stress or strain time history. By using a spectral description for the response of, say, an engine or suspension bracket, the requirement to collect and store large arrays of data can be avoided. In some situations the data might be collected and stored directly as PSD's, or alternatively a time series might be converted to a PSD using standard transformation techniques. Figure 1 highlights the equivalence between a time signal and its corresponding PSD. The transformation between ***time domain***, ie the time history of the loading, and the ***frequency domain***, ie a PSD, should not trouble the reader. The PSD simply shows the frequency content of the time signal and is an alternative way of specifying the time signal. It can be obtained from a time signal by utilizing the ***Fast Fourier Transform*** **(FFT).** Transforming from the frequency domain to the time domain is also a relatively easy task which can be done using the ***Inverse Fourier Transform*** **(IFT).** However, when transforming in this direction the random phase angles attributable to each frequency component have to be generated.

Secondly, the ***test engineer*** assessing the reliability of prototypes may be interested in spectral tools because such an approach allows the structural condition of the component to be monitored by continuous inspection of the system transfer function.

However, the most important benefit of working with PSD's is relevant to the ***structural analysis*** or designer because of the more sophisticated analysis options with which they can be used. In particular, dynamically responsive structures, or structures subjected to irregular loading patterns, can be efficiently and accurately analysed using a linear transfer function analysis to relate an input PSD of loading to an output PSD of response. Such approaches are widely used in nearly all engineering industries. The intercooler example shown in Figure 2 is one of many that could be used.

For all three of these design scenarios the fatigue designer is presented with a PSD of stress or strain with which to perform his fatigue calculation. There is therefore a requirement for a reliable, accurate and robust spectral fatigue design tool. Such a tool allows the designer to estimate the rainflow range content and hence fatigue damage from the PSD.

Technical background

The first serious effort at providing a solution for estimating fatigue damage from PSD's was undertaken by SO Rice (1954). He developed the very important relationships for the number of upward zeros per second (E[0]) and peaks per second (E[P]) in a random signal expressed solely in terms of their spectral moments m_n. The irregularity factor, a very useful term for characterising the type of structural response encountered, was defined as E[0]/E[P]. This means that it varies between 0 (so called white noise containing a broad range of frequencies) and 1 (a classical narrow band signal containing only one predominant frequency).

$$E[0] = \sqrt{\frac{m_2}{m_0}} \qquad E[P] = \sqrt{\frac{m_4}{m_2}} \qquad \gamma = \frac{E[0]}{E[P]} = \sqrt{\frac{m_2^2}{m_0 m_4}}$$

The relevant spectral moments are easily computed from a one sided PSD G(f) in units of Hertz using the following expression.

$$m_n = \int_0^\infty f^n \, G(f) \, df$$

JS Bendat (1964) developed the theoretical basis for the so called ***Narrow Band*** solution. Again this expression was defined solely in terms of the spectral moments up to m_4. However, the fact that this solution was suitable only for a specific class of response conditions was an unhelpful limitation for the practical engineer.

Sherratt and Dirlik (Dirlik -1985) and then Sherratt and Bishop (1989, 1990) undertook much useful work in extending these restricted solutions during the period 1975 to 1990. This research work solved many of the theoretical problems which existed. In particular a theoretical solution was obtained to estimate rainflow ranges of stress or strain from any class of PSD.

However, many potential recipients of the technology were undoubtedly put off by the complexity of the techniques. Furthermore, implementation of the theoretical work into usable software was itself a complicated process with many potential numerical instability and inaccuracy pitfalls for the unsuspecting software writer. Because of this, work since 1990 has concentrated on making the techniques more widely applicable to the practical engineer (see for instance, Bishop - 1991, 1994, 1995). The rest of this article therefore addresses the application of this theoretical work using state of the art techniques. No theoretical background is provided since this is readily available in the references.

When should the techniques be used?

The fatigue designers task can be conveniently separated into ***response prediction*** and ***fatigue prediction*** as shown below. Both response and fatigue prediction will either be carried out in the time domain (ie, conventional stress or strain time series analysis) or in the frequency domain (ie using PSD's for the stress and strain information). The correct choice between time or frequency domain will be influenced by a number of issues which are primarily dependent on the type of analysis to be performed, ie, [A], [B] or [C] below. There are also a number of considerations which are relevant to the fatigue prediction stage [D]. These issues are discussed below.

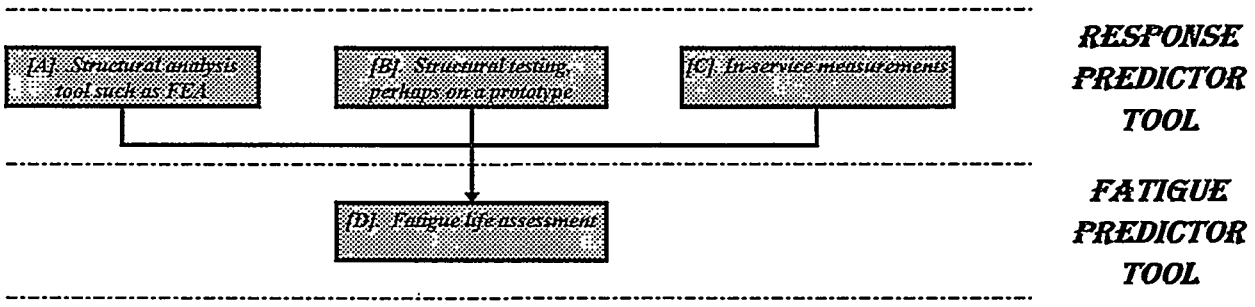

[A]. Fatigue analysis with responses estimated using analytical or computational models such as Finite Element Analysis

An important question facing the designer is what are his analysis options? It may be that because of the nature of the structure being analysed the analysis route is already determined. For instance, many deepwater offshore oil platforms can only be satisfactorily designed in the frequency domain, thereby producing frequency domain results. In this case a frequency based fatigue calculation is the only option. Alternatively, the nature of the fatigue damage mechanism, or the structural system, may determine that only a time based approach is applicable. If either of these scenarios is true then the correct approach is already defined. However, there is often a choice and it is always worth considering if a frequency based analysis, perhaps in parallel with a time based approach, may provide an enhanced analysis capability. A recent analysis (Bishop et al, 1995) of an engine intercooler highlighted just such a situation where the analysis was considerably enhanced by the inclusion of a frequency based approach.

In general, for any system, there are three main analysis options as described below. Figure 2 highlights these options for the engine intercooler.

Deterministic (steady state). This is the most common type of analysis where the response of a structure to a deterministic, usually a sine wave, loading function is found. This type of analysis is severely limited for random or irregular loading functions because of its inability to properly characterise the true nature of the loading history.

Time domain (transient). In a world with infinitely powerful computers this would be the ideal form of analysis because the truly random nature of the loading can be retained and non-linearities can be catered for. Its main, and important, limitation is that because it is so computationally expensive it is not really suitable as a fast design tool.

Frequency domain (spectral). For systems which are not too non-linear (see next section) this approach offers all the advantages of the transient approach whilst being as fast as the deterministic method. In many design situations it is therefore an attractive option.

A very important question, if a spectral approach is being considered, concerns system linearity. In order to obtain the output (PSD) response of any system we need its ***transfer function***. This transfer function has to obey the following,

This is the basis of any frequency based structural analysis including FEA. Fortunately, even non-linear systems can often be linearised for certain operating conditions, thereby enabling a frequency based approach to be used.

[B]. Fatigue analysis with loads obtained from a prototype such as a test vehicle

If laboratory tests are being undertaken an important question is do the results need to be compared with, for instance, FEA results? The intercooler example demonstrates that frequency based FEA can be a powerful qualitative as well as quantitative tool for the reliability assessment of certain components. If this is likely then frequency based tests and fatigue calculations may be appropriate.

Another important question might be is any structural condition monitoring required, or beneficial? Frequency based measurements are very useful for determining any changes in structural behaviour or performance. Any change in the system transfer function is a useful indicator that some structural change has taken place, such as the growth of a crack. If such structural monitoring is likely to be beneficial then frequency based tests and fatigue calculations may be appropriate.

[C]. Fatigue analysis with loads measured directly from in-service components

If loads are being measured directly from in service components, are data storage problems likely to be an issue, either in terms of hard disk space or speed of acquisition? An acquisition rate of one fifth of that for time domain measurements can usually capture the frequency domain data required for a fatigue analysis with the same level of accuracy. Furthermore, there can also be a significant reduction in storage space required for the frequency domain data. For instance, a PSD can usually be characterised using approximately 1000 points. On the other hand, a truly random time signal may need 100,000 points or more for the same level of accuracy in the fatigue calculation.

[D]. Fatigue life assessment

An important and difficult question for the design engineer is concerned with whether the engineering process is stationary, Gaussian and random. Firstly, on the question of how Gaussian (sometimes referred to as 'normality') particular data is. If we calculate the percentage of time that response data spends within a particular stress bin and plot this as a ***probability density function*** **(pdf)** we require that its pdf follows the ***Gaussian*** bell shape. Fortunately there is a theoretical explanation to explain why nearly all engineering components and structures exhibit Gaussian behaviour. This is called the ***Central Limit Theorem.*** This states, in very general terms, that the response of any system will be Gaussian as long as the number of processes contributing to this system response is reasonably large and that no one process dominates. This is true even if the individual processes are not Gaussian. Practical fatigue calculations have shown that the fatigue predictor tool used for this article is quite robust to some variation from a strictly Gaussian signal (see Bishop et al 1994).

If the signal is ***stationary*** it means that the general characteristics, such as rms, don't change with time. For most engineering processes this is true. Furthermore, even where the signal characteristics are changing slowly with time the complete response process can usually be broken up into a number of shorter stationary processes.

Finally, and perhaps most importantly, is the signal ***random***? If it isn't then a time based approach is likely to be the best approach. For instance, if a small number of transients dominate the fatigue damage then it is almost impossible for a frequency based fatigue predictor to properly identify these. This is an example, referred to in the Central Limit Theorem, where one process dominates the rest. If such transient or deterministic inputs are relatively small, in comparison to the rest of the response data, then a frequency based calculation may still be possible.

Irrespective of the above issues it is still worth considering if the advantages of working in the frequency domain outweigh any possible errors. If a frequency based fatigue predictor is coupled up with a frequency based load predictor, such as an FEA program, then a designer has the ability to undertake rapid design optimisation. He may then choose to use a time based calculation for the final 'proving' analysis calculation. In such a case any loss of accuracy involved in working in the frequency domain is far outweighed by the increased design capability. This is therefore something which should be carefully considered.

A simple worked example.

In order to illustrate the mechanism of spectral fatigue calculations it is worth performing some simple hand calculations on the PSD shown in Figure 3. Approximate hand calculations have been performed in both the time and frequency domains. The results from the hand calculations have then been compared with the results from a proprietory software package called *FATIMAS-SPECTRAL* which has been developed by nCode International.

Hand calculation in the time domain. An approximate visualisation of the original time signal can be obtained by adding together two sine waves, one for each block in the PSD, where the amplitude of each is obtained (approximately) from 1.41 times the root mean square (rms) value. And since the rms of each block can be calculated (approximately) from its area we get the following stress ranges, as shown in Figure 4.

Sine wave 1 at 1Hz with a stress range of $\sqrt{10000}$ **x 1.41 x 2 = 282MPa**
Sine wave 2 at 10Hz with a stress range of $\sqrt{2500}$ **x 1.41 x 2 = 141MPa**

If we use a typical steel with S-N data of the form $N = 1.0E+15 * S^{-4.2}$ we get

N(141MPa) = 9.4E+5 **N(282MPa) = 5.1E+4**
N(315MPa) = 3.2E+4 **N(423MPa) = 9.3E+3**

An approximate Palmgren-Miner damage calculation on the time signal then gives;

$$E[D] = \frac{10}{9.4E+5} + \frac{1}{9.3E+3} = \mathbf{1.18E\text{-}4}$$

This corresponds to a fatigue life of ***8462 secs***

Hand calculation in the frequency domain. Moments can be computed easily from the PSD using the expression given earlier.

$$m_n = 40000 * 1^n * 1 + 10000 * 10^n * 1$$

$m_0 = 12\,500$ $m_1 = 35\,000$ $m_2 = 260\,000$ $m_4 = 25\,010\,000$

From which we can compute
E[0] = 4.6 upward zero crossings per second and
E[P] = 9.8 peaks per second
$\gamma = 0.465$
rms = $\sqrt{m_0}$ **= 112 MPa**
An equivalent sine wave magnitude = 112*1.41*2 = **315MPa**

$$\mathbf{E[D]} = \frac{9.8}{3.2E+4} = \mathbf{3.1E\text{-}4}$$

This corresponds to a fatigue life of ***3265 secs***

Note: This calculation is based on representing the constant frequency varying amplitude function with a sine wave.

Frequency domain calculation using FATIMAS-SPECTRAL.

The following results were obtained using the nCode software package.

Fatigue life using Narrow Band formula = ***1472 secs***
Fatigue life using Dirlik = ***7650 secs***

A more advanced example

The above calculation is useful for the practical designer as a means of identifying the steps involved in a frequency domain fatigue calculation. Since very close agreement between the various results would not be expected a more rigorous assessment of the techniques has been undertaken by applying the tools to a variety of engineering systems including, for example, automotive components, wind turbine blades, agricultural machinery and offshore platform joints. Results have shown that the tools are surprisingly accurate and robust for a wide range of applications. As an example a random time signal of length 5000 seconds has been analysed using ***FATIMAS-SPECTRAL.*** A representation of the time signal, and its PSD computed using standard FFT techniques, is given in Figure 1. The following results were obtained for a CLASSB weld specification.

Fatigue life estimate using rainflow counting etc.....	**Time domain**	-	***20.48 Hours***
Fatigue life (frequency domain) using	**Dirlik solution.**	-	***18.07 Hours***
	Narrow Band solution	-	***10.58 Hours***
	Tunna solution	-	***59.10 Hours***
	Wirsching solution	-	***13.30 Hours***
	Hancock solution	-	***16.26 Hours***
	Kam and Dover solution	-	***20.16 Hours***
	Steinberg solution	-	***9.91 Hours***

The choice of frequency domain solution will depend on the industrial application involved as well as the desired level of accuracy. Generally the Dirlik solution has been found to give the best results when compared with the corresponding time domain result. This is particularly true if the data is not truly Gaussian, stationary and random (see for instance Bishop et al - 1994). Further research work is ongoing at UCL, in partnership with nCode International, to look at mixed deterministic and random signals and more generally non-Gaussian signals. Any new advances which are made with the research will in due course, be incorporated into ***FATIMAS-SPECTRAL***.

References

- Rice, SO. (1954). Mathematical analysis of random noise. Selected papers on noise and stochastic processes, Dover, New York.
- Bendat, JS. (1964). Probability functions for random responses. NASA report on contract NAS-5-4590.
- Dirlik, T. (1985) Application of computers in Fatigue Analysis, University of Warwick Thesis, 1985.
- Bishop, NWM and Sherratt, F. (1989). Fatigue life prediction from power spectral density data. Part 1, traditional approaches and Part 2, recent developments. Environmental Engineering, Vol.2, Nos. 1 and 2.
- Bishop, NWM and Sherratt, F. (1990). A theoretical solution for the estimation of rainflow ranges from power spectral density data. Fatigue Fract. Engng. Mater. Struct., 13 no.4,.
- Bishop, NWM (1991). Dynamic fatigue response of deepwater offshore structures subjected to random loading, Structural Engineering Review, SER 76/11.
- Bishop, NWM et al. (1994). Methods for the rapid fatigue evaluation of fatigue damage on the HOWDEN HWP330 wind turbine, BWEA Conference, York.
- Bishop, NWM, Lack, LW, Li, T, and Kerr, S.. (1995). Analytical fatigue life assessment of vibration induced fatigue damage. Paper presented to MSC World Users Conference, Universal City, Los Angeles.

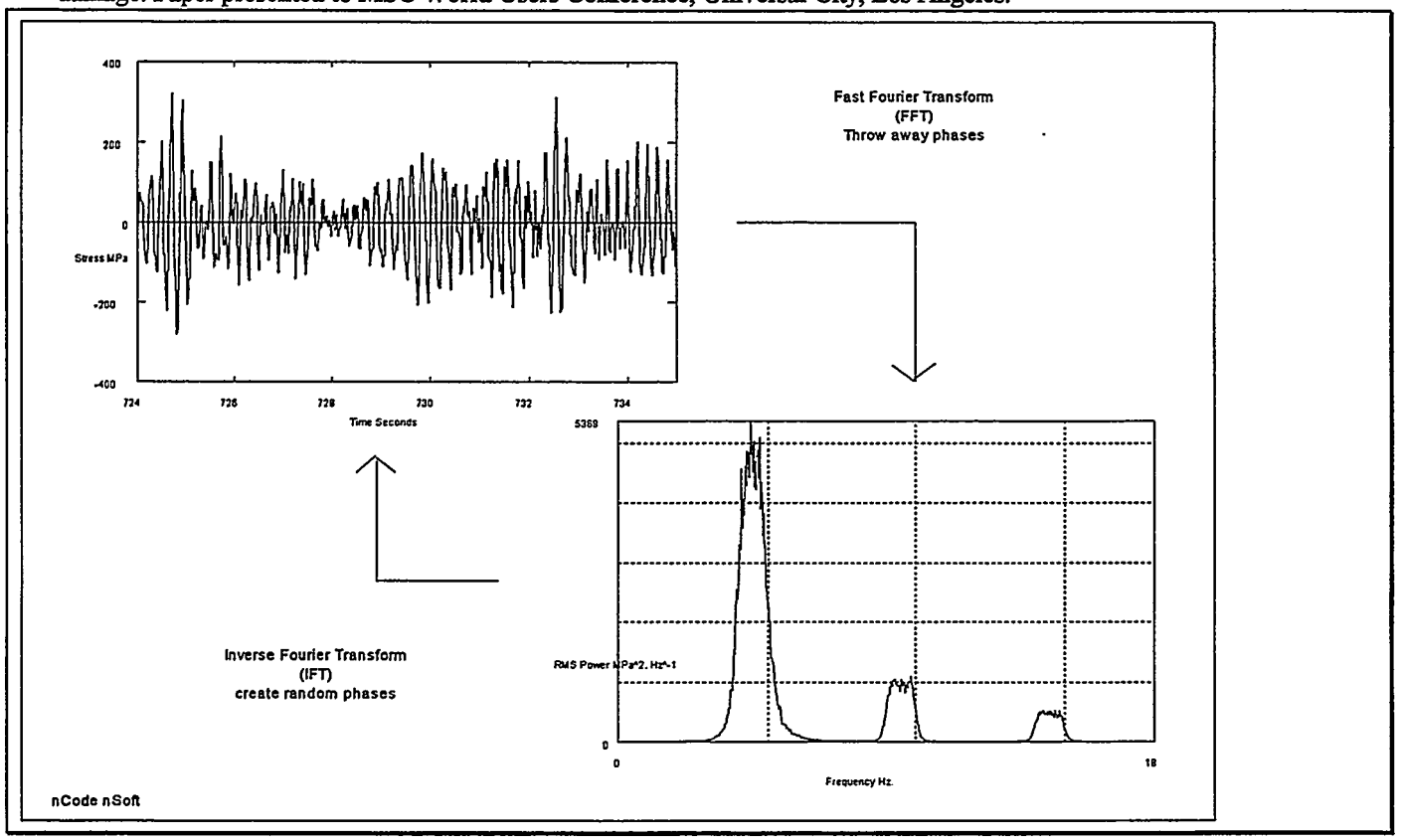

Figure 1. The relationship between a PSD and its equivalent time signal

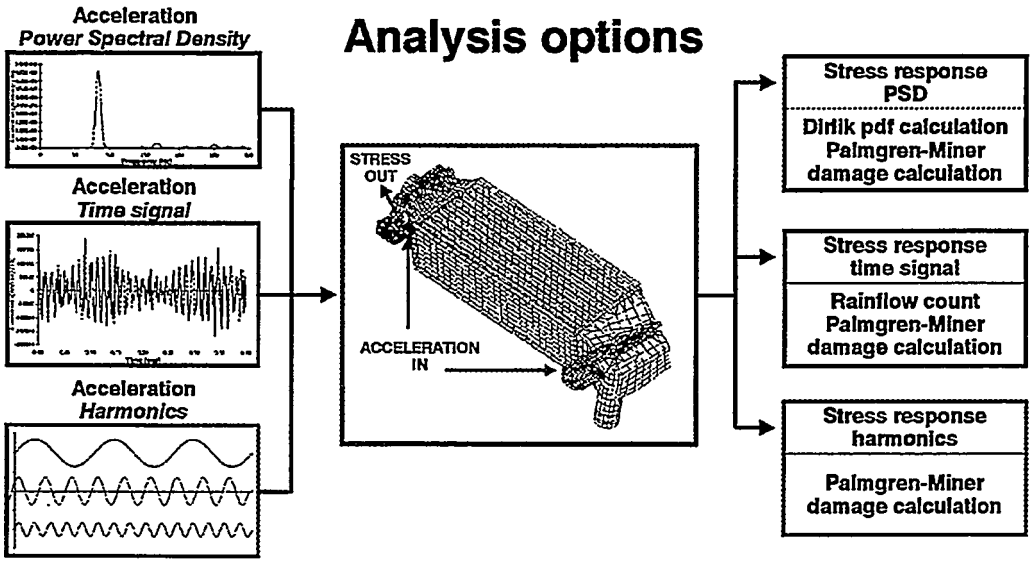

Figure 2. The analysis options available to the design engineer (see Bishop et al - 1995)

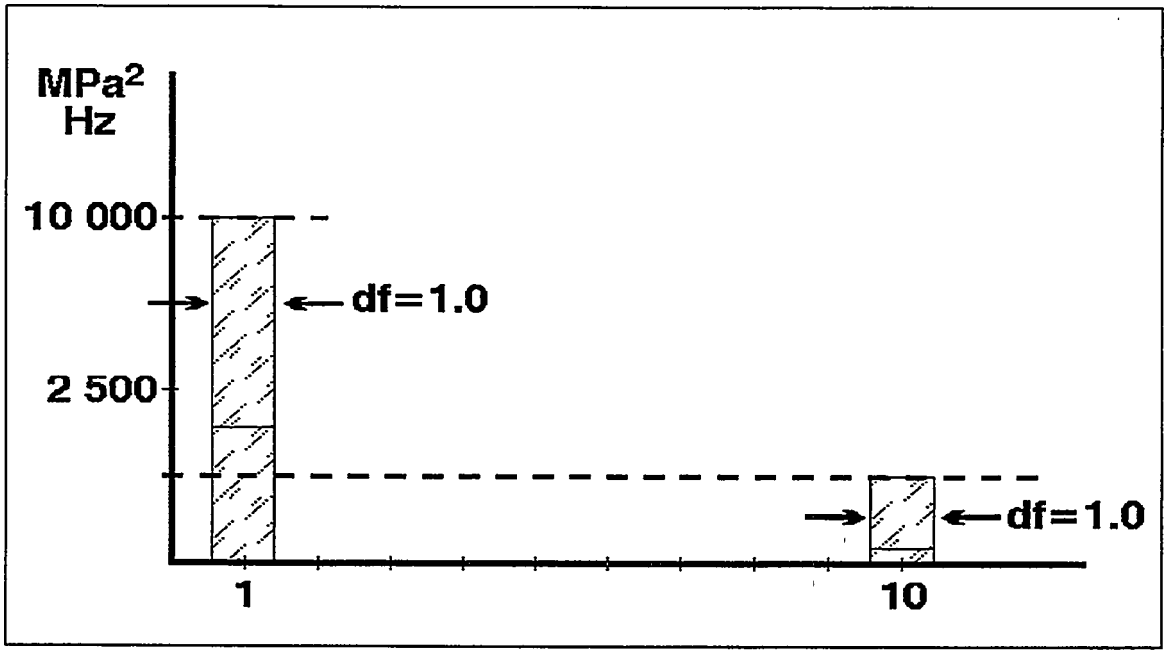

Figure 3. A simple two peaked PSD used to perform hand calculations

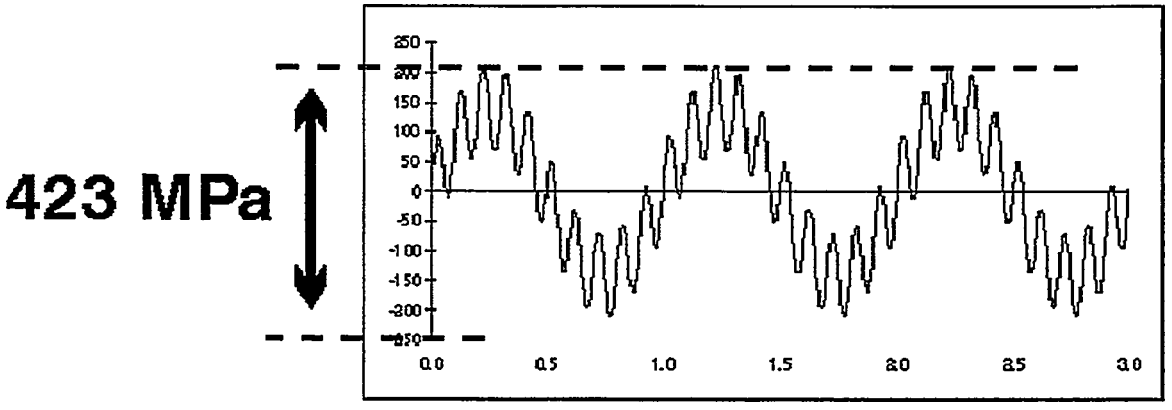

Figure 4. The sum of a sine wave at 1Hz with range 282MPa and sine wave at 10Hz with range 141MPa

4. Symposium on Wind Turbine Fatigue
held at DLR Stuttart, Germany, 1. -2. February 1996

Holger Söker, Deutsches Windenergie-Institut

Rainflow Counting Revisited

Introduction

Based on DEWI's working experience in the field of wind turbine fatigue and by taking a look across the borders of wind energy industry into automotive engineering this paper tries to highlight the author's ideas as of how load spectra generation for use in wind turbine design and testing may be enhanced.

DEWI's background in wind turbine fatigue is focussed on measurements of load spectra using on line monitoring methods[1]. The objective of this work is to verify calculated load spectra with actual measurements and this way to add to the knowledge of wind turbine fatigue behaviour. An underlying intention is to complement complex numerical simulation methods with easy to use and cost efficient, standardized measurement and evaluation methods.Beside the compilation of a rather simle and robust measurement technique emphasis has been placed on the identification of key parameters that govern the loading situation of a wind turbine component using statistical methods.

As state of the art method the rainflow counting technique is presently applied everywhere in fatigue analysis. However, the author feels that the potential of this technique is not fully recognized in wind energy industries as it is used, most of the times, as a mere data reduction technique disregarding some of the inherent information of the rainflow counting results. The ideas described in the following aim at exploitation of this information and making it available for use in the design and verification process.

Why is Rainflow Counting Used?

As a starting point it seems to be wise to recollect the major characteristics that made rainflow counting the most commonly used method for statistical evaluation of load time histories in fatigue analysis.

Since the development of this cycle counting technique it has found wide acceptance for its appreciation of the actual behaviour of material under cyclic loading. The technique virtually decomposes a given load time history in load cycles corresponding to the stress - strain hysteresis cycles as seen by the material. A special feature is that large cycles engulfing smaller ones are detected and counted as well simulating the material's ability to memorize these big cycles. As a two parametric counting technique it retains not only the range and average value of the analysed load cycles, but also their direction i.e. upward or downward pointing load cycles.

The most important characteristics of rainflow counting are:

damage equivalence:	two time series that result in the same RC-result are equivalent with respect to the damage they cause
data reduction:	the technique has capability for strong data reduction enabling its user to store, handle and evaluate large amounts of data
simplicity:	its algorithm is easily implemented in computer code and the presentation schemes are easily interpretable, once fully understood
reconstruction:	rainflow data allows for reconstruction of time series from the reduced data
real time contraction:	methods for construction of a shortened time series that is damage equivalent to the original time series are available
extrapolation:	the technique allows for extrapolation and superposition

In Europe's wind energy community only the data reduction capability of RC is fully recognized and put to use.

DEWI

What are the problems in fatigue load estimation?

To arrive at dependable load estimates basically two approaches are possible: load calculation by means of complex numerical simulation (time or frequency domain) or estimation on the bases of rather simply calculated parameters and a model for the expected load characteristics. The first alternative needs costly labour (time domain) and highly specified skills on the side of the design engineers. The latter method is a lot less demanding with respect to labour and complexity, however, it needs some inbuilt conservatism in order to make up for uncertainty in the estimation model. At this point it should be realized that there is *not* a decision to be met regarding which of both ways should be chosen. We should rather be interested in finding a way to make available methods complement each other. Such a way should establish a reasonably conservative load description and at the same time enhance design speed and cost effectiveness.

Generally, any estimation method is based on experience i.e. knowledge from the past and a way of extrapolating it into the future by means of qualified gesses. To make experience from the past efficiently accessable, most of the time, some statistical processing of the information will be necessary. The type of statistical process employed should correspond to the nature of the data processed and to the sort of result needed. Now, looking at the above mentioned characteristics of rainflow counting it becomes clear why it has become such a powerful technique.

High quality sources of experience are measurements, given that the measurement data are reliable and have actually been evaluated. In the case of load measurements data varification and evaluation are the cost driving activities which lead to rather expensive measurement campaigns. This is why such measurements are triggered in R&D projects as well as in the wind turbine certification process when there is either subsidies involved or the high cost are outweighed by the risc of failure. Due to the variety of employed measurement systems and sometimes very specific objectives, the data structure varies greatly. In case of certification measurements accessability of data is, of course, restricted due to the competitiveness of the market. As a consequence many measurements cannot be further evaluated but are burried in the archives.

When discussing the usefulness of measurements the questions of transferability of the measurements to other sites, other external condtions and/or other wind turbine concepts arise. Here a lack of experience with respect to the governing physical as well as mathematical parameters of fatigue characteristics (s.a. wind speed, turbulence, wind direction, wind shear, dimensions, masses, inertia, control system) becomes obvious. Some of these parameters are known to be of importance, but their effects on wind turbine fatigue loading are sometimes not well understood. Mathematical parameters associated with the statistical model used could be of the Weibull -type: scaling and form parameters. To the author's knowledge a comprehensive set of these parameters is lacking up to date. Thus measurements are often one-way products: they are used for one purpose only.

What is the Cure

A cure for the problems quoted above could be a better exploitation of the benefits offered by the rainflow counting technique:

With respect to the measurement technique the implication is to use automatically operating systems that reduce data on-line. Such a system should feature techniques for detection and repair of erroneous data - this could be done possibly employing an expert system that has the available knowledge on data plausibility encoded.

Once data quality is assured, the rainflow counts must be evaluated, aiming at developing a thorough understanding of the pattern to be found. Typical pattern of the counts can be expected due to the fatigue loading characteristics of the measured load quantity. Depending on the load quantity that is measured, the external conditions and the wind turbine configuration (geometry as well as control strategy) typical counts will be produced by the method. Also transients from a given state of operation to another will show this model character and even erroneous data will probably form destinct pattern in the rainflow counts.

DEWI

Possible Action

Adopting the above philosophy as a complement to numerical simulations and time series measurements, a possible action is to start a data base of rainflow counts for a set of qualifying loads (s.a. recommended by the IEA-Recommended Practises for Wind Turbine Testing and Evaluation 3. Fatigue Loads [2]). For each of these loads the gathered counts should be sorted for external conditions, wind turbine configuration as well as external conditions. The objectives of such an action must be:

- find the scaling and shape parameter for the rainflow counted fatigue load distributions (which are known to be mixtures of Weibull distributions) and examine their relation to actual physical parameters (s.a. wind speed, turbulence, wind direction, wind shear a.s.o.) and turbine design parameters (s.a. dimensions, masses, inertia, control system a.s.o.)

- determine the proper time scale of the rainflow counts i.e. are they to be expanded to periods of 10 minutes, hours, days, weeks or even months in order to enable a good estimate of the wind turbines duty cycle

- develop a method to setup and extrapolate comprehensive fatigue load spectra from that data base

Conclusion and Perspective

The described ideas have evolved from the working experience of DEWI spiced up with loans from automotive engineering where these methods are already applied [3]. To the author's mind there is nothing wrong with adopting already existing know-how for use in wind energy, even if there might be a *natural* dislike of that *conservative* industry on the side of the wind energy engineers.

The suggested data base and associated methods to synthesize fatigue load spectra could be of great value in the begin of the design process, where the designer needs some estimate to start with. Of course the further design work cannot do without aeroelastic simulation or even load measurements. However, their amount might be diminished, saving money and labour. More than that, the opportunity for small enterprises with rather limited financial background to still be able to develop wind turbines may be ensured in future.

References

[1] Söker, H (editor): Monitoring Fatigue Loads on Wind Turbines Using Cycle Counting Data Acquisition Systems: Final report of Joule 2 contract no. JOU2-CT92-0175 for the Commission of the European Union, Directorate General XII for Science, Research and Development / DEWI Deutsches Windenergie-Institut (Wilhelmshaven) (Editor). Wilhelmshaven, Germany, 1995.

[2] P.H.Madsen e.a., Recommended Practices P. H. Madsen e. a.: Recommended Practices for Wind Turbine Testing, 3. Fatigue Loads 2. Edition 1990, Submitted to the Committee of the International Energy Agency Programme for Research and Development on Wind Energy Conversion Systems.

[3] N.N.: "Rainflow"-das Signalanalyseverfahren der Betriebsfestigkeit. Haus der Technik e.V. (editor): Proceedings of a workshop held at Essen, 2-3 March 1993.

JOU2-CT92-0175

MONITORING FATIGUE LOADS ON WIND TURBINES USING CYCLE COUNTING DATA ACQUISITION SYSTEMS

FINAL REPORT

H.SÖKER (EDITOR)

JULY 1995

Participants

Germany	Deutsches Windenergie-Institut (DEWI)	H.Seifert H.Söker T.Kramkowski	(Resp. Scientist)
Greece	Center for Renewable Energy Sources(CRES)	A.Fragoulis P.Vionis D.Foussekis	(Resp. Scientist)
Sweden	The Aeronautical Research Institute of Sweden (FFA)	J.A.Dahlberg M.Poppen	(Resp. Scientist)

ABSTRACT

As in any industrial application, the duration of a wind turbine's life is a key parameter for the evaluation of its economic potential. Assuming a service life of 20 years, components of the turbine have to withstand a number of load cycles of up to 10^8. Such numbers of load cycles impose high demands on the fatigue characteristics of both, the used materials and the design. Nevertheless, fatigue loading of wind turbine components still remains a parameter of high uncertainty in the design of wind turbines. The specific features of these fatigue loads can be expected to vary with the type of turbine and the site of operation. In order to ensure the reliability of the next generation of larger scale wind turbines improved load assumptions will be of vital importance.

Within the scope of the presented research program DEWI, C.R.E.S. and FFA monitored fatigue loads of serial produced wind turbines by means of a monitoring method that uses on-line cycle counting techniques. The blade root bending moments of two pitch controlled, variable speed wind turbines operating in the Hamswehrum wind farm, and also that of a stall controlled, fixed speed wind turbine operating in CRES' complex terrain test site, were measured by DEWI and CRES. In parallel FFA used their database of time series measurements of blade root bending moments on a stall controlled, fixed speed turbine at Alsvik windfarm in order to derive semi-empirical fatigue load data.

The experiences gained from application of the on-line measurement technique are discussed with respect to performance, data quality, reliability and cost effectiveness. Investigations on the effects of windfarm and complex terrain operation on the fatigue loads of wind turbine rotor blades are presented.

SUMMARY

This report describes the work and the results of the project MONITORING FATIGUE LOADS ON WIND TURBINES USING CYCLE COUNTING DATA ACQUISITION SYSTEMS which was carried out by DEWI, CRES and FFA within the framework of the JOULE II research and development program on non nuclear energy of the European Commission. The contributions of DEWI and CRES were co-funded by the European Comission through a contracted 50% reimbursement of the estimated total cost (contract: JOU2-CT92-0175). The work was carried out by the following participants:

Germany	Deutsches Windenergie-Institut (DEWI)	H.Seifert	(Resp. Scientist) (General Project Manager)
		H.Söker	
		T.Kramkowski	
Greece	Center for Renewable Energy Sources(CRES)	A.Fragoulis	(Resp. Scientist)
		P.Vionis	(CRES Project Manager)
		D.Foussekis	
Sweden	The Aeronautical Research Institute of Sweden (FFA)	J.A.Dahlberg	(Resp. Scientist) (FFA Project Manager)
		M.Poppen	

The objective of the project was to investigate the influence of wind turbine configuration and site parameters on the fatigue loads of series produced wind turbines by means of a continuous monitoring method capable of on-line cycle counting techniques.

SCOPE

Components of the turbine have to withstand numbers of load cycles of up to 10^8 imposing high demands on the fatigue characteristics of both, the used materials and the design. Nevertheless, fatigue loading of wind turbine components still remains a parameter of high uncertainty in the design of wind turbines. The specific features of these fatigue loads can be expected to vary with the type of turbine and the site of operation. In order to ensure the reliability of the next generation of larger scale wind turbines improved load assumptions will be of vital importance. Within the scope of the project statistically approved fatigue load data were to be measured by means of the proposed on-line cycle counting method and evaluated with respect to the influences of wind farm operation, complex terrain and wind turbine configuration on the component fatigue loads. The results are meant to support the development of procedures for more exact load assumptions and the investigation of existing load prediction methods.

WORK ORGANIZATION & TASKS

Each of the participants carried out measurements at their proposed sites :

The blade root bending moments of two pitch controlled, variable speed wind turbines operating in the Hamswehrum wind farm, and also that of a stall controlled, fixed speed wind turbine operating in CRES' complex terrain test site, were measured by DEWI and CRES. In parallel FFA used their database of time series measurements of blade root bending moments on a stall controlled, fixed speed turbine at Alsvik wind farm in order to derive semi-empirical fatigue load data.

The work was organized in 6 tasks as follows:

1 Development of DAS and measurement program
2 Instrumentation and calibration of measurement equipment
3 Measurement campaign
4 Comparison with FFA data
5 Evaluation of data; foundation of data base for load spectra
6 Conclusive work; final report

The project started in December 1992 and ended in February 1995 with a total duration of 27 month. The project was extended by incorporation of two Central European partners, Institute for Informatics, Bukarest, Rumania (ICI) and the Research Institute Energovyzkum, Brno, Tchech Republic (EGV) under a supplementary agreement (ERBCIPDCT930334). The new partners contribute in the field of data acquisition systems and tower load measurements.

RESULTS AND CONCLUSIONS

The presented project delivered on-line counted Rainflow matrices that show that the method of long time monitoring of fatigue loads leads to reliable and statistically approved results, given that the proper measures are taken to maintain the data acquisition system. Compared to the cost of large scale wind turbines the cost of the proposed monitoring method are marginal, whereas the results can help to save material without diminishing safety.

The results show clearly that the suggested method is a valid approach to the problem of determining the characteristics of fatigue loading on different wind turbine concepts and varying site conditions. The monitored data were proven reliable and statistically meaningful due to the prolonged period of continuous observation compared to short time series measurement campaigns. For its cost effectiveness the method offers the opportunity to perform such measurements at various turbines in order to collect the whole variety of typical loading situations that specific turbines will feel at specific sites. Generalizing this information will improve the load assumptions. These findings could be enforced by a first application under commercial conditions as described above.

With respect to the effects of complex terrain and wind farm operation the following can be concluded:

The loading for a wind turbine in the second row of the Hamswehrum wind farm are found to be increased by 23% in flapwise and by 13% in edgewise direction. The results are well in line with those determined in other projects dedicated to the problem of increased loads in wind farms.

For the conditions studied, fatigue loading on the blade root, of a fixed speed stall controlled wind turbine operating in specific wake conditions turns out to be more severe than single turbine operation in complex terrain, which though experiences remarkably higher fatigue loading compared to the single wind turbine operating in flat terrain. However, it must be pointed out that the results obtained depend strongly on the material's fatigue properties. Additionally, the severity of fatigue loading in stall operation has been explicitly shown.

Simulation of fixed speed, stall controlled turbine operation in the windfarm of Hamswehrum, indicates that the wake effects on the fatigue loading on this type of turbine concept can be expected to be stronger than those on the fatigue loading of a wind turbine with variable speed, pitch control concept. This conclusion is valid given that no stall or pitching actions occur.

DAMAGE ESTIMATES FOR EUROPEAN AND U.S. SITES USING THE U.S. HIGH-CYCLE FATIGUE DATA BASE

Herbert J. Sutherland
Wind Energy Technology
Sandia National Laboratories
Albuquerque, NM 87185-0708
Phone: (505)844-2037
Fax: (505)845-9500
E-Mail: hjsuthe@sandia.gov

ABSTRACT

This paper uses two high-cycle fatigue data bases, one for typical U.S. blade materials and one for European materials, to analyze the service lifetime of a wind turbine blade subjected to the WISPER load spectrum for northern European sites [Ten Have, 1992] and the WISPER protocol load spectrum for U.S. wind farm sites [Kelley, 1995]. The U.S. data base, developed by Mandell, et al. (1995), contains over 2200 data points that were obtained using coupon testing procedures. These data are used to construct a Goodman diagram that is suitable for analyzing wind turbine blades. This result is compared to the Goodman diagram derived from the European fatigue data base FACT [DeSmet and Bach, 1994]. The LIFE2 fatigue analysis code for wind turbines [Sutherland and Schluter, 1989] is then used to predict the service lifetime of a turbine blade subjected to the two loading histories. The results of this study indicate that the WISPER load spectrum from northern European sites significantly underestimates the WISPER protocol load spectrum from a U.S. wind farm site; i.e., the WISPER load spectrum significantly underestimates the number and magnitude of the loads observed at a U.S. wind farm site. Further, the analyses demonstrate that the European and the U.S. fatigue material data bases are in general agreement for the prediction of tensile failures. However, for compressive failures, the two data bases are significantly different, with the U.S. data base predicting significantly shorter service lifetimes than the European data base.

INTRODUCTION

In recent papers, Mandell, et al. (1995), Samborsky and Mandell (1996) and Sutherland and Mandell (1996) have brought together the extensive set of S-N fatigue data that was developed at Montana State University (MSU) under the auspices of the U.S. DOE's Wind Energy Program. The data base, herein called the MSU/DOE data base, now contains over 2200 data points with test results for typical U.S. wind turbine blade materials, i.e., E-glass fiber composites with polyester, vinyl ester and epoxy matrices and with a variety of fiber contents and architectures. Specimens were tested over a range of 10^3 to $5x10^8$ cycles and at R values of 2, 10, -1, 0.5 and 0.1 (the R value is defined to be the algebraic ratio of the minimum stress σ_{min} to the maximum stress σ_{max} in one cycle). Supporting tests for ultimate tensile, ultimate compression, and modulus were also conducted for inclusion in the data base. The fatigue data are from constant-amplitude S-N tests that were conducted using conventional coupon test procedures and a specialized, high-speed coupon test procedure. The latter testing procedure was developed at MSU especially for these tests to permit high-cycle fatigue testing in a timely manner, see Mandell, et al. (1994).

Mandell, et al. (1993) have demonstrated that the data from the various fiberglass composite materials in the data base may be characterized by a power law curve fit when they are normalized to the ultimate tensile or compressive strength of the composite. Starting with the normalized curve fits at various R values, a Goodman diagram is constructed and then normalized to typical wind turbine blade properties. This normalization is required because the relatively small coupons in the data base perform significantly better than the relatively large composite structures used in typical blades.

To illustrate the use of these data, the Goodman diagram is used by the LIFE2 fatigue analysis code for wind turbines [Sutherland and Schluter, 1989] to analyze two distinct loading environments. The first is the WInd turbine reference SPEctRum, WISPER, herein called the European load spectrum, that was developed by Ten Have (1992) to be a loading standard that reproduces the general character of flap loads on a wind turbine blade. This load spectrum represents a more or less homogeneous view of the service environment seen by turbines operating individually in near-uniform terrain in the proximity to the ocean. The second load spectrum, herein called the U.S. wind farm load spectrum, was developed by Kelley (1995). In this formulation, the WISPER development protocol is applied to data from a California wind farm to obtain a load spectrum that is representative of the service environment for multi-row wind farms at continental sites dominated by complex terrain (i.e., mountain passes).

Fatigue analyses are used to compare the MSU/DOE fatigue characterization to the European data base FACT developed by DeSmet and Bach, (1994). Here, we demonstrate that the two data bases are in general agreement for tensile failure of the blade, but are significantly different in compression. Moreover, the MSU/DOE data base predicts the critical failure mode to be compressive, while the FACT data base predicts the mode to be tensile.

Fatigue analyses are also used to demonstrate the impact of the two operating environments on the predicted lifetime of the two characterizations. The analyses demonstrate that the WISPER load spectrum from northern European sites significantly underestimates the WISPER protocol load spectrum from a U.S. wind farm site; i.e., the WISPER load spectrum significantly underestimates the number and magnitude of the loads observed at a U.S. wind farm site.

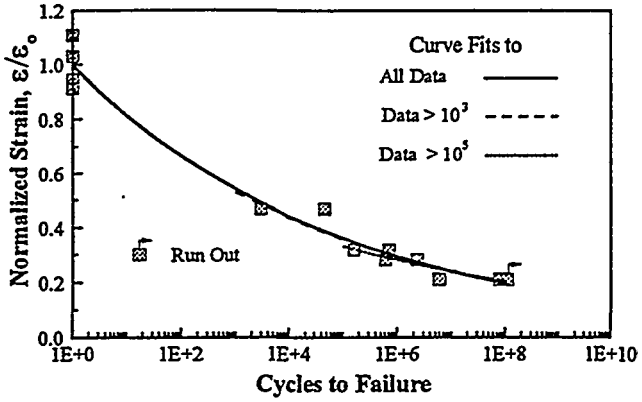

Figure 1. High cycle S-N data for R=0.1 with selected curve fits to the data.

MATERIAL CHARACTERIZATION

The MSU/DOE Data Base

The initial U.S. fatigue data base was reported by Mandell, Reed and Samborsky (1992). These data were obtained from constant-amplitude S-N tests using traditional coupon tests. The coupons were typically 25 to 50 mm (one to two inches) wide and 4 to 8 mm (an eighth to a quarter inch) thick. The internal hysteretic heating of these polymer-based materials, combined with their poor heat transfer characteristics, limited the testing frequency to below 20 Hz. Typically, these tests were run at a frequency of 10 Hz.

To cover the entire range of interest for wind turbine applications, the S-N data must extend to a minimum of 10^8 cycles. Using traditional techniques, one test would require over one hundred days to complete. Thus, an appropriate fatigue data base for wind turbine applications would be very difficult and time consuming to build when tests are limited to 10 or 20 Hz cyclic rates. To overcome this difficulty, Creed (1993) and Mandell, et al. (1994) developed a new testing technique that permits testing at frequencies up to 100 Hz, thus shortening the test period for 10^8 cycles to just eleven days. Adequate heat transfer is achieved in this technique by using relatively thin specimens, approximately 1.5 mm (0.06 inch) thick. This thickness limits the number of fiberglass layers to fewer than 10. Details of the test development and validation are discussed by Creed (1993) and Mandell, et al. (1995). The validation process included a detailed comparison of the S-N fatigue data produced using the relatively thin coupons to data produced using standard coupons. The comparison showed that the S-N data were within experimental scatter of one another.

As discussed by Sutherland and Mandell (1996), the data base now contains over 2200 data points with test results for E-glass fiber composites with polyester, vinyl ester and epoxy matrices. Many of the specimens used in these tests were supplied by U.S. wind turbine blade manufacturers. Other specimens were constructed to systematically study the effect on fatigue properties of variations in composite structure, e.g., fiber content and reinforcement architecture. The data base contains test results that span a range of 10^3 to $5x10^8$ cycles and R values of 2, 10, -1, 0.5 and 0.1. Supporting tests for ultimate tensile, ultimate compression, and modulus were also conducted for inclusion in the data base. A typical data set for uniaxial fiber lay-ups and an R value of 0.1 is shown in Figure 1.

Power Law Fit

The fiberglass composite data contained in the data base cover a wide range of properties. Mandell, et al. (1993) demonstrated that the constant amplitude, S-N fatigue data may be characterized by a power law curve fit of the form:

$$\frac{\varepsilon}{\varepsilon_o} = C N^{-(1/m)} \quad , \qquad [1]$$

where ε is the maximum cyclic strain if the coupon fails in tension or the minimum cyclic strain if the coupon fails in compression, ε_o is the ultimate tensile strain ε_{uts} or ultimate compression strain ε_{ucs} (for tensile and compressive failure, respectively), N is the number of cycles to failure, and m and C are the curve fitting parameters. The mean fits for uniaxial fiber lay-ups are summarized in Table I. The fits for an R value of 0.1

Table I: Power law fit of the fatigue data for uniaxial fiber lay-ups.

R	Power Law Coefficients with Range of Applicability					
Value	1 to 10^8		10^3 to 10^8 Cycles		10^5 to 10^8 Cycles	
	C	m	C	m	C	m
0.1	1	11.3	0.969	11.6	0.740	14.3
0.5	1	15.4	0.977	16.0	0.977	16.0
-1	1	14.9	1.124	13.2	1.124	13.2
10	1	18.0	0.862	22.5	0.802	24.9
2	1	31.2	0.859	47.8	0.802	61.7

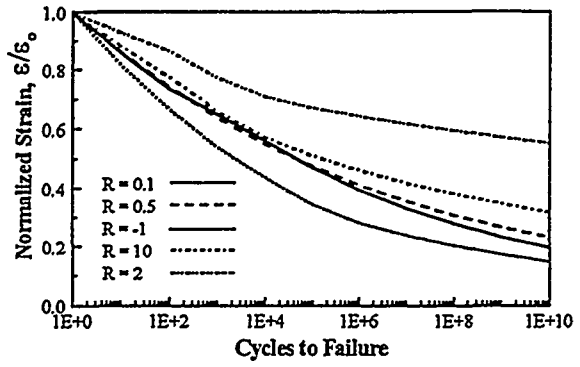

Figure 2a. Semilog plot.

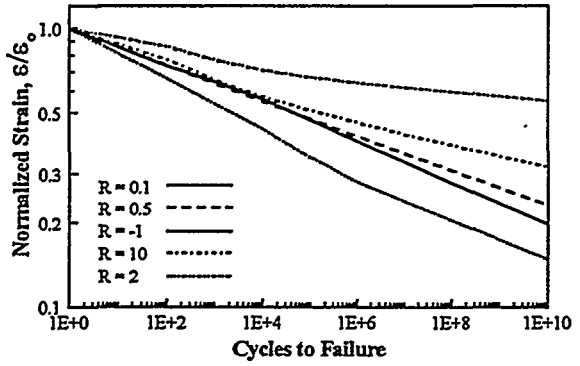

Figure 2b. Log-log plot.

Figure 2. S-N diagram for fiberglass composites normalized to failure strain.

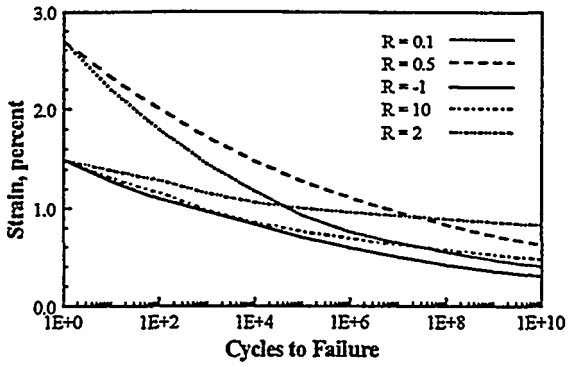

Figure 3. S-N diagram for fiberglass composites based on the MSU/DOE data base.

are shown in Figure 1. In this table, the first set of parameters (labeled 1 to 10^8 cycles) is the best fit parameters when all of the S-N data and the ultimate strain are considered (the lead coefficient C has been set to one in these fits to reflect the correct ultimate strain of the material). The second set (labeled 10^3 to 10^8 cycles) is the parameters for fits to the S-N data with lifetimes that are greater than 10^3 cycles. The third set (labeled 10^5 to 10^8 cycles) is the parameters for fits to the data with lifetimes that are greater than 10^5 cycles. In the latter two sets, the value of C is not restricted to a value of one.

To obtain the "best" overall fits shown in Figure 2, the first set of parameters was used from 1 to 10^3 cycles, the second from 10^3 to 10^5 and the final from 10^5 to 10^{10}. At the intersections, an average value was used. Note that the data underlying these fits are limited to approximately 10^8 cycles. Thus, from 10^8 to 10^{10} cycles, the power law fits are extrapolations of the 10^5 to 10^8 data.

Goodman Diagram

The data cited in the previous section describe the normalized behavior of the composites. To use this characterization in a service lifetime calculation, ε_o must be denormalized by the ultimate tensile (ε_{uts}) and compressive (ε_{ucs}) failure strain of the material under consideration. Typical values for industrial blade laminates are 2.7 percent and 1.5 percent, respectively [Mandell et al. 1995]. The normalized data presented in Figure 2 are scaled to these values to obtain the S-N diagram shown in Figure 3 and the Goodman diagram shown in Figure 4. In Figure 4, the plot has been normalized to ε_{uts} using the ratio of 2.7 to 1.5 for the tensile-to-compressive ratio.

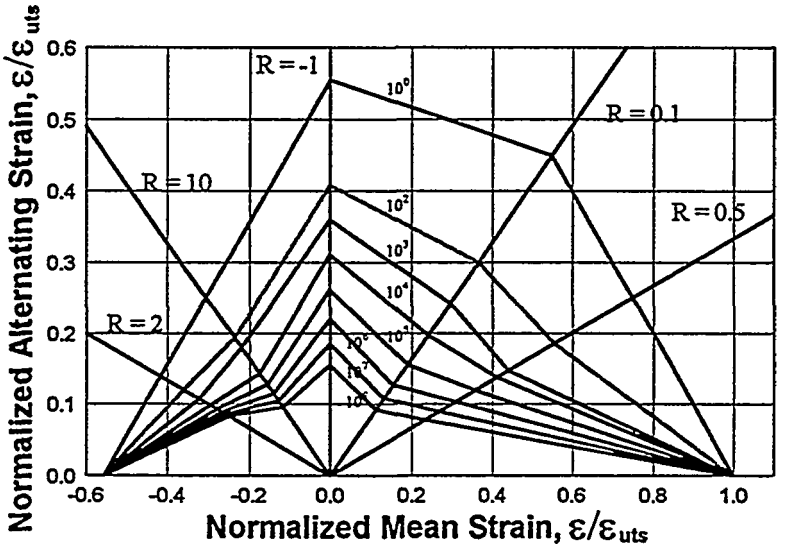

Figure 4. Normalized Goodman diagram for fiberglass composites based on the MSU/DOE data base.

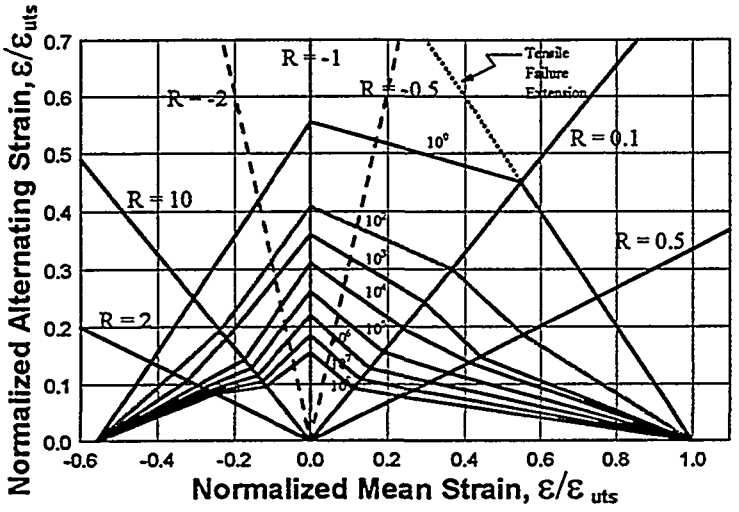

Figure 5. Goodman diagram with tensile failure extension and constant R values based on the MSU/DOE data base.

When comparing Figures 3 and 4, one notes that the Goodman diagram is based on curve fits to the ultimate tensile and compressive strains and curve fits at five R values. Between these five constant R value lines, a Goodman diagram was constructed using straight lines. This construction technique is a reasonable approximation between R values of 2, 10 and -1 and the ultimate compressive strain, and between R values of 0.1 and 0.5 and the ultimate tensile strain, because the failure mechanisms for the former are all compressive and for the latter they are all tensile. However, somewhere between an R value of -1 and 0.1, the failure mechanism changes from compressive to tensile. The transition between the two is not defined in the data base. In the rendition of the Goodman diagram shown in Figure 4, this region is also bridged with straight lines.

In Figure 5, the Goodman diagram shown in Figure 4 has been redrawn with the tensile failure extension, indicated by the dashed line, into an R range of -1 to 0.1. As shown by this extension, a tensile failure mechanism in this range will produce significantly higher strains to failure. Thus, we have chosen a conservative estimate of a Goodman diagram in this region.

In the FACT data base [DeSmet and Bach, 1994], ε_{uts} and ε_{ucs} are 2.58 percent and 1.94 percent, respectively. These values produce an almost symmetric Goodman diagram. A symmetric diagram implies that there are only small differences between tensile and compressive failures. Thus, for tensile failure (R values between 0 and 1), the MSU/DOE and the FACT data bases are in general agreement. However, for compressive failures, there are significant differences in the strain to failure, with the MSU/DOE data base predicting lower strains to failure and shorter service lifetimes. The effects of these differences on predicted service lifetimes are demonstrated below in the sample fatigue analysis.

The discrepancy in the compressive strain to failure between the two data bases may reflect a difference in the compression test methodology. In particular, the compressive tests conducted at MSU used gauge sections with no lateral constraints, whereas, the FACT data base has a preponderance of data obtained from compression tests with lateral constraints. The in the compressive strain discrepancy can also indicate that the materials contained in the FACT data base are significantly different from those contained in the MSU/DOE data base. Until definitive tests are conducted, these differences will remain unresolved.

WISPER PROTOCOL LOAD SPECTRA

The European load spectrum (the WISPER load spectrum) was developed by an international working group composed of thirteen different European research institutes and manufacturers [Ten Have, 1992]. The objective of the effort was to specify variable-amplitude (or spectral) test-loading histories that incorporate the major features seen in the root flapwise (out-of-plane) bending of horizontal-axis wind turbine (HAWT) blades. The European load spectrum is derived from eight load cases that are called "classes" or "modes." The first two classes are the loads for discrete events, specifically turbine start-up (Class 1) and stopping (Class 2). The six remaining classes, 3 through 8, define the load histories for continuous operation of the turbines over their operating wind speed range. Class 3 contains representative data for mean wind speeds below 9 m/s. Classes 4 through 7 contain data for mean wind speeds of 9-11, 11-13, 13-15, and 15-17 m/s, respectively. Finally, Mode 8 describes the loads for mean wind speeds exceeding 17 m/s. Only classes 3 thorough 8 are used in the analyses presented here.

Kelley (1995) found that the WISPER development protocol could be successfully applied to the U.S. wind farm operating environment. He constructed a U.S. wind farm load spectrum using an operating data set that was collected from two adjacent Micon 65/13 horizontal-axis wind turbines. These turbines are located in Row 37 of a 41-row wind farm in San Gorgonio Pass, California. This location is near the center of a group of turbines that is characterized by low energy production and higher fatigue damage relative to other turbine locations within the wind farm. The two turbines were identical except for their rotors. One turbine had a 17-m rotor that was based on the NREL (SERI) thin-airfoil family, and the other had a 16-m rotor consisting of reconditioned, original-equipment AeroStar blades. [Tangler et al. (1990) present a complete discussion of these tests.] In all, 397 10-minute records were collected over a wide range of inflow conditions.

Kelley (1995) followed the WISPER development protocol to form the load cycle matrices for Modes 3 through 7. Data from both the NREL and AeroStar loads data were used to determine these matrices. The U.S. wind farm and the European distributions are compared with one another in Figure 6. As shown in this figure, the San Gorgonio (U.S. wind farm)

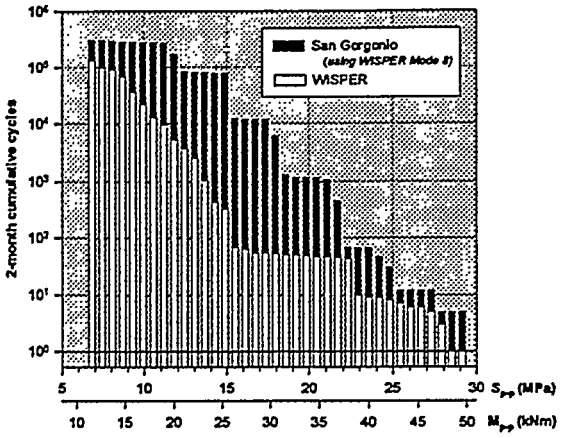

Figure 6. Cumulative 2-month reference alternating load spectra.

spectrum differs significantly from the European load spectrum (WISPER), which is based on the loads from singly-sited turbines located in relatively smooth terrain. The U.S. wind farm load spectrum contained many more and larger loading cycles than the European load spectrum. And, Sutherland and Kelly (1995) showed that the wind farm load spectrum is significantly more damaging.

Both the European and the U.S. load spectra are normalized to an amplitude range of 1 to 64, with zero load equal to 25. To convert the normalized ranges to strains requires a detailed knowledge of the design and the loads on the turbine blade. Because we are not analyzing a particular turbine blade here, we assume that the maximum nominal strain level in the blade is 0.4 percent (this strain level is commonly used in the wind industry as the maximum allowable nominal strain for the blades).

As noted above, both spectra are flap bending moment spectra. Therefore, the blade is subjected to tensile strains on one side (up wind) and compressive strains on the other (down wind). The cyclic loads on both the tensile and compressive side are considered in this analysis.

PREDICTION OF SERVICE LIFETIME

The LIFE2 analysis code for wind turbines [Sutherland and Schluter, 1989] is a PC-based, menu-driven numerical analysis package that leads a user through the steps required to characterize the loading and material properties. Miner's rule or a linear crack propagation rule is then used to calculate the time to failure. Only Miner's rule is used here.

Input Parameters

The LIFE2 code requires four sets of input variables: 1) the wind speed distribution for the turbine site as an average annual distribution, 2) the material fatigue properties, 3) a joint distribution of mean strain and strain amplitude (or stress) for the various operational states of the turbine, and 4) a miscellaneous set of parameters that describe the operational parameters for the turbine (e.g., the cut-in and cut-out wind speed) and the stress concentration factor(s) for the turbine component. The reader is referred to Sutherland, Veers and Ashwill (1994) for a complete description of these input parameters.

For this analysis, we assume that the turbine is located at a Rayleigh site with an average wind speed of 6.3 m/s (14 mph). The fatigue properties for the MSU/DOE data base are the numerical equivalent of the data contained in the Goodman diagram shown in Figure 4. A similar numerical formulation was developed for the FACT data base by the author from the Goodman diagram developed by DeSmet and Bach (1994). Another fatigue data base, developed by Kensche (1992), was also used in the calculations. As the results of the latter two data bases are in general agreement, the analyses based on the Kensche data base are not reported here. The third input data set for the LIFE2 code is the U.S. wind farm and the European load spectra that are described above. Figures 7a and 7b present representative samples of the alternating component of the cyclic strain distribution, from class 5 and 7 wind speed bins for the

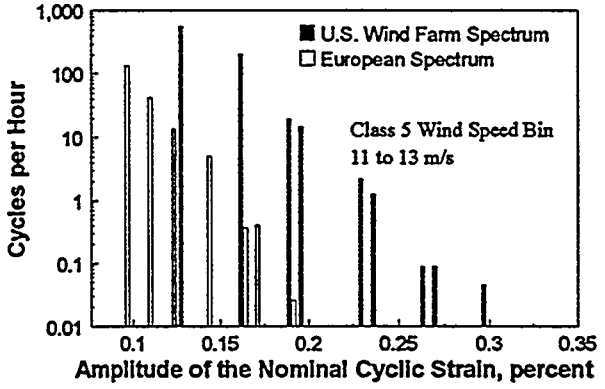

a. Strain spectra for Class 5 Wind Speed Bin.

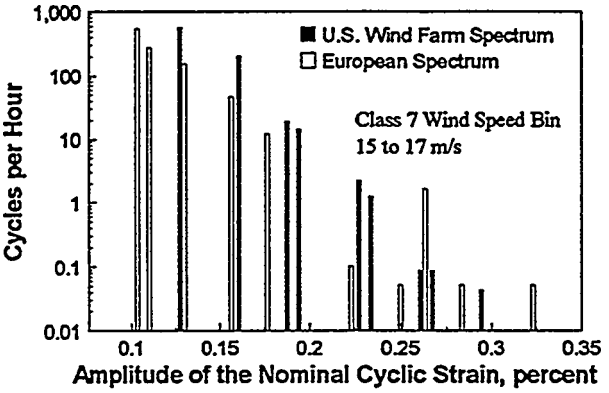

b. Strain spectra for Class 7 Wind Speed Bin.

Figure 7. Typical load spectra.

Table II. Predicted service lifetime in years.

Bending Direction	U.S. Wind Farm Spectrum		European Spectrum	
	MSU/DOE	FACT	MSU/DOE	FACT
Tensile	44.9	67.5	186.	618.
Compressive	23.5	136.	90.0	1130

European and the U.S. wind farm data bases. Complete descriptions of these distributions are given by Kelley (1995). The fourth and final input set describes the operation of the turbine and the stress concentration factor. For these calculations, the turbine is assumed to operate between 5.4 m/s (12 mph) and 25 m/s (56 mph). The stress concentration factor is assumed to be 2.5.

Damage Calculations

The input parameters described above were used in the LIFE2 code to predict service lifetimes. The results of these analyses are summarized in Table II.

First, the predicted service lifetimes in Table II illustrate that the WISPER load spectrum from northern European sites (the European spectrum) significantly underestimates the WISPER protocol load spectrum from a U.S. wind farm site (the U.S. wind farm spectrum); i.e., the WISPER protocol overestimates the service lifetime at this U.S. site. And, second, Table II illustrates that the MSU/DOE data base predicts the blade will fail in compression and at shorter lifetimes than predicted by the FACT data base.

Comparison of the Spectral Loads: As shown in Figure 6 and analyzed by Kelley (1995) and Sutherland and Kelley (1995), the WISPER load spectrum for U.S. wind farms contains many more cycles than does the European spectrum, and the wind farm spectrum is more damaging. The latter conclusion is illustrated in Table II by comparing the predicted lifetimes in the first column to the third column and the second to the fourth. In all cases, the European load spectrum significantly overestimates the service lifetime at the U.S. wind farm site.

A more detailed comparison of the damage is shown in Figure 8. In this figure we examine the damage $\mathcal{D}$ associated with each load spectrum. The damage at strain ε_i is defined by Miner's Rule to be

$$\mathcal{D}(\varepsilon_i) = \frac{n\left[(\varepsilon_i)_a, (\varepsilon_i)_m\right]}{N\left[(\varepsilon_i)_a, (\varepsilon_i)_m\right]} \quad , \qquad [2]$$

where n is the number of cycles in the spectrum at alternating strain $(\varepsilon_i)_a$, mean strain $(\varepsilon_i)_m$ and N is the number of cycles to failure at the same strain level. The total damage is simply the sum of the damage over all strain cycles in the spectrum. By Miner's Rule, failure occurs when the total damage accumulates to one, or inversely, when the damage is summed over all stress cycles in time t, the service lifetime of the component is equal to the reciprocal of the damage.

As shown in Figure 8, the damage is concentrated in the mid-range wind speed bins (i.e., wind speed classes 4, 5 and 6) for the U.S. wind farm spectrum and in the upper wind speed bins (i.e., wind speed classes 7 and 8) for the European load spectrum. This result could be anticipated by a close examination of Figure 7. As shown in Figure 7a, the strain cycles in Class 5 for the U.S. wind farm spectrum have more

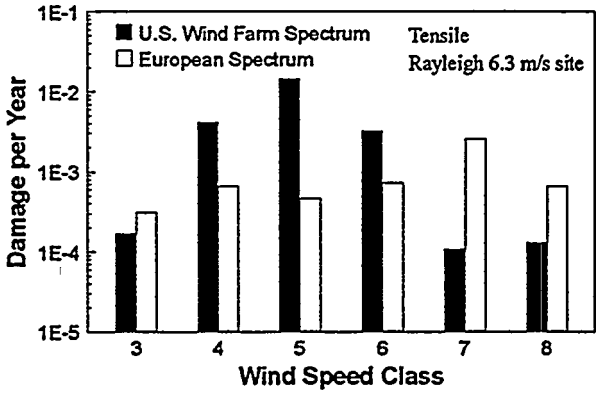

a. MSU/DOE fatigue data base.

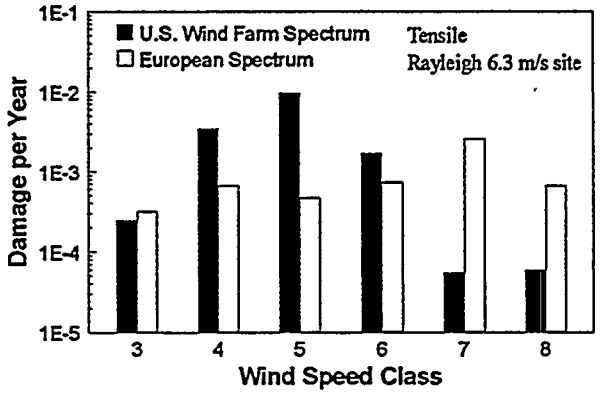

b. FACT data base.

Figure 8. The damage spectra for the two fatigue data bases by wind speed bin.

cycles at higher amplitudes than the European spectrum. Figure 7b, illustrates that in Class 7, the distributions are reversed, with the European spectrum containing more cycles at higher amplitudes. Again, when the damage for all wind speed classes are totaled, the European spectrum is less damaging than the U.S. wind farm spectrum.

One must be careful in drawing general conclusions from these observations. These analyses are based on a limited set of data from two almost identical turbines located at a single, U.S. wind farm site. Their limited nature precludes us from determining if this "U.S. wind farm spectrum" is representative of the load spectra on other turbines in different wind farms. Also, one should remember that the WISPER spectrum was never intended to duplicate the actual load spectrum on a turbine blade. This spectrum is a fatigue test loading standard based on variable amplitude load cycles for flap bending of HAWT blades on multiple turbines.

Comparison of Material Data Bases: The predicted service lifetimes shown in Table II illustrate that the MSU/DOE data base predicts, for both the U.S. and the European load spectra, that the blade will fail in compression and at shorter lifetimes than predicted by the FACT data base. These observations are drawn by comparing the first column to the second and the third to the fourth. The prediction of compressive failure is due to the asymmetry in the Goodman diagram of the MSU/DOE database, and the prediction of shorter lifetimes is due to the higher ultimate strains measured for the materials contained in the FACT data base.

To examine the asymmetry in greater detail, we will examine the damage rate (see Equation 2) produced by the U.S. wind farm strain spectrum in wind speed class 5 that is discussed above and shown in Figure 7a. The damage associated with these strain cycles is shown in Figures 9.

As illustrated in Figure 9a and in Table II, compressive strains produce significantly more damage than equivalent tensile loads when the MSU/DOE data base is used to determine the damage. This result is directly related to the strong asymmetry between compression and tension failures in the MSU/DOE data base that is characterized by the Goodman diagram shown in Figure 4. Consider the component of the strain distribution in the class 5 wind speed bin, shown in Figure 7a, that is located near a nominal alternating strain amplitude of 0.3 percent. This component has a rate of accumulation of approximately 0.045 cycles per hour and nominal amplitude of 0.3 percent strain and a nominal mean of 0.1 percent strain. For tensile bending with a stress concentration factor of 2.5, this converts to 1.0 percent maximum strain and -0.5 percent minimum strain. For compressive bending, this converts to 0.5 percent maximum strain and -1.0 percent minimum strain. Thus, R equals -0.5 for tension and -2 for compression. As shown in the Goodman diagram in Figure 5, the tensile failure strains to failure (see the R equal -0.5 dashed line in the Figure) are higher than the compressive failure strains (R equal -2 dashed line) for most alternating strains. This observation translates to a lower service lifetime in compression.

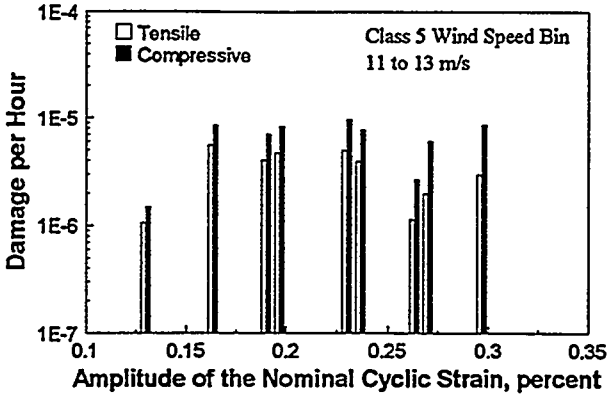

a. Damage spectra using the MSU/DOE data base.

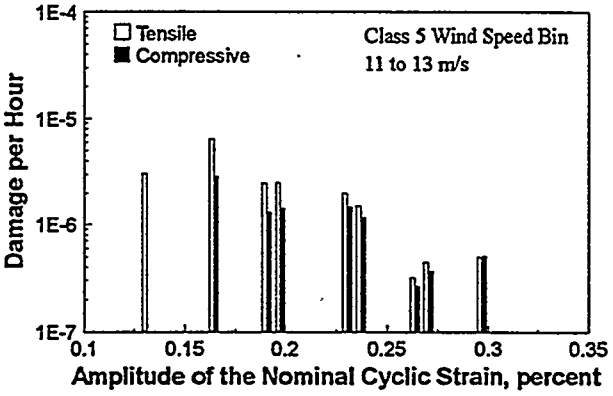

b. Damage spectra using the FACT data base.

Figure 9. Typical tensile and compressive damage spectra for the class 5 wind speed bin.

Likewise, as illustrated in Figure 9b and in Table II, tensile strains produce significantly more damage than equivalent compressive loads when the FACT data base is used to determine the damage. This result is attributed to the approximately symmetric Goodman diagram in the FACT data base.

As one may deduce from the predicted service lifetimes in Table II, similar results are obtained for the European load spectrum.

CONCLUDING COMMENTS

The MSU/DOE data base contains over 2200 data points with test results for fiberglass composites with polyester, vinyl ester and epoxy matrices and with a variety of fiber contents. These data may be characterized by a power law curve fit when normalized to their ultimate tensile and compression failure strains. The Goodman diagram constructed from these data displays a significant asymmetry between the tensile and compressive failure zones. A similar diagram constructed from the FACT data base does not display a pronounced asymmetry.

The fatigue calculations demonstrate the significance of these differences in the Goodman diagrams for the MSU/DOE and the FACT fatigue data bases. For both load spectra used in this example, the data bases predict similar lifetimes in tension, but in compression, the data bases predict very different lifetimes. The FACT data base predicts the critical failure mode to be tensile, and the MSU/DOE data base predicts the critical mode to be compressive. As discussed in detail above, these differences are a direct result of the asymmetric MSU/DOE Goodman diagram and the approximately symmetric FACT Goodman diagram. We hypothesize that the differences may be attributed to testing methods (lateral constraints). However, these differences could also indicate that the materials contained in the FACT data base are significantly different from those contained in the MSU/DOE data base. Until definitive tests are conducted, these differences will remain unresolved.

The analyses presented here further illustrate that the European load spectrum from northern European sites (the WISPER load spectrum) significantly underestimates a U.S. wind farm load spectrum (the WISPER protocol load spectrum derived from wind turbine loads data at a U.S. wind farm site); i.e., the European load spectrum significantly underestimates the number and magnitude of the loads observed at a U.S. wind farm site. Significantly more fatigue damage is occurring at the U.S. site because the inflow in the wind farm environment produces more cycles and higher loads in the turbine. Thus, there are fundamental differences in the two service environments.

ACKNOWLEDGMENTS

This work is supported by the U.S. Department of Energy under contract DE-AC04-94AL85000.

The author wishes to extend special acknowledgments to Neil Kelley and John Mandell. As cited in the paper, the author has drawn heavily upon their work for the data and the analyses presented in this paper.

REFERENCES

Creed, R.F., Jr., 1993, *High Cycle Tensile Fatigue of Unidirectional Fiberglass Composite Tested at High Frequency*, M.S. Thesis, Dept. of Chemical Engineering, Montana State University, Bozeman.

DeSmet, B.J. and P.W. Bach, 1994, *DATABASE FACT: Fatigue of Composites for Wind Turbines*, ECN-C--94-045, ECN, Petten, the Netherlands.

Kelley, N.D., 1995, "A Comparison of Measured Wind Park Load Histories With The WISPER and WISPERX Load Spectra," *Wind Energy 1995*, SED-Vol. 16, ASME, p. 107.

Kensche, C.W., 1992, *High Cycle Fatigue of Glass Fibre Reinforced Epoxy Materials for Wind Turbines*, DLR-FB 92-17, DLR, Stuttgart.

Mandell, J.F., Sutherland, H.J., Creed, R.J., Jr., Belinky, A.J., and Wei, G., 1995, "High Cycle Tensile and Compressive Fatigue of Glass Fiber-Dominated Composites," ASTM, *Sixth Symposium on Composites: Fatigue and Fracture*, in publication.

Mandell, J.F., Creed, R.J., Jr., Pan, Q., Combs, D.W., and Shrinivas, M., 1994, "Fatigue of Fiberglass Generic Materials and Substructures," *Wind Energy 1994*, SED-Vol. 15, ASME, p. 207.Mandell, J.F., Reed, R.M., Samborsky, D.D., and Pan, Q., 1993, "Fatigue Performance of Wind Turbine Blade Composite Materials," *Wind Energy 1993*, SED-Vol. 14, ASME, p. 191.

Mandell, J.F., Reed, R.M., and Samborsky, D.D.,1992, *Fatigue of Fiberglass Wind Turbine Materials*, SAND92-7005, Sandia National Laboratories, Albuquerque.

Samborsky, D.D., and Mandell, J.F., 1996, "Fatigue Resistant Fiberglass Laminates for Wind Turbine Blades," *Wind Energy 1996*, ASME, in publication.

Sutherland, H.J., and Kelley, N.D., 1995, "Fatigue Damage Estimate Comparisons for Northern European and U.S. Wind Farm Loading Environments," *Proceedings of WindPower '95*, AWEA, Washington, DC.

Sutherland, H.J., and Mandell, J.F., 1996, "Application of the U.S. High Cycle Fatigue Data Base to Wind Turbine Blade Lifetime Predictions," *Wind Energy 1996*, ASME, in publication.

Sutherland, H.J., and Schluter, L.L., 1989, "The LIFE2 Computer Code - Numerical Formulation and Input Parameters," *Proc. WindPower '89*, SERI/TP-257-3628, American Wind Energy Association, Washington, DC.

Sutherland, H.J., Veers, P.S., and Ashwill, T.D., 1994, "Fatigue Life Prediction for Wind Turbines: A Case Study on Loading Spectra and Parameter Sensitivity," *Case Studies for Fatigue Education*, ASTM STP 1250, p. 174.

Tangler, J., Smith B., Jager D., and Olsen, T.,1990, *Atmospheric Performance of the SERI Thin-Airfoil Family*, SERI/TP-257-3939, Solar Energy Research Institute, Golden, CO.

Ten Have, A.A., 1992, *WISPER and WISPERX: Final Definition of Two Standardized Fatigue Loading Sequences for Wind Turbine Blades*, NLR-TP-91476U, National Aerospace Laboratory NLR, Amsterdam, the Netherlands.

Fourth IEA Symposium on Wind Turbine Fatigue
February 1-2, 1996
DLR, Stuttgart, Germany

FATIGUE TESTING OF A CARBON FIBRE COMPOSITE WIND TURBINE BLADE WITH ASSOCIATED MATERIAL CHARACTERISATION

by: G A Lowe & D J Richardson
Faculty of Engineering, University of the West of England
Bristol, UK

1 Introduction

Within the EC project JOULE 2, the University of the West of England (UWE) tested a carbon fibre reinforced epoxy (CFRE) full scale wind turbine blade together with an associated material test coupon programme.

All the work was closely linked with the manufacturer Polymarin BV of the Netherlands, who designed and manufactured the blade and provided test specimens, the UWE carried out the research into the validation of the design calculations together with a check of the strength and fatigue life of the blade.

2 Blade Manufacture

The 8.5 metre blade developed by Polymarin in collaboration with UWE has two unusual features; the blade is made from CFRE and it is produced by the Resin Transfer Moulding (RTM) manufacturing process. The main reason for using CFRE was because of a requirement for high blade stiffness by the wind turbine operator for use in a variable speed passive control wind turbine system.

The RTM process was chosen for a number of reasons, but mainly to increase the production rate, increase the quality, and improve the safety of the labour force because of the closed nature of the process rather than the traditional open hand lay-up method of manufacture.

3 Test Programme

The development of the RTM process for manufacturing the blades was successfully completed in the early stages of the research [1]. The results of the material characterisation and the full scale blade tests was divided into two sections, namely:

* Characterisation of the CFRE material used in the manufacture of the blade.
* Full scale structural tests of the 8.5 metre wind turbine blade.

4 Material Characterisation

Flat test plates were produced by the RTM manufacturing process to simulate as closely as possible the characteristics of the blade material. The plates were manufactured from woven unidirectional carbon fibre, 80% in uni-direction fabric and 20% of +/- 45 degree fabric. The volume fraction of the plates was 44%.

Various testing methods were employed to determine the main material properties but these were essentially standard tensile and flexural tests; non standard compressive testing where short specimens were held in special clamps to give a 'fixed ended' condition, and fatigue testing.

The static tests were devised so that Polymarin could check whether the theoretical values used in the design of the blade were correct. The following table summarises some of the main material properties found from the test programme.

Table 1: Material Properties

Material Property	Average Value (from 5 tests)
Tensile Strength	1537 MPa
Tensile Modulus	103 GPa
Tensile Failure Strain	1.42%
Flexural Strength	1022 MPa
Compressive Strength	696 MPa

There was some surprise that the compressive strength of the material was one half of the tensile strength, it was later found [2] that this was not unusual for CFRE materials, especially woven fabrics manufactured by the RTM process.

5 Fatigue Testing of the Coupon Specimens

Tensile fatigue testing was conducted at an R-ratio of 0.1 at two stress levels, three coupons were tested at each stress level. The main purpose of these tests was to check whether the fatigue curve used by Polymarin in the design of the blade was appropriate.

A 10% drop in modulus was originally chosen as a pseudo failure criterion and the modulus of the specimens was measured periodically throughout each test. However, a drop in modulus was generally observed but very difficult to measure and therefore each fatigue test was continued until the specimen completely failed. Two stress levels were mainly considered. None of the specimens cycled at the lower stress level actually failed and the tests were eventually stopped due to the amount of machine time taken.

Figure 1 shows the S-N graph for life to failure. The graph shows the test results superimposed onto the curve used by Polymarin, high lighting the fact that their calculations were conservative.

6 Full Scale Wind Turbine Blade Testing

The 8.5 metres CFRE wind turbine blade was subjected to a number of static and fatigue tests in the Structures Testing Laboratory at the UWE.

The blade was mounted onto the "strong wall" of the laboratory so that it formed a cantilever in the horizontal axis. The blade was fastened to the strong wall with the actual fittings that are used to mount the blade to the hub of the turbine, therefore exactly simulating the 'in service' blade fixture.

A static limit load test was first performed on the blade to see if it was capable of withstanding the maximum bending moment received in service; this was successfully achieved.

7 'Design Life' Fatigue Test of Wind Turbine Blade

A full scale blade fatigue test was conducted to check that both the blade and the root fitting were capable of withstanding an equivalent 20 year design life. The blade was cycled in fatigue at an R-ratio of -0.1 in the flapwise direction. The cumulative damage of the blade for 20 years service life was transferred into equivalent damage for one million cycles. The calculations dictated that the blade was cycled with a 4.5 kN load at a distance of 4.8 metres from the blade root this induce a maximum strain of 16% of the tensile failure strain. Figure 2 shows the test arrangement.

The following data was captured by the automatic logging system:

(a) Stiffness
(b) Hysteresis Area
(c) Maximum and Minimum Strain
(d) Fatigue Life (using fatigue fuses)
(e) Maximum and Minimum Load and Deflection

A total of 14 strain gauges were mounted at defined locations on the blade. The location of each gauge was specified from the high strain areas of Polymarin's finite element model and from the results of a strain survey carried out at UWE.

7.1 Blade Fatigue Test Results

The instrumentation indicated that the blade had not suffered any significant damage after being subjected to one million fatigue cycles; in fact the load/deflection graph that was plotted at the start of the test was virtually identical to the graph after one million fatigue cycles. Figure 3 shows the final load/deflection graph superimposed onto the initial graph.

Graphs were plotted of strain versus number of cycles for each strain gauge and for stiffness and hysteresis area versus number of cycles. All of the graphs indicated that any damage inflicted onto the blade by the fatigue test was negligible.

7.2 Performance of the Fatigue Fuses

The fatigue fuse is made up of four flat specimens (legs), each leg has a special notch pattern that produces a stress concentration and therefore induces failure at different fatigue lives [3].

The fuses responded as anticipated, giving an indication of the fatigue damage that the CFRE material had been subjected to, both on the blade and on the test coupons.

The principle of the fatigue fuse is that each of the four legs gradually fail, indicating the amount of fatigue damage that they have encountered. The first two legs of each fatigue fuse failed at the predicted number of cycles, but the remainder of the legs did not fail due to poor adhesion between the fuse and the adhesive layer. This premature failure of the adhesive prevented a definitive test of the fatigue fuse, but the data that was obtained gave increased confidence in the application of fatigue fuses for condition monitoring of carbon composite structures.

8 Accelerated Fatigue Testing of the Blade

The load on the blade was increased by 50% and the fatigue test continued. The test was performed to determine whether continued fatigue testing would cause any damage to the blade or to the blade root and to give Polymarin confidence in the design and in the RTM manufacturing process. The maximum strain induced in the blade due to this increased load was 23% of the tensile failure strain.

8.1 Accelerated Fatigue Test Results

A crack appeared after some 50,000 fatigue cycles at a distance of 1.92 metres from the blade root, the length of the crack was 150 mm. The crack formed at the end of one of the layers that reinforce the blade root. The two strain gauges in the vicinity of the crack indicated that damage suddenly appeared, rather than gradually building up over a period of time. The instrumentation and visual appearance of the damage indicated that the crack appeared at a resin rich area.

Damage built up at the extreme ends of the crack over the following 50,000 fatigue cycles in the form of local delamination. The fatigue test of the blade continued but the damage did not noticeably grow because the load appeared to redistribute around the crack forming a new state of equilibrium. The blade has now endured over 500,000 fatigue cycles.

Figure 4 shows the maximum strain versus the number of fatigue cycles for the two strain gauges located in the vicinity of the crack. The strain on gauge 'F3' increases slightly and then dropped by 100 microstrain when the crack appeared; this indicating that the load was redistributed. However the strain then started to rise again to its original value, indicating that further fatigue damage enabled the load to transfer back to its original path. The strain on gauge 'F2' gradually reduced over the period of the accelerated fatigue test, also indicating a redistribution of load.

The global blade instrumentation (hysteresis area and stiffness) did not indicate that a crack had formed in the structure; this was not a surprise because similar cracks were not detected by such instrumentation in the JOULE 1 programme [4].

The damage that was detected as a result of the fatigue test will be used by Polymarin to enable them to improve the design of the blade and the RTM manufacturing process.

9 Conclusions

The tested properties of the CFRE material were in good agreement with the theoretical calculations used to design the blade, with the exception of the compressive strength of the material which was approximately a half of the tensile strength. However, it was noted, from other sources of information, that it is quite common for woven unidirectional material produced by the RTM process to be much stronger in tension that compression.

A number of different measuring techniques were used to monitor damage, generally they were successful, although the blade was so well designed that the stiffness and hysteresis area changes were small over the period of the fatigue test. Further fatigue testing will be conducted to provide a decisive evaluation of the suitability of fatigue fuses for condition monitoring of composite structures.

The wind turbine blade conformed to its design criteria under test, both statically and in fatigue and should not suffer any structural problems when in service. Lessons were learnt with regard to the design of the blade and the RTM process from the blade tests; mainly related to the buckling characteristics of the skins and fatigue crack growth due to joins in the layers of the fabric. The knowledge gained from the blade fatigue test will be used by Polymarin to improve this blade and in the design and manufacture of future wind blades and other optimum light weight structural components.

A wind turbine blade very rarely fails due to basic material fatigue. This research has shown that detailed design and manufacturing considerations, such as where any joins in the layers of fabric should be positioned, are key criteria to achieving the optimum fatigue resistance of wind blades or other large structures.

Reference

[1] RTM hollow mouldings: from fiction to fact
Reinforced Plastics, April 1994, Volume 38, Number 4.
ISSN 0034-3617
Published by Elsevier

[2] Design Data for Reinforced Plastics
Hancox N L, Mayer R M
Page 118, table 5.14, Properties of Unidirectional Carbon Fibre Composites.
Published by Chapman & Hall

[3] Fatigue Monitoring with Fuses
De La Veaus, R, Mcglinchey, J.
Materials Evaluation, August 1991, Volume 49, pages 1042-1045
ISSN 0025-5317

[4] Fatigue Properties of Wingblade Materials and Components manufactured by the Transverse Filament Winding Process.
Lowe G A, Satterly N D.
Proc. of the E C Wind Energy Conference, Travemunde, 1993

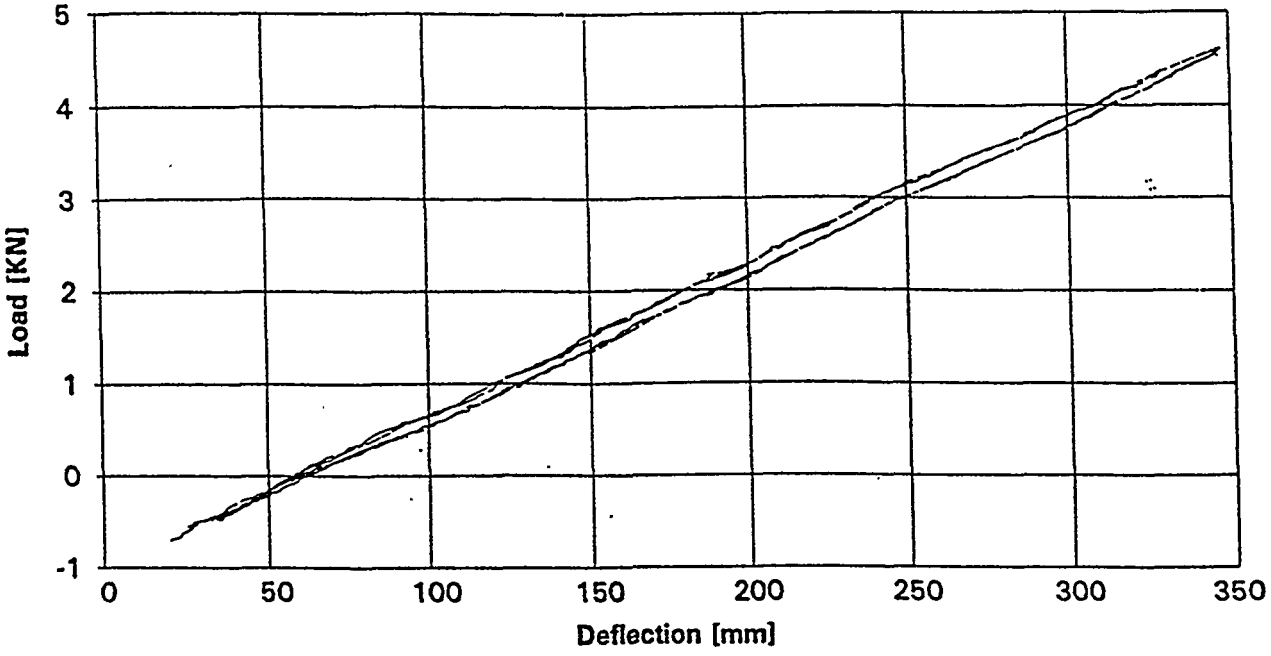

Figure 3: Load Versus Deflection Plot (Initial & Final Graphs)

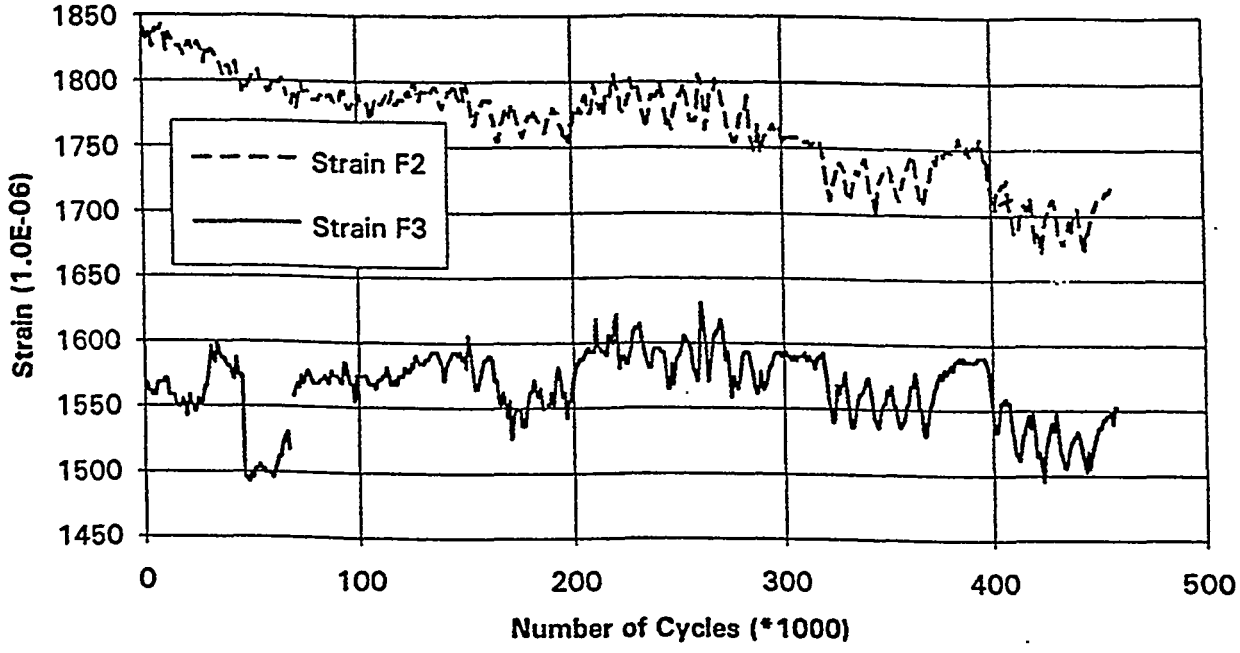

Figure 4: Strain History of Gauges F2 & F3 at the Area of Damage

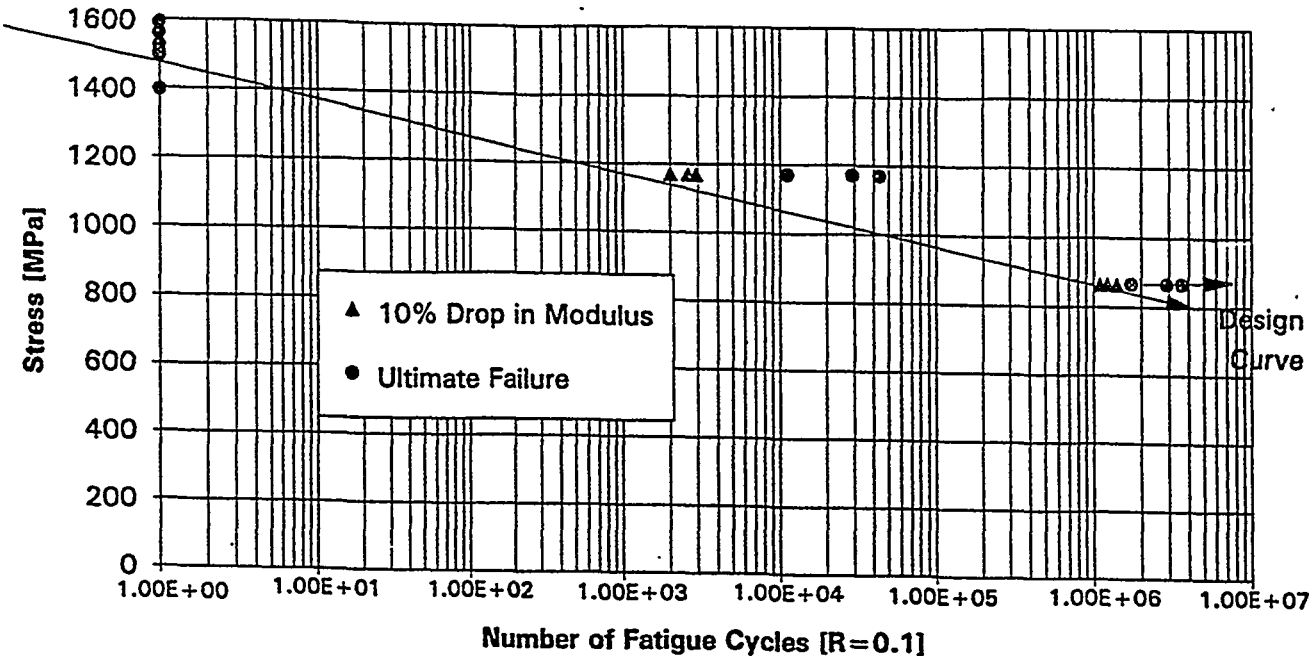

Figure 1: Unidirectional CFRE Fatigue Test Results

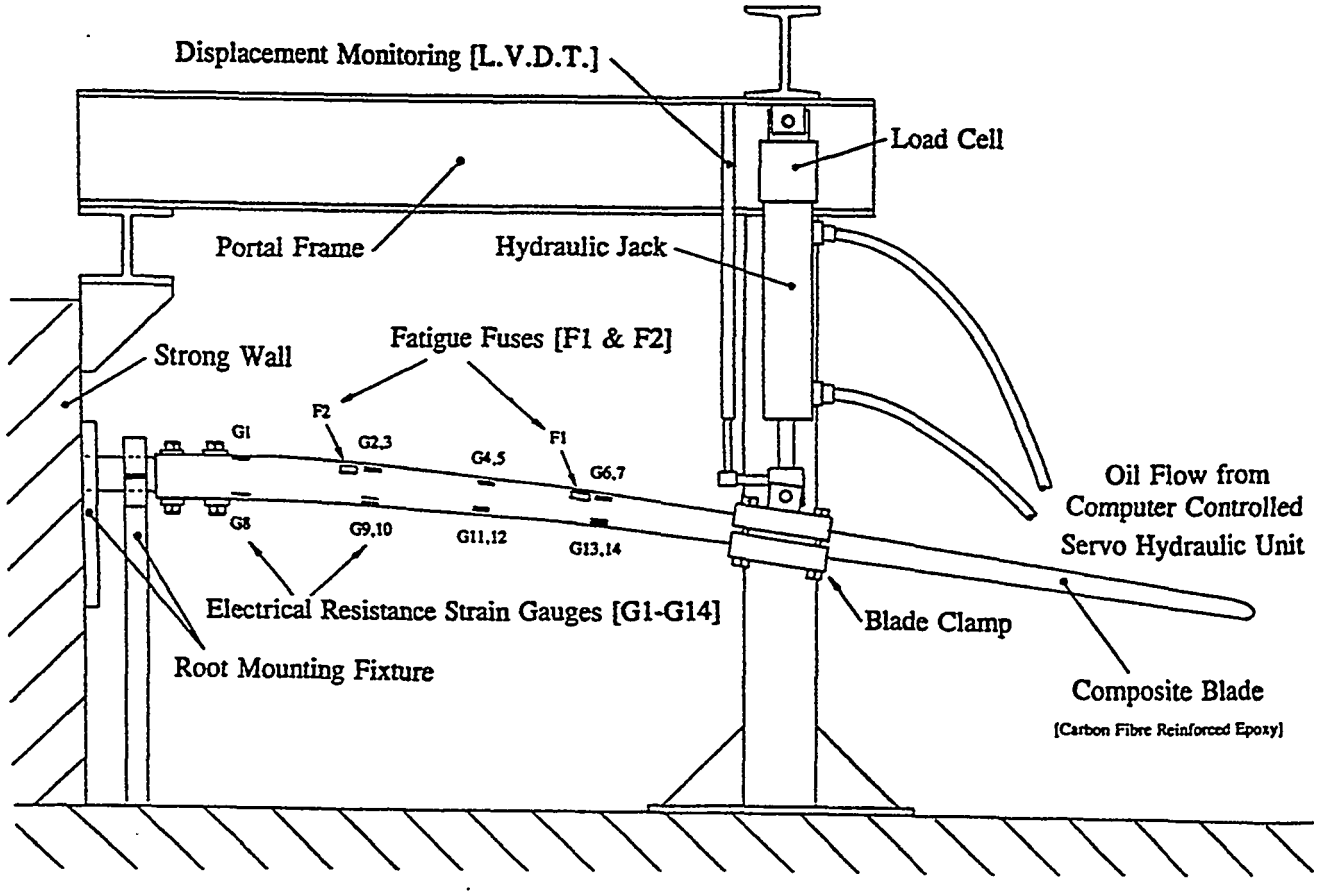

Figure 2: Fatigue Testing Arrangement of CFRE Blade

Fourth Symposium on Wind Turbine Fatigue
February 1-2, 1996
DLR, Stuttgart, Germany

The Carbon Fibre Market and Uses for Composite Wind Blades

J R Lowe
Tenax Fibers GmbH & Co. KG
Kasinostraße 19-21, D-42103
Wuppertal, Germany.

Abstract

Due to its excellent fatigue properties, low weight and high stiffness, carbon fibre reinforced plastic (CFRP) is the ideal material to use for the manufacture of wind blades. The present use of CFRP in the wind energy sector however is very low in comparison to glass fibre reinforced plastic (GFRP) materials. The main reason for this low use of CFRP is cost since at present times carbon fibre is valued ten times as much as glass fibre. This paper introduces carbon fibre as an alternative material to glass and examines the use of CFRP components in other high fatigue applications.

1. Introduction

Carbon fibre use has risen steadily since 1980 when world wide capacity was only 1000 tonnes. Its present capacity is in the region of 10,000 tonnes per annum. This remarkable growth was due to several factors, the energy crises of the 1970s, the growth in the civilian aerospace sector, military requirements and the high performance sporting goods market, where items such as tennis racquets and golf clubs have become just as much a fashion item(1,2).

After the end of the cold war the military market reduced causing a decline mainly in the US market, which in turn affected the world situation.

Almost half of the carbon fibre yarn sold in Europe is woven into fabric which is then prepregged, approximately 27% goes into unidirectional prepregs. Other processes becoming more important away from the aerospace industry are RTM, filament winding and pultrusion.

Filament winding is becoming more important due to the requirement of high specification light weight pressure vessels, used for gas propulsion vehicles among other things. Applications where rotational mass and energy savings are also relevant such as large print rollers and flywheels. Many composite manufacturers previously reliant on the defense industry have managed to successfully use their expertise to find new and diversified industrial markets.

The aerospace market within Europe is still a very stable sales platform for the carbon fibre industry, consuming an estimated 40% of the available yarn. Within this sector there are also areas such as highly engineered small aircraft and gliders which consume large quantities of materials.

For the future use of CFRP for aerospace applications it is no secret that Airbus Industries, Boeing and other manufacturers are looking forward to producing a future aircraft with a carbon fibre reinforced plastic structure. Throughout the aerospace industry cost, weight and performance on aircraft will be the primary drivers for the future.

The use of carbon filament yarn for wind blades is presently limited with only a few examples within the European sector. The market is dominated with manufacturers using glass fibres and traditional hand laminating techniques.

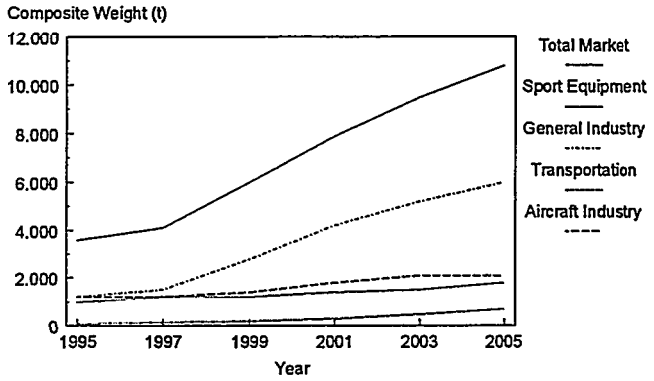

European CFRP-Market 1995-2005

Figure 1

Wind blades are only one of the industrial applications which are seen to be the largest growing market for CFRP since the material is becoming more available and more widely accepted by industry and consumers alike (Figure 1).

2. Manufacture of PAN based Carbon Filament yarns

Carbon fibres are produced either from coal-tar pitch or from polyacrylonitrile fibres as a precursor, and of these the PAN process is the most important (3). In this process (Figure 2) the PAN fibre is first stretched at high temperature in the presence of oxygen (oxidation stabilisation). During this stage the hydrogen is removed with the formation of a ladder polymer which is made up of condensed pyridine rings. In the subsequent heat treatment under an inert atmosphere, hydrogen and nitrogen are removed. Temperatures between 1200°C and 1800°C (carbonisation) give fibres with high strength (HTA type), high extension to break and high strength (UTS type), or intermediate modulus (IMS type). Temperatures above 2000°C and 3000°C (graphitization) give high modulus fibres (HMS) and ultra high modulus fibres (UMS).

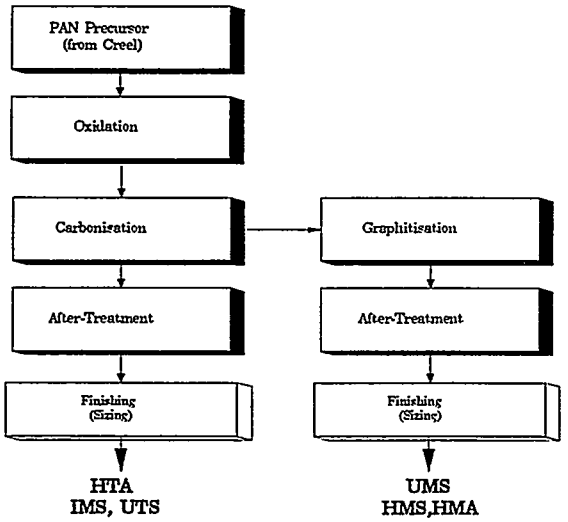

Carbon Fibre Processing

Figure 2

Next the fibres undergo surface treatment so as to increase the concentration of polar groups at the fibre surface. This improves the impregnation with the matrix material and the adhesion between the fibre and matrix. The final fibre finish has the effect of making it easier to process the comparatively brittle carbon fibres without damage, so as to produce fabrics, to braid or to wind.

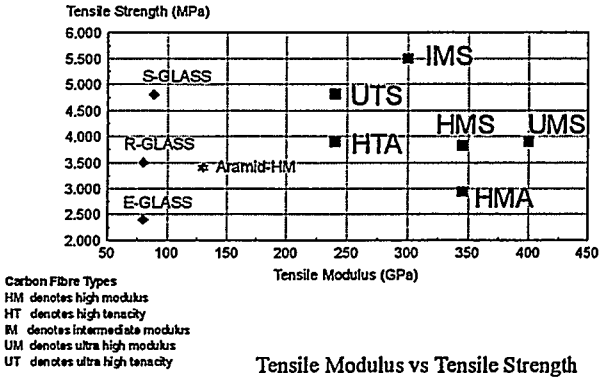

Tensile Modulus vs Tensile Strength for Tenax Fibers Yarns

Figure 3

3. Development Trends for PAN based Carbon Filament Yarns

In the last two decades much was achieved developing new classes and types of fibre as improvements in mechanical performance were sought (Figure 4). Today customers and designers can choose from high tenacity (HTA) yarns, high strain (UTS), intermediate modulus (IMS), high modulus (HMS) and ultra high modulus (UMS), with other individual derivatives (Figure 3). It is believed that the development of these materials by classical means such as precursor or processing modification is approaching a maximum. The activities of the carbon fibre producers over the next decade will be directed to optimising yarn production processes for the different applications. No principal expansion in the range of yarn types is to be expected.

4. Fatigue Properties of HTA Carbon Filament Yarns

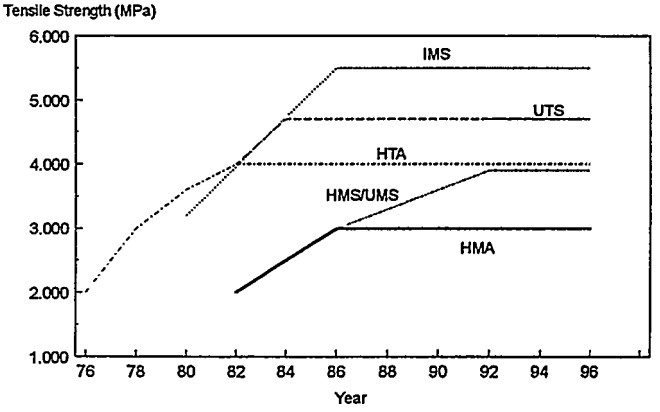

Improvement of Fibre Properties

Figure 4

The wind blades of a wind generator can be cycled in fatigue several million times, and as such one of the most important material properties of use to the wind turbine designer is the fatigue properties of the blade material (4). Due to price vs performance restrictions the HTA yarn will be realistically the only yarn of interest to the to the industry.

A selection of prepregs and fabric styles was available for laminate manufacture, including; plain weave fabric using Tenax HTA 5131 200tex yarn with Ciba 913 resin, unidirectional prepreg using Tenax HTA 5131 800tex with Ciba 913 resin, five harness satin using Tenax HTA 5131 200tex yarn with Ciba 914 resin (5) and plain weave fabric using Tenax HTA 5131 200tex yarn (for hand lamination).

Prepreg laminate manufacture was undertaken according to individual manufacturing specifications. For hand laminated specimens a Shell GE163 / Epikure 113 epoxide resin was cured at room temperature and post cured at 60°C for 15 hours. Each panel was C-scanned, with micrographs taken in the warp and weft directions. Specimens were cut from a predescribed cutting plan. Fatigue testing was undertaken in the Tenax Fibers laboratories at room temperature. A special testing fixture was used to prevent buckling in the specimen when tensile-compressive testing was underway (R=-1).

Testing results can be seen in Figures 5 and 6, with testing to R=-1 and R=0.1. Shear failures were apparent in all ±45° specimens. E-Glass values were taken from information supplied by Owens Corning Fiberglass(6).

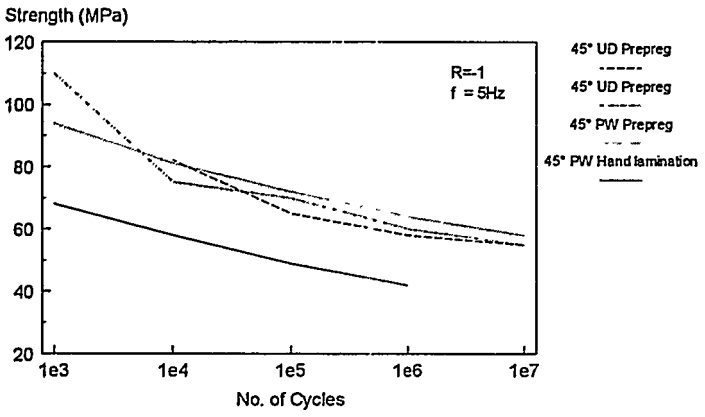

Fatigue of 45° tensile-compression fatigue (R=-1). for Tenax HTA 5131 laminates in epoxy resins.

Figure 5

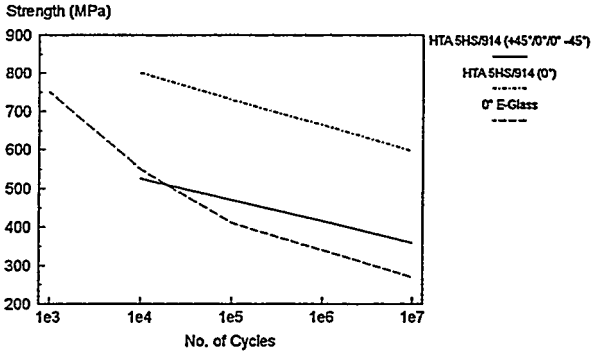

Fatigue Comparisons of woven Tenax HTA laminates with 0° E-Glass at R=0.1

Figure 6

5. Examples of Carbon Filament Yarn usage in High Fatigue Components

5.1 Aerospace, Helicopter Rotor Blades

The use of advanced composites has offered improvements in helicopter rotors due to improved aerodynamic geometry, damage tolerance, lower costs and weight reductions (7). The composite blades give increased performance due to their higher fatigue tolerances compared with that of metals. When composite blades were compared under test condition's with metal ones the fatigue life of the composite was proved to be much greater (Figure 7).

Although the initial costs of composite blades is slightly higher than for the aluminium, the life time savings run to half of what could be expected for a metal blade.

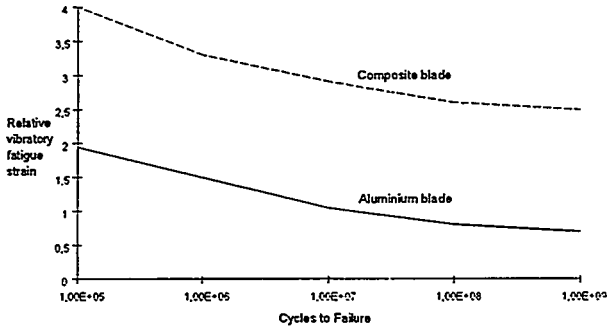

Comparison of fatigue strain capabilities between composite and aluminium blades

Figure 7

5.2 Pressure Vessels

An industry which is expanding at a rapid rate is that of the filament wound pressure vessel manufacturing sector. Low weight filament wound high pressure vessels are becoming increasingly popular in the transport sector where the vessels are used for the storage of natural gas as an alternative to traditional petroleum based fuels. These vessels are subjected to pressure fatigue loading during a lifetime of being filled and unfilled with pressurised gas. Carbon fibre (CFRP) is used in preference to glass (GFRP) because of a better fatigue life and strain performance.

The reason for this increased usage is the rising legislative and environmental pressures on automotive emissions. Major uses at present are for public transport buses and coaches within urban environments.

Certification of filament wound pressure vessels is a major issue within Europe[8], there is a growing interest in a European ISO standard, which should become a reality in the next couple of years.

The market for these pressure vessels is expected to rise in coming years as the use of natural gas propulsion becomes more accepted and CFRP is accepted in preference to more traditional metal materials such as aluminium and steel.

5.3 Wind Turbine Blades

Due to the cost drivers within a very competitive industry, CFRP is seldom but increasingly used for the manufacture of blades. In an industry which is still dominated by labour intensive, hand laminating techniques glass fibre reinforced plastic, ie E-glass and unsaturated polyester resin, are the primary materials.

In specific applications CFRP has played a role in the european wind energy sector. Eight metre CFRP blades are in full production with two major manufacturers. In predominantly GFRP blades CFRP has found niches, for example the tip shaft of blades which are produced from carbon filament wound structures.

6. Advantages and Barriers of using CFRP in Wind Blades

6.1 Cost

From a technical standpoint (ie mechanical properties and fatigue life) CFRP is the ideal material for the production of wind blades. However as mentioned previously cost is the major reason that CFRP is not in more widespread use in the industry. In the future the cost of the yarn per kilogramme will reduce slightly as volume increases. Another factor in the cost of materials used for component manufacture is the weaving cost for the production of fabric.

The use of heavier tow yarns, heavier fabrics and more direct placement tow techniques during component manufacture (filament winding, braiding) would assist in cost reduction exercises, but in general the relatively high unit price in comparison to other fibres is due to the high processing cost and is compensated by a more structurally advanced material.

Maintenance reductions and low inspection for wind blades due to the extended fatigue life and higher mechanical properties would also incur an operating cost saving.

6.2 Processing

Apart from a few small blade manufacturers (8-9m), the majority of the industry is steeped in hand laminating tradition using GFRP and lower cost unsaturated polyester resins. Efficiency in processing where large savings and better quality manufacture can be made will result is lower wastage, possibly allowing the future use of CFRP.

6.3 Life cycle

The fatigue life of CFRP is essentially better than GFRP and thus long term life cycle savings can be made.

6.4 Weight Reduction

The much higher stiffness and rigidity of using CFRP allows better efficiency of the overall turbine and the design can be improved, at lower overall weights. Due to thinner structures however buckling of stresses skins and structures could complicate designs and manufacture.

6.5 Material Specifications and Testing Requirements

At present there are no European material specifications or specific testing standards common procedures relating to the wind blade manufacturing industry. Due to this factor the material requirements and needs for the wind blade manufacturing industry are obscure. Existing standards used within this sector require examination and any new specifications and universal testing methods have to be considered together, as a complete system. This will be necessary to maintain a competitive european industry.

7.0 Conclusions

- Better and more unified specifications are required in the European wind blade manufacturing sector with possibly an ISO standard.
- Better manufacturing methods and processing costs will increase use of CFRP.
- Higher material property and longer life requirements will demand the use of CFRP materials.

References

1. Kinsella, M.A., Carbon Fibre, A European View of the Applications, The Professor Anthony Kelly Symposium, 1994, Elsevier.
2. Blumberg, H., Carbon and Aramid Fibres, Kunststoffe German Plastics, 77. Jahrgang 1987/10.
3. Stolze. R., Reinforcing Fibres and Matrix Materials for High Performance Composite Materials, Kunststoffe German Plastics, 11. Jahrgang 1987.
4. Lowe, G.A. & Satterly, N.D., Fatigue Properties and Design of Wing Blades for Wind Turbines, Final Report for ETSU contract W/44/00230. UWE 1993.
5. Cler, S., Fatigue Properties of Composites Materials Autoclave Processed from Carbon-Epoxy Woven Fabric Prepregs, 36th International SAMPE Symposium, April 15-18, 1991.
6. Owens Corning Technical Information.
7. Salkind, M.J., The Twin Beam Composite Rotor Blade, Fibre Science and Technology, 4.75, pp91-102.
8. Mayer, R.M., Design with Reinforced Plastics, Design Council, 1992.

FATIGUE BEHAVIOUR OF FIBREGLASS WIND TURBINE BLADE MATERIAL UNDER VARIABLE AMPLITUDE LOADING.

D.R.V. van Delft[♦], G.D. de Winkel[♦], P.A. Joosse[♠]
[♦]Delft University of Technology, STEVIN laboratory
P.O. box 5048, 2600 GA DELFT, THE NETHERLANDS
[♠]Stork Product Engineering b.v.
P.O. box 379, 1000 AJ AMSTERDAM, THE NETHERLANDS

ABSTRACT: In the work presented here fatigue tests with the WISPER and WISPERX load sequence have been carried out and analysed. The test programme includes tests at low stress levels which results in fatigue lives of 50 millions of cycles. The results are compared with constant amplitude tests in the very high cycle range, carried out in a previous programme. The results are also compared with ECN results in the lower cycle range (on identical specimens). It appeared, that the difference between the fatigue life of the specimens tested with the WISPER and the WISPERX load sequence is larger than can be expected from the theoretical damage rates. Moreover, the slope of the S-N data differs from theoretical values obtained by using commonly applied design rules.

NOTATION

a,b	Constants
N	Number of cycles
N_f	Number of cycles at failure
R	Ratio between minimum and maximum stress during a cycle.
UCS	Ultimate compressive strength
UTS	Ultimate tensile strength
σ_{amp}, S_{amp}	Stress amplitude of a cycle
$\Delta\sigma, S_{range}$	Stress range during a cycle (=2.S_{amp})

1 INTRODUCTION

In the structural design of a wind turbine rotor blade a fatigue analysis is important. In the design operational life the number of cycles in the fatigue loading is in the order of 100 to 1000 millions. The design loading is a variable amplitude loading. The stress spectrum is different for the different turbines and locations on the blade.
The design curves for fatigue are merely based on results of tests on coupons loaded with a constant amplitude. The compilation from the design stress spectrum to these constant amplitude results is based on rules (Miner, Goodman etc.) established for other materials.

To check to validity of these rules, variable amplitude tests on coupons have been carried out using the standard WISPER or WISPERX test load sequence. The fatigue test programme using variable amplitude loading reported here is a follow-up of a test programme using constant amplitude loading. In this previous programme [1] tests on a rather low stress level were carried out in order to obtain the fatigue behaviour in the very high cycle range (500 millions of cycles). Together with tests carried out at ECN on the same specimen at the lower cycle range, the S-N curve could be established.

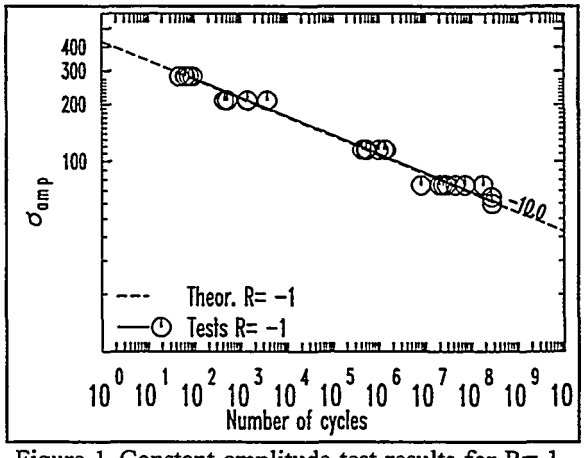

Figure 1 Constant amplitude test results for R=-1

For this research programme on variable amplitude loading, tests were carried out at ECN and TU-Delft using the same specimen. Again the lower and high cycle range tests were carried out at ECN and the Stevin laboratory of TU-Delft respectively. The material used for the specimen was considered to be typical for glass fibre reinforced material used for rotor blades.

2 FATIGUE FORMULATIONS

In design rules the S-N curve for constant amplitude loading at an R-ratio of -1 is used as a basis. Basically two possibilities are applied for the relation between the stress (or strain) and the number of cycles:

$$\log(N_f) = a + b.\Delta\sigma \quad (1)$$

$$\log(N_f) = a + b.\log(\Delta\sigma) \quad (2)$$

or alternatively:

$$N_f = a.\sigma_{amp}^{b} \quad (3)$$

The constant b in these formulae is referred to as the slope of the S-N curve. From the constant amplitude test results[1] it was concluded that the relation between Stress (or Strain) and Number of cycles is a double logarithmic one (log-log) which is expressed by equation (2). These test results for R=-1 are given in fig.1 together with the linear regression lines using equation (2). Also plotted in this figure is a dashed line with a slope of -10 which intersects at vertical axis (N=1) at the UTS value. Apparently this line describes the fatigue behaviour of this material at R=-1 accurately. This line is expressed by:

$$N_f = \left(\frac{\sigma_{amp}}{UTS}\right)^{-10} \quad (4)$$

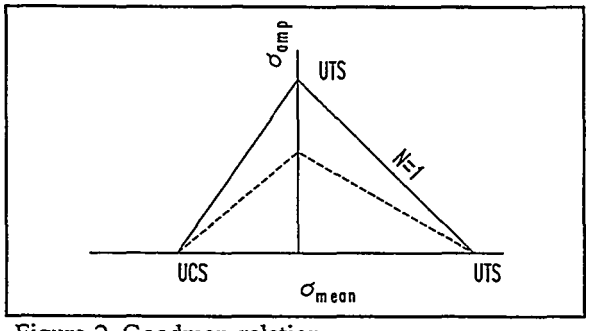

Figure 2 Goodman relation

To obtain the number of cycles to failure for other R-values, Goodman type relations can be applied. In many design codes the Goodman relation given in fig. 2 is used. This diagram gives the relation between the amplitude of a stress cycle and the mean value for a arbitrary number of cycles. Using this relation together with equation (4) leads to the following fatigue formulation:

$$\sigma_{mean} > 0: \quad N_f = \left(\frac{\sigma_{amp}}{UTS\left(1-\frac{\sigma_{mean}}{UTS}\right)}\right)^{-10}$$
$$\sigma_{mean} < 0: \quad N_f = \left(\frac{\sigma_{amp}}{UTS\left(1-\frac{\sigma_{mean}}{UCS}\right)}\right)^{-10} \quad (5)$$

For a mean stress level of zero (R=-1) this reduces to equation (4).

3 THE WISPER AND WISPERX LOAD SEQUENCE

3.1 WISPER

In order to test material under variable amplitude, the WISPER load sequence was established[2]. This load sequence is based on measured data and therefore will contain cycle sequences being more or less representative for blade material. However, it is supposed to be a load sequence for material testing only and not for design purposes.

3.2 WISPERX

To reduce testing time, the WISPERX load sequence was established by omitting the small cycles the WISPER load sequence. This resulted in a reduction of the number of cycles by a factor of 10. Since only the small cycles are omitted, the difference in damage rate could be expected to be negligible. However, the actual calculated difference in damage rate between the WISPER and WISPERX spectrum will depend on the fatigue formulation applied (slope in S-N curve, Goodman relation etc.)

3.3 Cycle counting results

In fig. 3, the cycle counting results (using the rainflow or range pair range counting procedure) are given. On the left side the result is given applying the counting procedure directly on the sequence, whereas on the right side the result is given applying the counting procedure in a

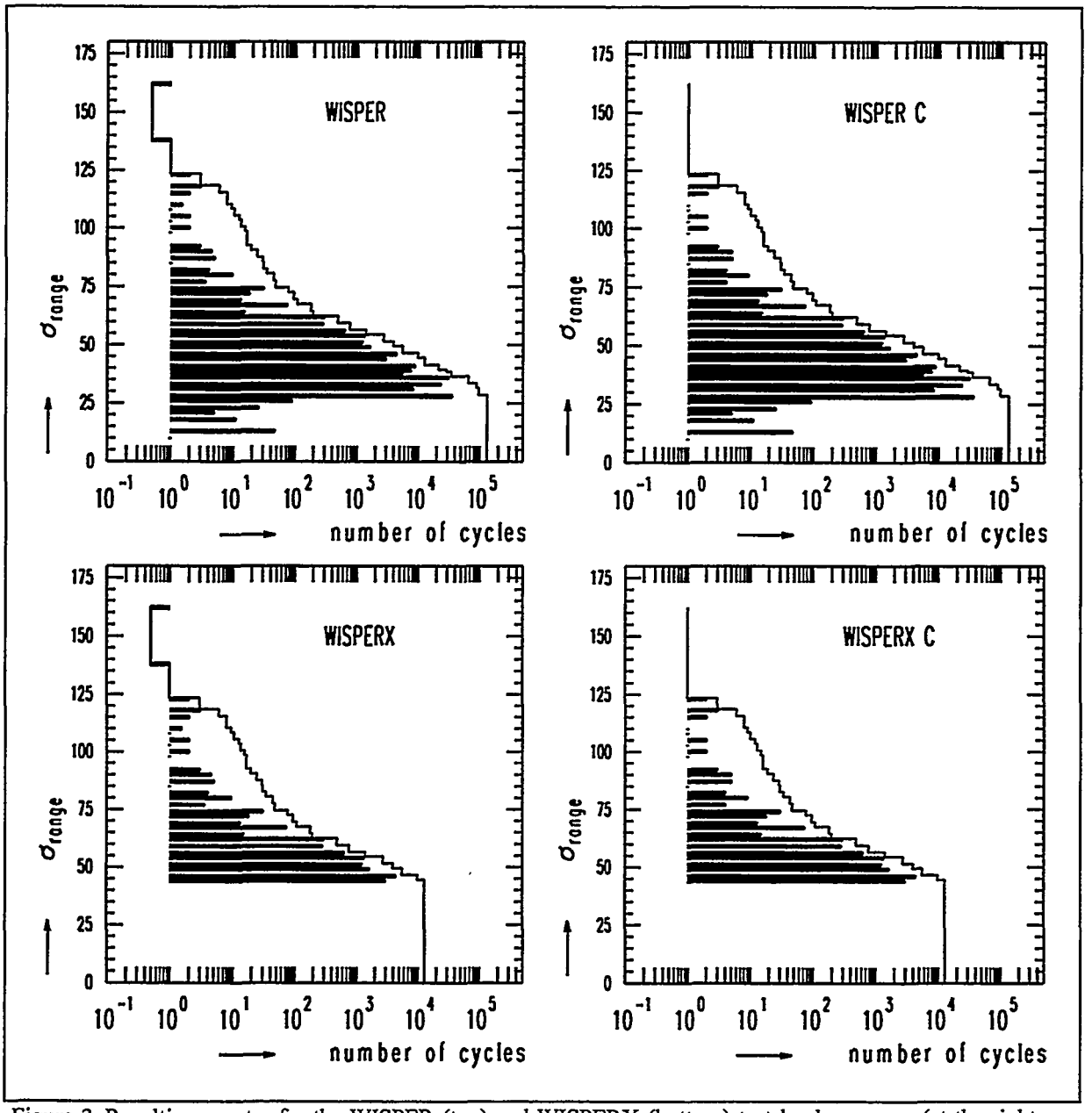

Figure 3 Resulting spectra for the WISPER (top) and WISPERX (bottom) test load sequence (at the right side: results using a cyclic counting procedure).

(see top of spectra) occur due to the fact that the test load sequence does not start at an overall maximum or minimum. Since the load sequence is repeated many times the cyclic counting is supposed to be the correct one to use.

3.4 Theoretical damage

Applying equation (5) and using a Miner summation, the theoretical number of sequences to failure can be calculated.

The results of such calculations are given in table I. In this table the number of sequences for a damage rate of 1. are given. These were calculated for a maximum stress level of 200 MPa and a material with a UTS and UCS value of 428 and 291 MPa respectively. Moreover, the slope of the line through the number of sequences for different stress levels are listed.

The differences between WISPER and WISPERX are negligible (whitin 10 percent). The differences between the cyclic and non cyclic rainflow counting is modest and in the order of 20 percent. The slopes of the S-N lines in table I is ca. -12. This is a little different from the slope of -10 for the R-value of -1, which was used as a starting point of the fatigue formulation.

TABLE I Theoretical number of sequences for standard load sequence WISPER and WISPERX

Load Sequence	Type of Counting	Number of sequences to failure at σ_{max}=200 [MPa]	Slope of S-N line
WISPERX	cyclic	3110.7	-11.6
WISPER	cyclic	2924.1	-11.8
WISPERX	non-cycl	3818.0	-12.0
WISPER	non-cycl.	3540.0	-12.2

4 EXPERIMENTAL

4.1 Test programme

Tests have been carried out with the WISPER and WISPERX load sequence at relatively low strain levels. The tests carried out are together with the results listed in table II

4.2 Material and specimen

The specimens used, are from the same batch as those use for the previous constant amplitude test programme[1]. The specimens are delivered by ECN and the same as the "batch one" specimens used in the ECN tests. The specimens were cut out from a glass fibre reinforced plastic plate of 8.5 mm thickness. This plate consists of 7 layers of 500g/m^2 unidirectional and 8 layers of 480g/m^2 ±45° glass fibre in a symmetrical hand lay-up. More detailed information about specimens is given in [3].

4.3 Testing

The same test rigs were used as for the constant amplitude tests [1]. Also the clamping and aligning of the specimens was done equally except for the fact that now only one specimen in a test rig was tested simultaneously.

The WISPER and WISPERX loading was applied to the specimen with sinusoidal shapes between each pair of extremes. The frequency of each cycle is proportional with the amplitude. The average frequency was approximately 16Hz. With the use mechanical ventilation this resulted in a measured temperature below 35 degrees Celsius at the surface of the specimen.

5 RESULTS

The results of the tests are given in table II. In fig. 4 the results are plotted including the test results from ECN using the specimens from the same batch. The dashed lines are the regression lines for the ECN results only.

TABLE II Test results

Test	Load Sequence	Smax [MPa]	Nunber of sequences	Nunber of Cycles
15	WISPERX	170	871	11,175,801
20	WISPERX	170	397	5,093,907
22	WISPERX	160	890	11,419,590
23	WISPERX	225	133	1,706,523
24	WISPERX	225	70	898,170
25	WISPER	170*	227	30,125,397
26	WISPER	160*	177	23,489,847
27	WISPER	170	454	60,250,794
28	WISPER	170	339	44,989,029
29	WISPERX	160	1495	19,182,345
30	WISPER	160	328	43,529,208

*) taken out before complete failure

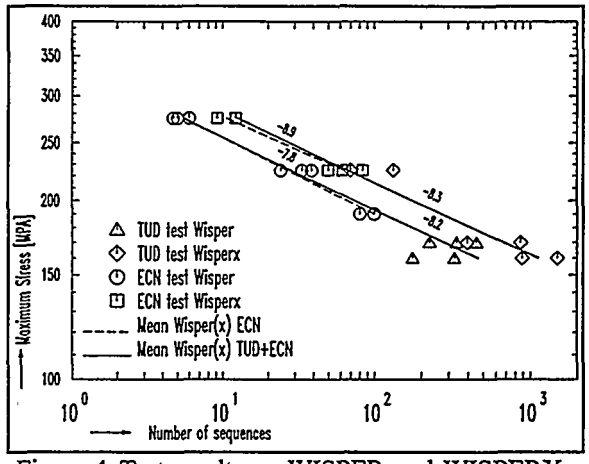

Figure 4 Test results on WISPER and WISPERX test (ECN results from [3])

6 DISCUSSION OF THE RESULTS

6.1 Difference between WISPER and WISPERX results

As shown in table I, the expected difference in number of sequences to failure between test results using the WISPER and WISPERX load sequence is expected to be negligible (les than 10 percent). Although not reported here, applying other Goodman type relations does not lead to different expectations.

However, the difference in the test results is significant and about a factor of two on number of sequences. Furthermore the slope of the S-N line is different from the theoretical expected value (about -8 instead of -12). This is true for the ECN results as well as for the TU-Delft results which coincide very accurately.

6.2 Comparison of test results with expected values

Applying equation (5) and using a Miner summation, the theoretical number of sequences to failure can be calculated.
By doing this for different stress levels (σ_{max}) a complete S-N curve can be obtained

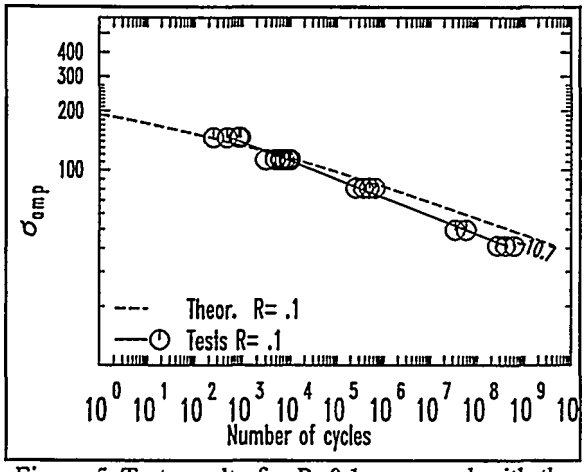

Figure 5 Test results for R=0.1 compared with the theoretical S-N curve.

For comparison this S-N curve is calculated for constant amplitude at R=0.1 and plotted in fig. 5 together with the test results from the previous programme. This curve is not a straight line due to the fact the Goodman relation is based on linear values of the stresses or strains. Although the slope of the tests and theoretical curve appears to be slightly different there is a good agreement. This supports that the S-N formulation is appropriate.

In fig. 6, the test results of the WISPER and WISPERX tests are given together with the theoretical S-N curves. It shows that the tests experience a fatigue life which is much shorter than expected, especially in case of the WISPER results. At the lower stress levels tested (S_{max}=150MPa) the WISPER test results show a fatigue life which is shorter by a factor of hundred. Furthermore the slope of an S-N curve based on the test is much "steeper" than for the theoretical line.

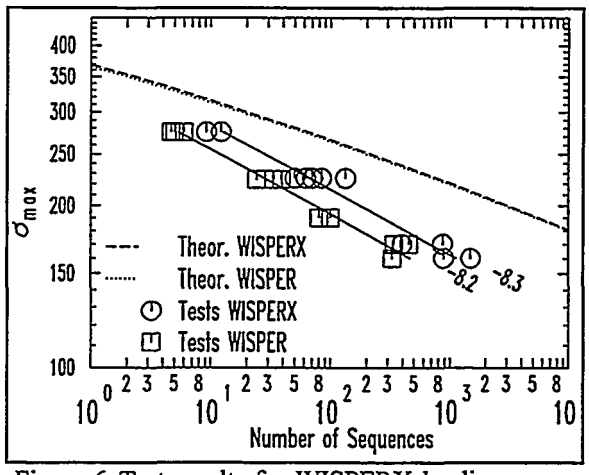

Figure 6 Test results for WISPERX loading compared with the theoretical S-N curve.

7 RELEVANCE OF THE RESULTS WITH RESPECT TO THE DESIGN SITUATION.

It appears that the assumed fatigue relation, which is in agreement with the constant amplitude test results, is not valid for the variable amplitude loading sequence. The variable amplitude loading situation leads to a much shorter than expected fatigue life. Due to the difference in slope the difference will be more pronounced at lower stress or strain levels.

For a typical design situation with for instance a maximum allowable stress level of 100 MPa, the fatigue life under the WISPER sequence appears to be more than a factor of 100 less than expected on the basis of accepted design fatigue formulations which have constant amplitude fatigue test results as a basis. On the basis of stress or strain level the difference is in the order of 1.5.

The reason why the WISPER and WISPERX load sequences are more severe than expected is not clear yet and has to be investigated in order to develop a more reliable fatigue formulation as is generally applied. These load sequences are also more or less artificial so the actual situation can be more benign or more detrimental than this factor of hundred in life. From the fact that the WISPER spectrum leads to a shorter number of passes, it could be concluded that in a variable amplitude load sequence the lower

amplitude cycles are more detrimental than expected according the currently applied fatigue formulations.

In many design codes (partial) safety factors are applied for the material strength and fatigue behaviour. This might be sufficient to cover the unexpected difference between the expected and actual fatigue lives for this material under variable amplitude (WISPER type) loading. However, most of the factors are needed to deal with the other differences in behaviour of the material under test and operational conditions. The test conditions are more benign than the operational condition with respect to ageing, humidity, temperature etc. Furthermore the fabrication of small specimens might result in a higher quality of the material than in a full scale blade.
If the applied safety factors are basically to cover these differences there might be not enough left to cover the possible unexpected lower fatigue life under variable (operational) loading.

9 CONCLUSIONS

Fatigue tests on GRP rotor blade material have been carried out using the WISPER and WISPERX load sequence.

- The test results suggest that the fatigue life under WISPER and WISPERX loading is about a factor of hundred less than could be expected from the currently applied fatigue formulations.
- The slope of the S-N curve following from the test results is different from the expected one (-8 instead of about -12).
- The fact that the fatigue lives (in number of passes) under WISPER is less than under WISPERX, might be an indication that especially the lower amplitude cycles are more detrimental than expected.
- It is questionable whether the level of the generally applied (partial) safety factors in the design are sufficient to cover this discrepancy.

10 REFERENCES

[1] D.R.V van Delft, P.A Joosse, H.D Rink
Fatigue Behaviour Of Fibreglass Wind Turbine Blade Material At The Very High Cycle Range
Proc. EWEC'94, pp 379-84, Thessaloniki 1994

[2] A.A. ten Have
WISPER: A Standardized Fatigue Load Sequence for HAWT blades.
Proc. EWEC'88

[3] P.W. Bach
Fatigue properties of glass- and glass/carbon-polyester composites for wind turbines.
ECN-C-92-072, November 1992

Which Slope for Gl-Ep Fatigue Curve?

Chr. W Kensche
DLR Stuttgart

4th IEA-Symposium on Wind Turbine Fatigue
1/2 February 1996

Objective

In many cases, the certificated fatigue life of rotor blades is assessed by symply using the slope of the specific material in an s-n curve in combination with a static value. The static values of the material must be known. The slope - if no measured properties are available - can be taken according to a proposal made in [1,2], if the blade shall have the GL-certification. For a long time, the slopes defined in [1] were in use, i.e. k=9 for glass-polyester (Gl-UP) and k=12 for glass-epoxy (Gl-Ep). In 1995, the figure for Gl-Ep was changed into k=10 [2]. From DLR-measurement on Gl-Ep and their evaluation, an increase of the slope anticipated for this material close to the first value might be possible.

Justification

DLR was involved in fatigue testing of Gl-Ep for wind turbine rotor blades mainly in two programmes of the EU, the Concerted Action "Material Testing" (CA) and JOULE 1, which took place from 1986 to 1993..

In the CA programme, the emphasis was on high cycle fatigue up to 10^8 load cycles. The tests are described and statistically evaluated by application of the Sendeckyj method in [3]. Two lay-ups were investigated, UD (Type 1A) and ±45°/UD (Type 2A). For considering the slopes, only the fatigue curves at stress ratios R=-1 were evaluated. The slope for 1A was k=10, for 2A it was k=8.5, see Tab.1, Fig.1 and Fig.2.

In the JOULE 1 programme again the 2A material was tested. The emphasis was to compare dry and wet conditioned material [4]. The statistical evaluation of the tests at the dry 2A material showed a slope of k=13, see Tab.1 and Fig.3.

Since the 2A material of the two programmes CA and JOULE 1 was identical, a pooling of the data was made which led to a slope k=11.5, see Tab.1 and Fig. 4. Fig.4 shows clearly that the three high cycle fatigue points are far below the mean curve. This indicates that the consideration of these points as sound tests was not correct. Indeed one of them was a runout, and the failure of the other specimens was doubtful. Therefore a second evaluation was made by censoring these three tests which resulted in a slope of k=12.1, see Tab.1. The censoring of runouts and doubtful results was also applied to the 1A material reported in [3] which resulted in a slope of k=11.2, see Tab.1. This indicates that a pooling of the data of 1A and 2A should be investigated.

The feed back of these evaluations is that in the CA programme, the lowest strain levels applied seem to have been too low. These long term test results ended too early. Thus, they steepen the slope of the fatigue curve. By means of the censoring possibility in using the Sendenckyj method, a correction was carried out which shows that a slope of k=11÷12 seems to be possible for the Gl-Ep material tested.

References

[1] *Richtlinie für die Zertifizierung von Windkraftanlagen, Chapter 5.2* Germanischer Lloyd, Ausgabe 1993

[2] *Mitteilung zur Änderung der Wöhlerlinie von GFK-Teilen aus Epoxid-Harzen,* Germanischer Lloyd, 07.07. 1995

[3] Ch.W. Kensche (ed.) et al., *Fatigue of materials and components for wind turbine rotor blades,* EUR 16684 EN, 1996

[4] Ch.W. Kensche, *Environmental Effects on Gl-Ep Material and Tests on Blade Components with T-Bolt Load Attachment,* DLR, FB 94-09

Programme	Lay-Up	Stress ratio	Weibull Parameters		Model Parameters			Correction by
		R	α	β	C	S	k=1/S	Censoring?
CA	UD	-1	13,405	2,447	0,196	0,1	10,0	no
CA	±45°/UD	-1	20,109	2,236	0,01744	0,11756	8,5	no
JOULE 1	±45°/UD	-1	15,812	2,312	0.92	0,0772	13,0	not necessary
JOULE 1 + CA	±45°/UD	-1	13,988	2,230	0,22	0,0868	11,5	no
JOULE 1 + CA	±45°/UD	-1	15,717	2,242	0,364	0,0824	12,1	yes
CA	UD	-1	16,477	2,478	0,624	0,08952	11,2	yes

Table 1: Slope and statistical paramaters of Gl-Ep fatigue curves

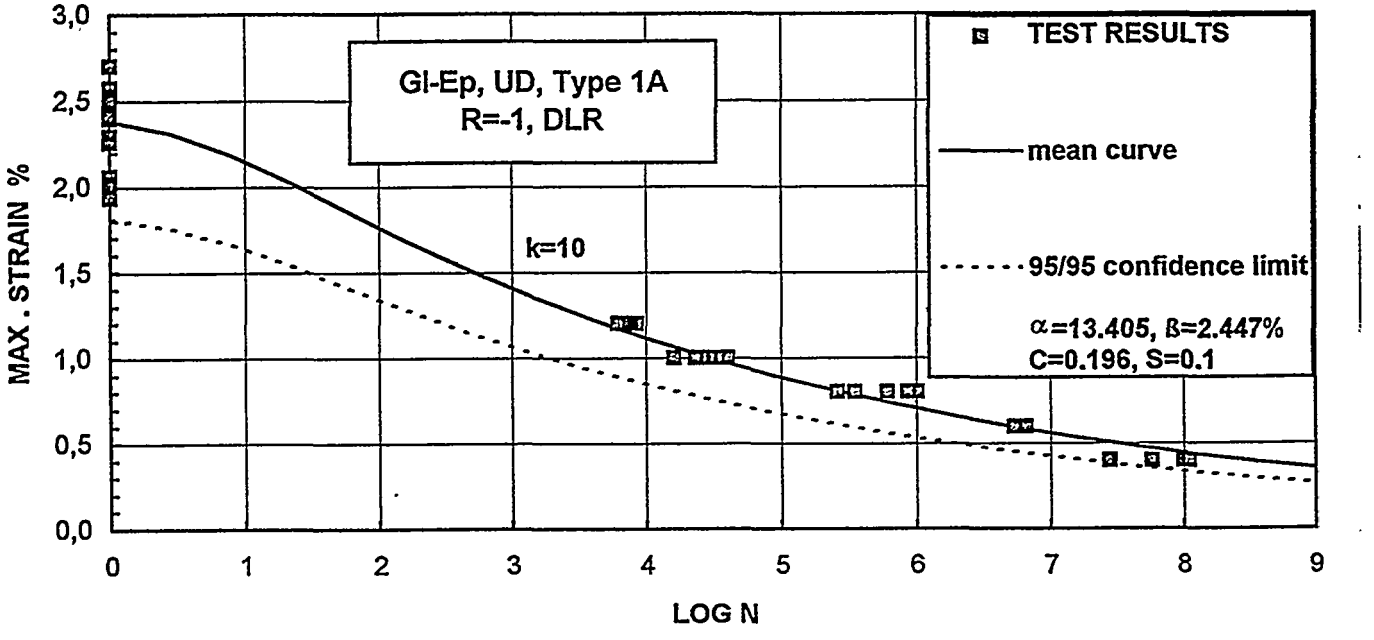

Figure 1: Fatigue curve of Gl-Ep, type 1A, programme CA, not censored

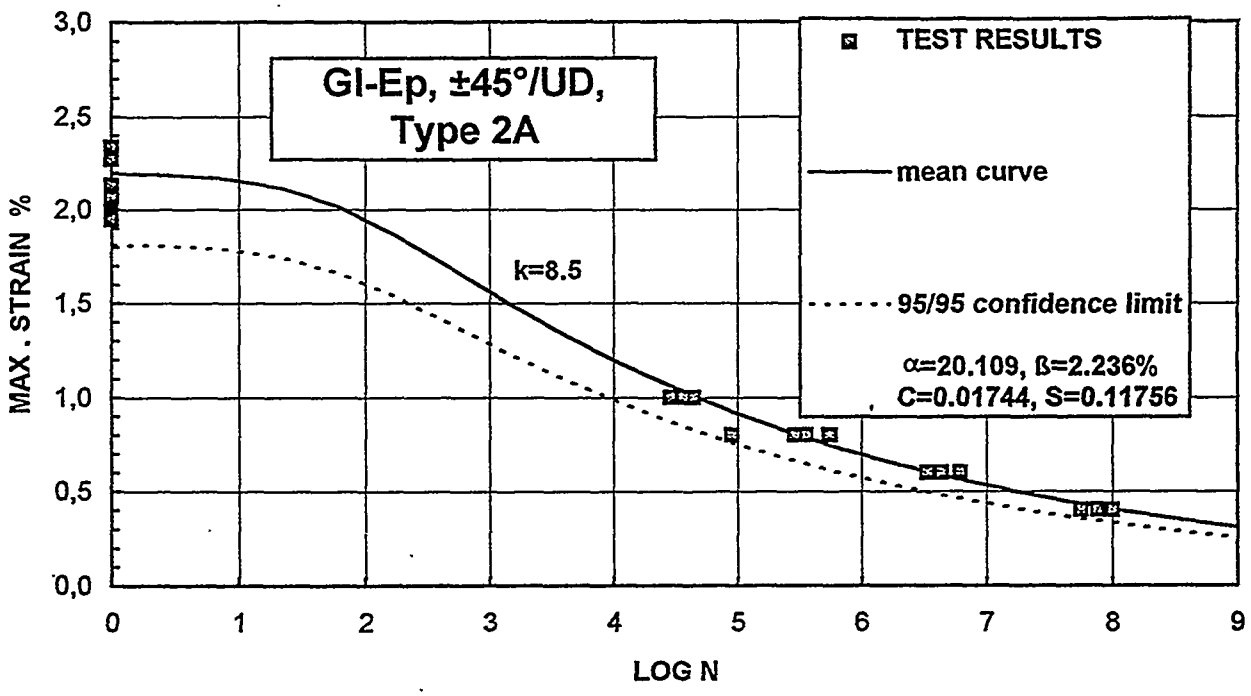

Figure 2: Fatigue curve of Gl-Ep, type 2A, programme CA, not censored

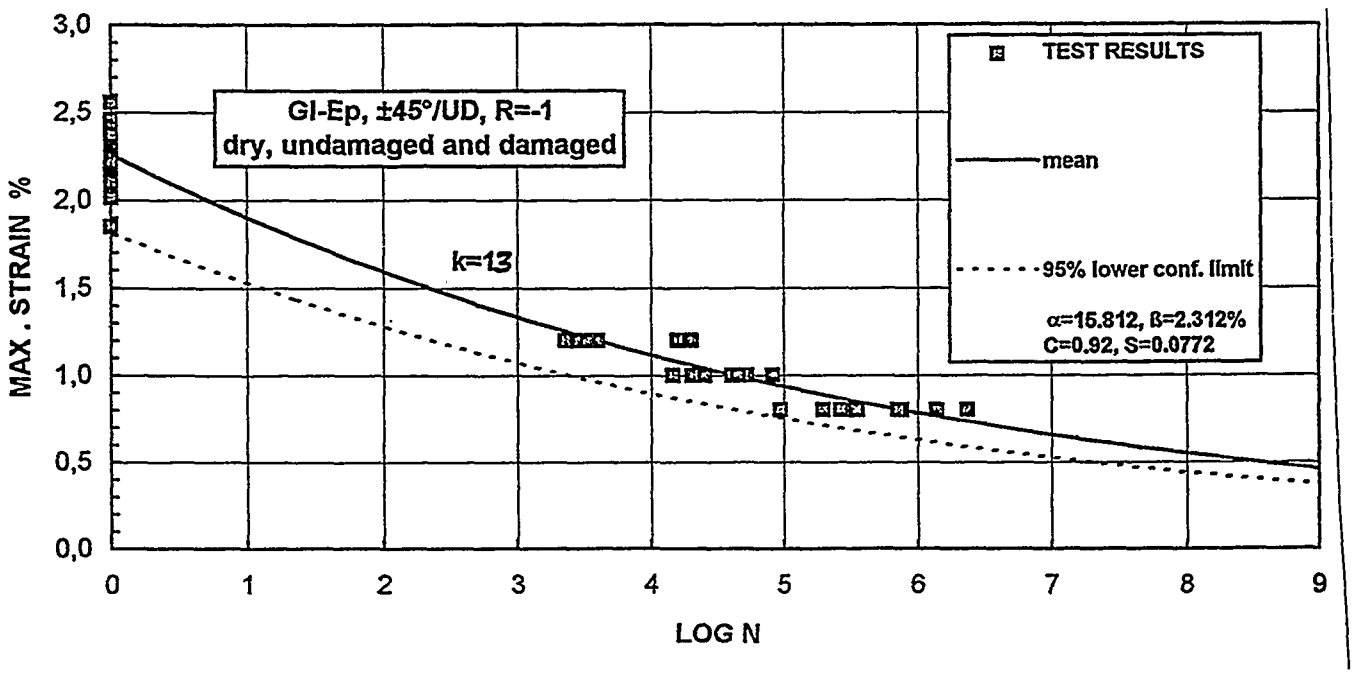

Figure 3: Fatigue curve of Gl-Ep, type 2A, programme JOULE 1, not censored

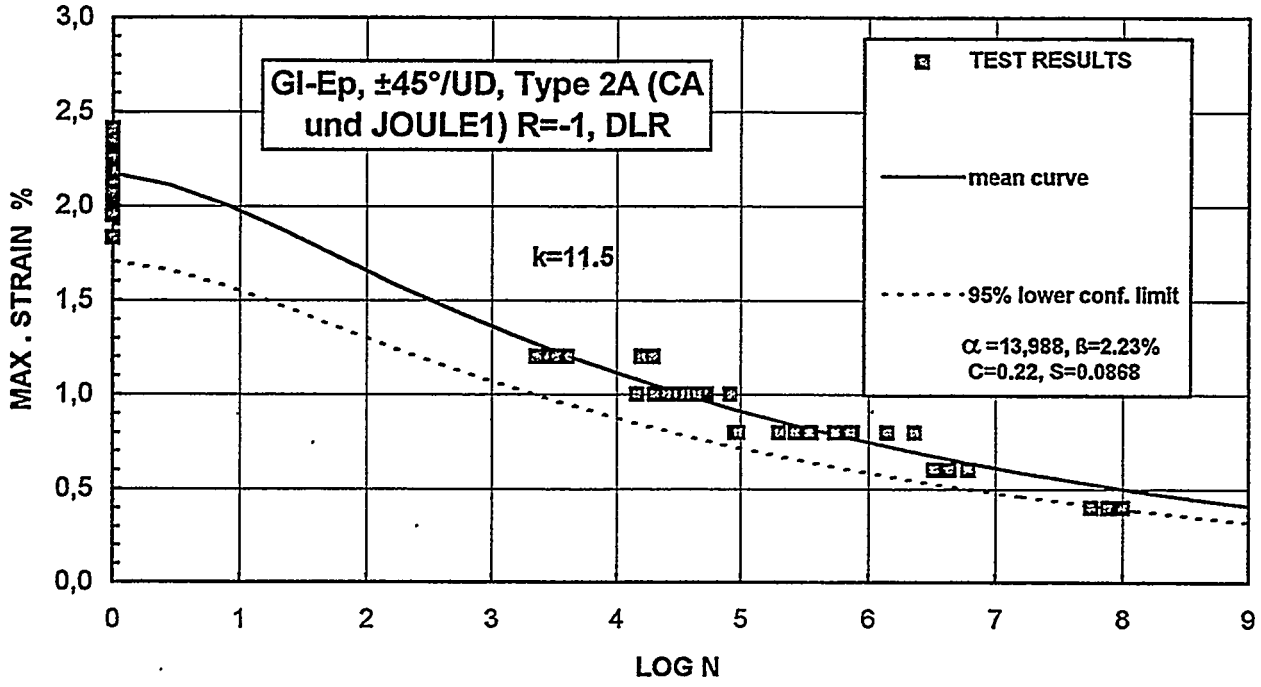

Figure 4: Fatigue curve of Gl-Ep, type 2A, pooled data of the programmes CA and JOULE 1, not censored

EN-WISPER: RESEARCH OVERVIEW AND CONSEQUENCES

Peter Joosse
Stork Product Engineering B.V.
Amsterdam, the Netherlands

ABSTRACT

Humidity can have a considerable effect on the fatigue life time of glass reinforced matrix products. Simple pre-conditioning of specimens have shown a degradation by a factor of 10. Within the EN-WISPER research an accelerated climatological cycle has been defined, based upon the Dutch climate. Pre-conditioning of fatigue specimens with this cycle does however not lead to a significant change of the fatigue lifetime. The paper reflects some of the discussions on possible follow-up work.

1 INTRODUCTION

A wind turbine rotor blade operates in an environment which can be best characterized as fluctuating: temperature, humidity and wind speed (magnitude and direction) change continuously. Fluctuations in the blade loads result mainly from wind fluctuations and can adequately be predicted by computer codes now available. The strength of the material is a function of the loads and the environment. The influence of the environment has been explored with simple pre-conditioning methods, e.g. as reported in [1] for bolted joints. This influence may be considerable: the lifetime may decrease one order of magnitude.
In the Netherlands it was felt necessary to verify whether a fluctuating environment would give more degradation in a (mechanical) fatigue loading. A research program was started within the Dutch national fatigue research on this topic. The research was carried out by KEMA and has in part already been reported at a former expert meeting [2].
Presently the research has been finished. In this contribution an overview will be given of the results with the aim to start a discussion on the necessity and the topics of this type of research.
Remarks made during the discussion which was held during the expert meeting are given.

2 SUMMARY OF RESEARCH

The EN-WISPER research has been carried out by KEMA and has been reported in full in [3] and [4]. The major results will be mentioned here without the will to be complete. Detail information can be found in the literature mentioned.

2.1 Objective of the research

In the past a wide range of specimens and fatigue loading types has been explored. A minor part of the fatigue research has been directed towards 'wet' specimens. These specimens showed a degradation in fatigue lifetime with a factor of 10-50, see e.g. [1] and [5].
It was expected that fluctuating climatological conditions would have a detrimental effect on the fatigue life.
It was assumed that this effect could be shown with a suitable pre-conditioning of the specimens. If pre-conditioning would not be valid a combination of climatological and mechanical spectra should be used.

The research was aimed towards the following topics:
-1- compare actual humidity level to coupons
-2- develop an accelerated cyclic environmental test to be used as pre-conditioner for load spectra
-3- compare test results of pre-conditioned test specimen with dry specimen

The actual humidity level should be measured from details of a commercial blade for which the life history is known.
The accelerated cyclic environmental test should be based upon the Dutch climate, but the generic approach should make other applications possible.
The combination of cyclic environmental testing in combination with a variable amplitude load testing is called EN-WISPER.

2.2 Results

A commercial blade of Aerpac, exposed outdoor to the environment for 4 years, has been used to measure the humidity level. Different coupons were taken from the blade. The measured humidity level is approx. 0.25%, which is claimed to correspond nicely to calculations. This level also corresponds to moisture levels found

after simple pre-conditioning (14 days in water) [1].

The environmental spectrum is based upon the Dutch climate, as monitored for four years at one site. For one year three different sites were monitored. Temperature and humidity were binned with a bin-size of 1 hour.
The increase of moisture content was calculated with the WW8GAIN program for this simplified yearly spectrum. Based upon the yearly spectrum a spectrum was then formulated with the aim to give a similar moisture up-take in one week.

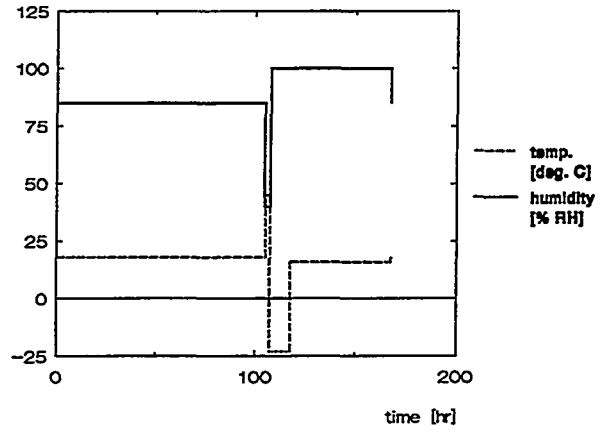

Fig. 1: Accelerated weekly climatological cycle

The weekly cycle as given in figure 1 is claimed to reach this aim. A typical example of the moisture up-take, as predicted by WW8GAIN, is given in figure 2.

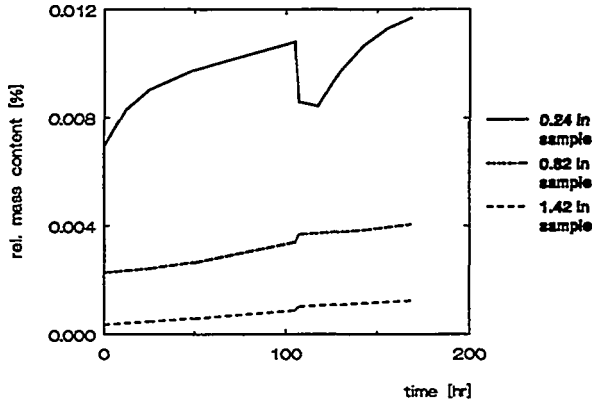

Fig. 2: Predicted result of weekly cycle.

The climatological cycling is carried out in a climate chamber using artificial water (pH=4). Specimens have been measured after each weekly cycle. It can be shown that equilibrium will not be reached after 20 weeks of exposure.
In cooperation with ECN several specimen types have been pre-conditioned for 20 weeks or more, the test results will be reported by ECN [4]. The results as given in figure 3 are preliminary results.

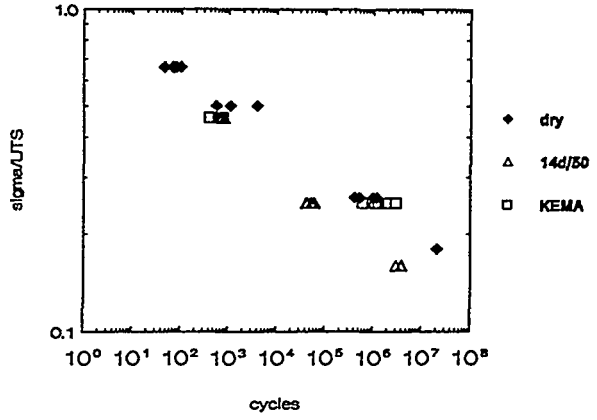

Fig. 3: ECN c.a. results (source: [3])

In the figure three batches of data are given:
'dry' unconditioned, dry tested,
'KEMA' conditioned at KEMA, sealed, dry tested,
'14d/50' conditioned 14 days at 50 °C, tested at 100% RH
From the results it can be concluded that there is no significant difference between the specimens tested dry. The specimens tested under 100% RH clearly show a decrease in life cycles.

3 CONSEQUENCES OF THE RESEARCH

At present not all results of the EN-WISPER research are available. Based upon the available information however, the following can be concluded.

1. Prolonged outdoor exposure of a commercial blade gives comparable moisture levels as the simple pre-conditioning method as used by ECN in the past. The results from the so-called 'wet' specimens seem therefore valid for wind turbine structures.
2. In view of the c.a. results there does not seem to be much influence of the history (dry or pre-conditioned) on the fatigue lifetime. A detrimental effect due to the environmental spectrum can not be shown from these data.
3. The testing conditions (wet or dry) seem to be dominant for this type of fatigue tests.

From these conclusions it follows that the prime ob-

jective of the research has not been met. realistic preconditioning of the specimen does not give a significantly different test result compared to non-conditioned specimens. The ambient climatological conditions during test, on the other hand, are dominant. Uncoupling of the environmental loading (temperature, humidity) and mechanical loading is therefore not allowed.

Assuming that the ambient climatological conditions are dominant should this therefore mean that a designer should take into account what percentage of time the product is in a wet environment ? For the Dutch climate this could mean that a rotor blade will be in a wet environment 30% of the time. Since the expected lifetime of a wet specimen is only 10%, this could lead to a overall reduction factor of approx. 1.15. For a off-shore turbine the reduction factor should then be 1.25.
It is clear that a methodology as given here would give rise to much discussion and confusion.

4 DISCUSSION ON FOLLOW-UP ACTIVITIES

As a consequence of the research a number of questions arise. Among them are:
- should a realistic fatigue spectrum exhibit a coupling between climatological and mechanical loading,
- which material factor shall be used to take into account the effect of environment ?

During the expert meeting several colleagues made their comments. The comments are given in the following.
- Since the inner layers do not reach a equilibrium state after 20 weeks of cyclic testing it may be wise to use thinner specimens for this type of testing.
- Matrix controlled mechanisms are more affected by climatological conditions. Fatigue testing in shear loading may therefore be more sensitive to the influence of humidity and temperature.
- It may be possible that one static test (on preconditioned specimens) gives enough information on the climatological influence.
- Matching the material reduction factor to the expected local environment seems to be a dangerous manner.
- For a thorough realistic spectrum a typical climate should be stated: wind, temperature and humidity. For typical control strategies (stall, pitch) a combination can be found for loads and environment. In view of the many possibilities it may be difficult to get consensus.
- To get a feeling for the influence of cyclic climatological conditions of fatigue test results a (climatological) block-loading could be used. The humidity level could be cycles between two extremes (e.g. 40% and 100% RH).

ACKNOWLEDGEMENT

The writer is indebted to mr. J.C.M. de Bruijn of KEMA for delivering the necessary information to serve as ammunition for this discussion. Furthermore the contribution of the participants of the 4. IEA symposium is gratefully acknowledged.
Inquiries on the EN-WISPER research should be directed towards J.C.M. de Bruijn, KEMA Inspection Technology, P.O. Box 9035, 6800 ET Arnhem, the Netherlands.
The EN-WISPER study is sponsored by NOVEM and the Dutch Electricity Distribution Companies.

LITERATURE

[1] P.W. Bach:"Fatigue properties of glass- and glass/carbon-polyester composites form wind turbines, *ECN report ECN-C--92-072*, November 1992
[2] J.C.M. de Bruijn et.al.: "EN-WISPER", *3rd IEA Symposium on Wind Turbine Fatigue*, 21-22 April 1994, Petten, the Netherlands
[3] J.C.M. de Bruijn: "EN-WISPER: Environmental influence on the fatigue behaviour of windtubine rotor blades, *KEMA document 50950-KIM 95-9313*, 20 November 1995
[4] P.W. Bach: "Results fatigue testing", *ECN*, to be published
[5] Ch.W. Kensche: "Lifetime of Gl-Ep Rotor Blade Material under Impact and Moisture", *3rd IEA Symposium on Wind Turbine Fatigue*, 21-22 April 1994, Petten, the Netherlands

IEC-TC88-WG8
Testing of rotor blades

D.R.V. van Delft (convener WG8)
Delft University of Technology
STEVIN laboratory
P.O. box 5048, 2600 GA DELFT, THE NETHERLANDS

ABSTRACT: In 1994 the TC88 of IEC installed a working group (WG8) to draft a guideline on blade testing. This paper gives a description of the task of the working group. Furthermore it gives a report of the progress of the work and summarizes the possible contents of the working group document on blade testing.

1 INTRODUCTION

Full scale tests can be used as a final verification of the structural design of a wind turbine rotor blade[1]. An increasing number of these tests are being carried out around the world. However, the methods of testing applied can differ in the various institutes (see photos 1-6). Also, the test load factors to be applied are based on the experience of the test laboratory, designer, national codes or certifying body. As a consequence the test load on the blade will differ and this may hinder or prevent general acceptance of the test results. This explains the need for a guideline or standard on blade testing. In 1994 the Technical Committee 88 (TC88) of the International Electrotechnical Commission (IEC) installed a Working Group (WG8) to draft a guideline on blade testing.

2 IEC-TC88-WG8

In 1988 the Technical Committee no. 88 (TC88) was established with the objective to develop standards for wind turbine generator systems (WTGS). At the start of the work of TC88, it installed three working groups which had to prepare the drafts on safety requirements. This has resulted in the international standard IEC 1400-1[2]. Later on TC88 installed

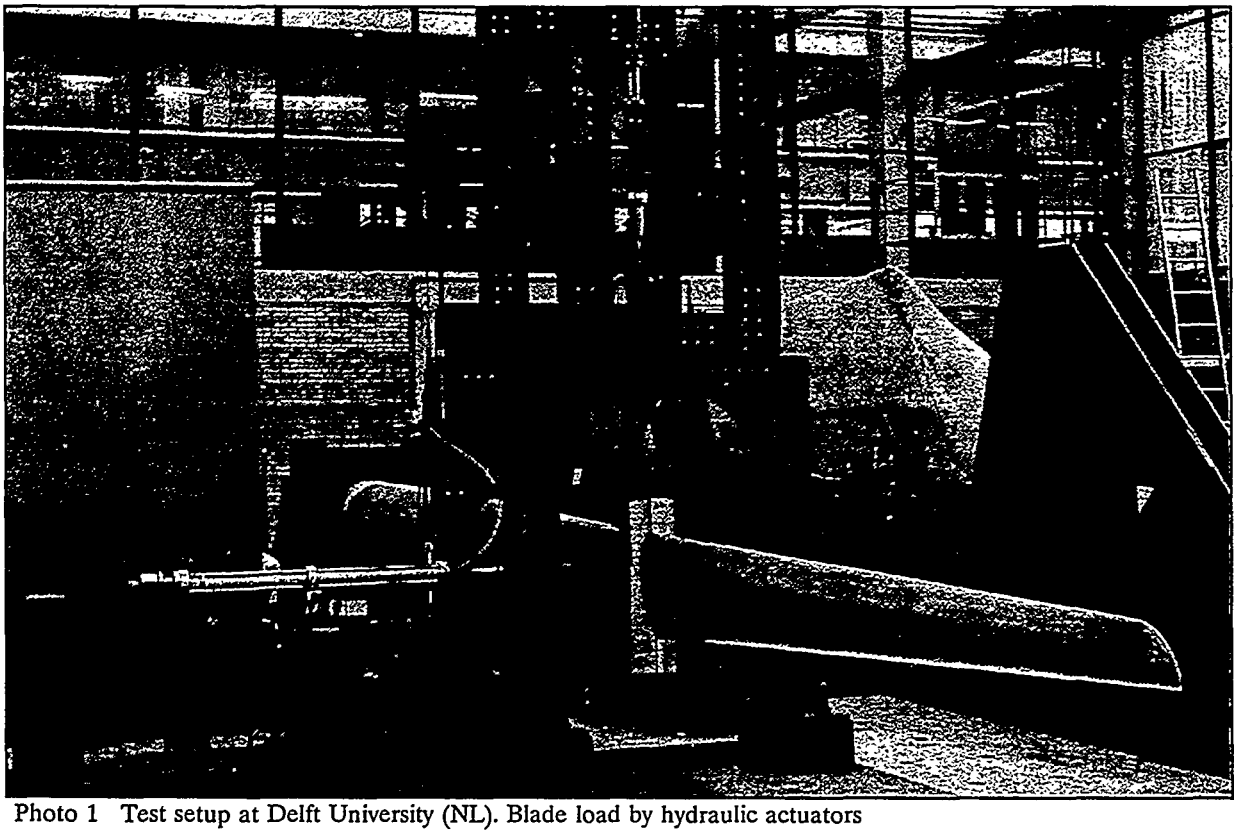

Photo 1 Test setup at Delft University (NL). Blade load by hydraulic actuators

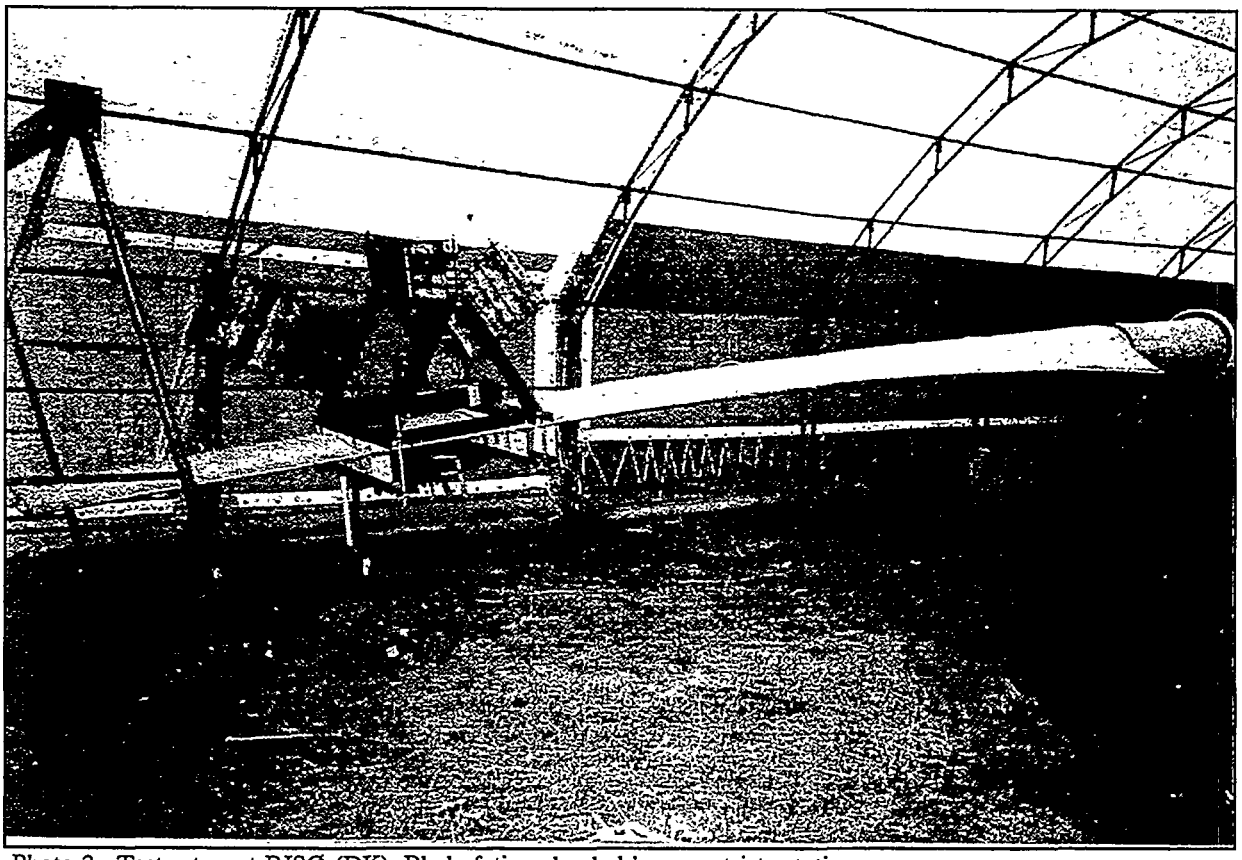

Photo 2 Test setup at RISØ (DK). Blade fatigue loaded by excentrict rotating mass

more working groups to draft standards or reports dealing with other aspects of WTGS. Untill now there are 11 working groups.

WG8 was installed in 1994 to draft a guideline on blade testing. The decision followed a proposal of the Netherlands but the need for a standard on structural testing of rotor blades was felt by many countries. The first WG8 meeting was held in May 1994.

3 TASK DESCRIPTION OF WG8

The WG8 was given the following task description:

To draw up a document that gives guidance for carrying out fatigue testing and ultimate strength tests on rotor blades as a possible part of the design verification. The work will include the following aspects:

- The methods and procedures for carrying out the tests
- The methods and procedures to evaluate the test loading with respect to the design loading
- The possibility to include the test results in the design assessment.

4 TIME SCHEDULE

After the first meeting in May 1994 six other meetings followed untill now. At this moment the WG considers that one or two more meetings are required to finalize the draft document. The next meeting is scheduled in October this year. The document is more or less complete but some sections are still being modified and have to be further reviewed and discussed.

The original target date for the draft was December 1995. However the WG felt that the draft at that time had not reached a sufficiently mature status. The working group draft is now expected to be finished by the end of 1996.

5 SCOPE OF THE DOCUMENT

The document is intended to be used as a guideline for full scale testing of blades of a WTGS as a possible part of a design verification of the integrity of the blade. The tests considered in the document are:

- static tests
- fatigue tests

It is assumed that the data required to define the

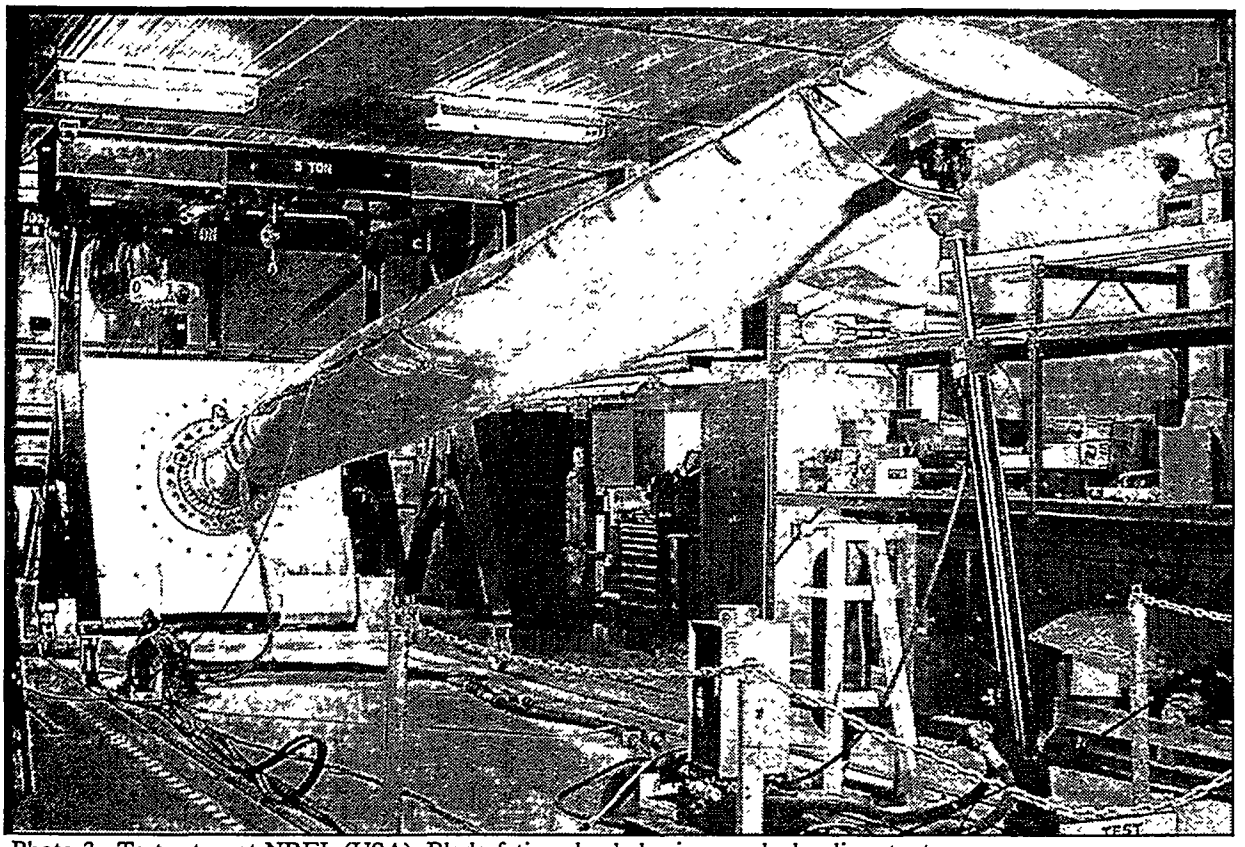

Photo 3 Test setup at NREL (USA). Blade fatigue loaded using one hydraulic actuator

parameters of the test are available. In the document the design loads and blade data are considered as starting points for establishing and the evaluation of the test loads. The evaluation of the design loads with respect to the actual loads are outside the scope of the document.
At the time this document will be finished full scale tests were carried out on blades of horizontal axis wind turbines. The blades were mostly made of reinforced plastics or wood/epoxy. However, most principles would be applicable to any WTGS configuration, size and material.

6 CONTENTS OF THE DOCUMENT

6.1 General

Currently full scale tests on rotor blades are carried out by various institutes (or manufacturers) in various ways. Some testing is done in a more complex way than others. Each of these tests may have its own advantages or disadvantages in terms of extensiveness or costs. It has not been the intention of the working group to prescribe in the document a particular test procedure or the hardware to be used.

However, it gives the procedures to evaluate the test result. It highlights various important aspects related to the different ways of testing. It gives guidance on general procedures, test load factors and reporting. The aim is that regardless of the test method applied it should be clear from the reporting which areas of the blade are tested to a sufficient level.

The main body of the existing draft deals with strength tests (Static and Fatigue). After some general introductory sections the document contains at this moment the following sections

- General Principles
- Blade Data
- Differences Between Design and Test Load Conditions
- Test Load
- Evaluation of Test Load Distribution
- Failure Modes
- Test Procedures and Methods
- Reporting

The contents of these sections will be briefly described here. It is however noted that the working group is working on the document so some parts might be modified.
In an annex other tests to determine physical properties of the blade will be discussed.
In another annex examples of the various test setups are given.

6.2 General Principles

This section discusses the purpose of a test, introduces the need for test load factors and addresses

the practical constraints of a test.

6.3 Blade Data

The blade data that is necessary to establish the test load and to report the test properly are given in this section. Some of the items are dimensions, material distribution, root fixing procedure, areas to be tested etc.

6.4 Differences Between Design and Test Load Conditions

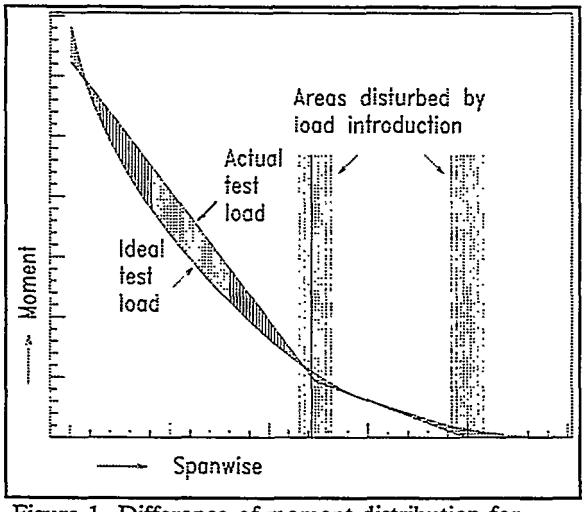

Figure 1 Difference of moment distribution for "ideal" and actual test load

These differences are mentioned and their possible implications are discussed. Some items are radial loads, load introduction, moment and shear distribution (see figure 1) etc.

6.5 Test Load

The description of the test load and some other aspects related to the test loads are discussed. This includes types of testing, test load duration, sequence of static and fatigue test etc.

6.6 Evaluation of Test Load Distribution

Normally during a test not the complete area of the blade is tested. This depends on the distribution of the severity of the test load and the design load. This can be different for each location. Procedures are given how to evaluate the test load severity with respect to the design load. Also, the partial safety and test load factors to be included are discussed

6.7 Failure Modes

Possible failure modes which should be monitored and/or reported are indicated.

6.8 Test Procedures and Methods

The various aspects of the different test methods are discussed. Guidance is given on the appropriate procedure for the different methods. Items discussed

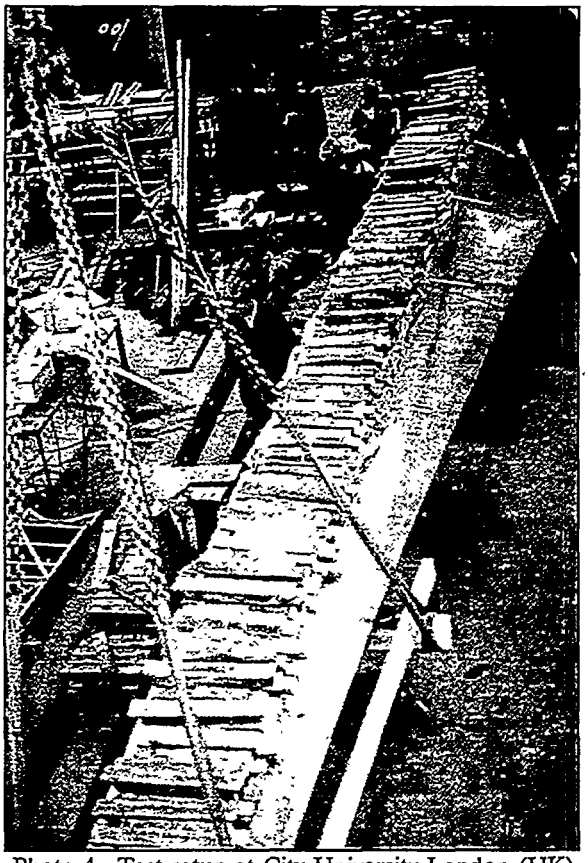

Photo 4 Test setup at City University London (UK). Blade loaded with sandbags and lead ingots ready for testing.

are test control issues, calibration, data collection, system errors and corrections, etc. The advantages and disadvantages of the different test methods are discussed.

6.9 Reporting

In this section is listed the items that should be reported. It is in a way a proposed table of contents of a full scale blade test report.

7 AUTHORS OF THE WORKING GROUP DRAFT

The following members have been actively involved in drafting the document:

D.R.V. van Delft	NL	DUT
Ch. Brokopf	DL	GL
A. Derrick	UK	NEL
M. Hancock	UK	Aerolam
J. Månsson	DK	LM
H. Matsumiya	JP	MITI
W. Musial	US	NREL
J. Olthoff	NL	Rotorline
A.J.P. van der Wekken	NL	ECN
M. Winther-Jensen	DK	RISØ
M.D. Zuteck	US	MDZ Consulting

8 CONCLUDING REMARKS

Most of the members of this working group are intensively involved in blade testing and blade design. Nevertheless it was found that the members had various approaches and opinions on how a blade test should be performed. Moreover in many cases it took some hours of discussion to completely understand the fundamentals of each other's arguments and to arrive at a consensus. This is due to the (sometimes surprising) complexity of full scale blade testing.

The members considered these discussion as fruitful since it increased the knowledge and mutual understanding of everyone. It is also essential in this process to make decisions on the basis of consensus. However, as a consequence a quite substantial amount of man-hours have proven necessary to fulfill this task.

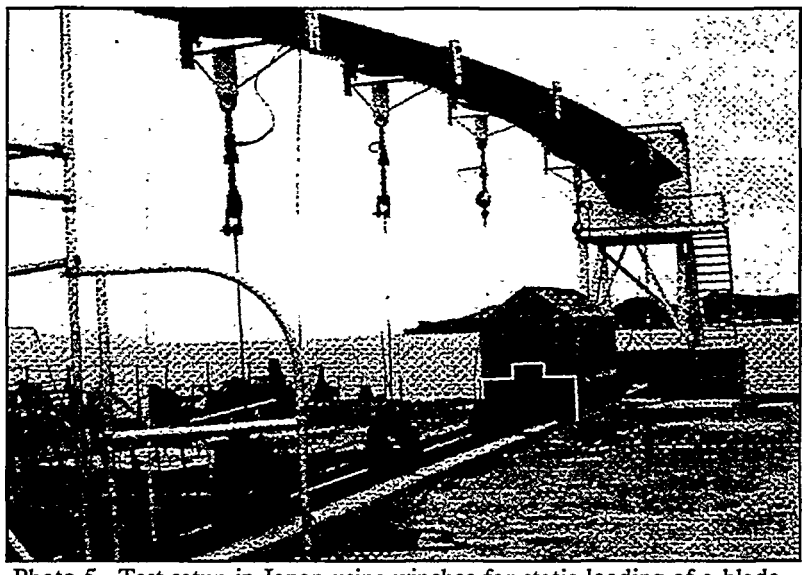

Photo 5 Test setup in Japan using winches for static loading of a blade.

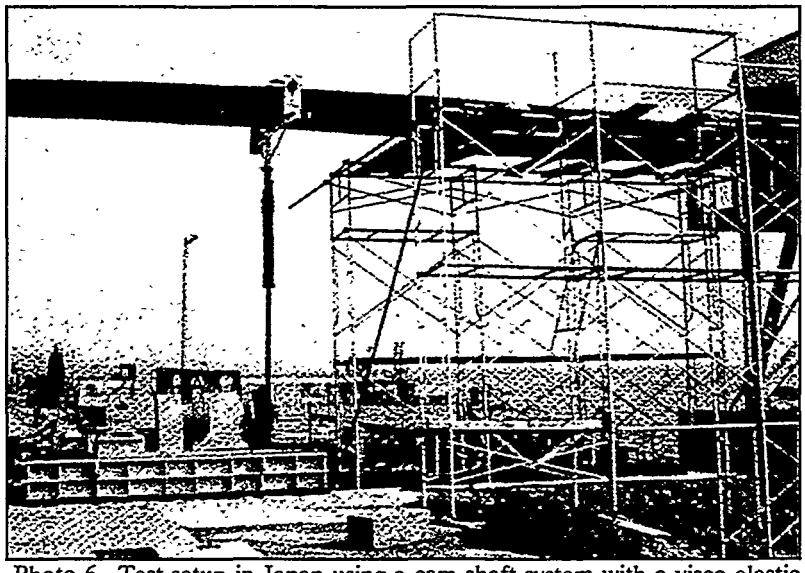

Photo 6 Test setup in Japan using a cam shaft system with a visco-elastic shaft for fatigue loading of a blade.

9 REFERENCES

[1] D.R.V.van Delft, J.L.van Leeuwen.
Full Scale Fatigue Testing of Wind Turbine Rotor Blades.
EWEC'94, Tessaloniki 1994

[2] IEC 1400-1: Wind turbine generator systems, part I: safety requirements.

IS THERE A FUTURE FOR MATERIAL FATIGUE RESEARCH?

Peter Joosse *
Bernard Bulder**
* Stork Product Engineering b.v., Amsterdam, the Netherlands
**ECN-Renewable Energy, Petten, the Netherlands

1 INTRODUCTION

Due to the fact that it is quite difficult to get new funding for (fundamental) wind turbine material related fatigue research the authors started a discussion with the following title:

Are there still wind turbine engineering specific fatigue problems?

and

What are the research goals for the fatigue experts in wind engineering for the second half of the 90^{ies}

In this paper the present status of the fatigue issue and the discussion following is reported.

2 PRESENT SITUATION

Technical status

In the field of fatigue research on glass reinforced plastics (GRP) a vast amount of fatigue results is available and agreement is at hand on the evaluation methodology to be used. Although consensus is not reached yet, the differences in the results of the analysis are moderate.

There is broad agreement that constant amplitude fatigue behaviour of GRP can be best described by a linear relationship between the logarithm of the cycles and the logarithm of the amplitude of either the strain or the normalised stress. The slope of the line is typically 1:10 for tension-compression fatigue (R=-1). For design purposes constant life lines are commonly given in the Goodman (or Haigh) diagram as straight lines between the static allowable (at a amplitude of zero) and the value at R=-1.

Fatigue research on wind turbine rotor blades has been very empirical in nature and has been directed to topics encountered in real practise. This has the advantage that solutions to the problems can be found relatively quick, but the disadvantage is that no thorough understanding of the fatigue problem is available.

Variable amplitude fatigue has been investigated also. It was commonly expected that a prediction based upon constant amplitude results and ordinary Miner-summation would be adequate. Only recently high cycle ($\geq 10^8$) WISPER results -as presented by van Delft have lead to different and troublesome conclusions.

Another long-term research with (at the moment) troublesome results deals with the environmental influence on fatigue.

Political status

In the Netherlands recently discussions have been held on the question which topics should be addressed in future wind energy research. As a conclusion NOVEM stated that there is no need for further basic research on material fatigue. This conclusion was based upon the following:

- at present, there is a adequate generic formulation available for constant amplitude fatigue of GRP,
- the influence of major parameters like load variations and climatological variations is well-known.

Applied research will still be useful for specific details or material usage, this type of research should be addressed by the manufacturer and a research institute.

In the Joule III round two proposals were forwarded on the topic of generic materials research:

- *"Blade Design"*: a follow-up of the Joule I and II funded research with a wider scope,
- *"ProFACT"*: aimed at evaluating all fatigue data available on wood/epoxy and fibre reinforced plastics (glass and carbon).

Both proposals were turned down. As a consequence no international R&D program will be running on fatigue research of (composite) wind turbine materials

As a result of the above stated it has become difficult, or even impossible, to start new, basic research on an international scale (or in the Netherlands). In view of the potential problems this means a serious draw back. The problem we face may be formulated as follows:

Nowadays we are not able to get (financial) support for basic research on the topic of material fatigue research. In the past we did, so what changed?

Several reasons may be possible:

1. the problem is solved for the most part, additional research will only increase useful knowledge by a small amount;
2. the problem is not solved, but there is no confidence that it will be solved soon, by us;
3. PR problem: problem is real and existing, but the audience is unwilling to invest money and time;
4. the attention is focused on a subject of more importance;
5. etc. etc. .. .

To the opinion of the writers there may be several reasons for the problem. The first step however is to check whether this problem is also experienced by other experts in the field and hear their perception on the cause(s). Following that, solutions may be found leading to consensus on the most important cause.

3 SUMMARY OF THE DISCUSSION

Is fatigue still a major design issue?

In general the difficulty with fatigue is, that errors in fatigue analysis or assumptions of fatigue will only show up several years after operation started (typically 5 years). Wind turbines, which are presently at

the age of 5 years, have been designed 5-7 years ago and are over-dimensioned due to the severe load assumptions.

Catastrophic failures known nowadays almost all result from faults in design (stress risers or the control system) or production (insufficient quality control). Fatigue failures become apparent over a relatively long time and there are suggestions that retrofitting due to fatigue failures are sometimes disguised as "standard" replacements.

The conclusion is that there may be more at hand that can be officially known.

Fatigue is found to be still dominant by the designers and blade manufacturers present at the meeting, although the importance has decreased. This is partly caused by the knowledge gained (which decreased the conservatism) and partly caused by re-definitions of the load cases. Extreme load cases have become more severe which puts more emphasis on buckling phenomena and shear loads (e.g. in the shear webs). However, now the wind turbine certification agency Germanischer Lloyd changed the slope of the S-N line for epoxy from 12 to 10, fatigue has become more important (the design driver) again in Germany.

An English study by W.S. Atkins [1] has concluded (1) that the potential cost reduction by increasing the knowledge on material fatigue is moderate. This is probably due to the observation that materials fatigue research is especially focused on blade material whereas the blade costs are 15-20% of the total turbine costs. At the same time it states (2) that the risk in not dealing with the problem is large.

It should be stressed that for the topic of fatigue the fatigue load calculations and the material properties are of equal importance. Benchmarks, like the REFSTRESS project [2], illustrate that the uncertainty in the load prediction can be high: predicted spectra of the flap bending moment show a relatively large scatter. The confidence level relating to fatigue life may therefore be increased more efficiently with enhancements in the load prediction methods.

Is there a problem and what is the reason?

The situation as given in this paper for the Netherlands and the Joule programme is confirmed by the experts present. The industry seems to have lost its interest in fatigue, an illustration of this is the modest (or even low) representation of the industry (except for the German companies) at the present meeting.

It should be noticed that the first conclusion of the W.S. Atkins report was remembered by those dealing with subsidies, but not the second one. This leads us to a possible reason for the problem we encounter:

although a lot of money was spend on fatigue research over the years, it still delivers new problems and therefore needs more money.

It seems to be a never ending story. This however means that we can not make clear to the decision makers that material fatigue research has paid off in the past and is still necessary: a *PR* problem. This is partly due to the fact that fatigue may be dominant for design, but it is not the only topic. (If fatigue were the only problem flexible rotor systems would be state-of-the-art now, which they are not). But is it only a PR problem? No it is not, significant cost reductions can be accomplished on the fields of the wind turbine, like an optimised control strategy, cheap blade production, optimised towers etc. To optimise these cost reductions a considerable R&D effort is needed.

It is true to say that the institutes investigating the fatigue problem continuously define new problems, whereas the industry is only interested in answers to the (already known) problems. As long as designers are not forced to use better fatigue formulations they will stick to the old ones. Changes can be forced by the certification institutes or by potential cost price reductions.

Which topics are worthwhile investigating?

Within certain fields the fatigue research is in an investigative, empirical phase; among others this holds for:

- variable amplitude fatigue,
- influence of humidity,
- different materials (e.g. bio-fibres),
- multi-axial fatigue,
- off-shore operation (include salt),
- carbon-epoxy laminates.

In other fields research has entered the evaluation phase:

- re-analysis of existing methods on a larger set of fatigue data (combination of the FACT database and the database of Mandell),
- statistical approach to fatigue data,
- modelling damage phenomena, this subject is not close to being solved within the next 3-5 years.

The above topics have a much broader significance than wind energy, financial sources should therefore be sought also outside this market. It should however be reminded that glass fibre is the dominant fibre used in wind turbine rotor blades, whereas this will be carbon fibre in the aero-space industry. The development of theory and insight in damage phenomena stems from the aero-space industry and therefore has its focus on carbon reinforced materials.

On the topic of predicting variable amplitude fatigue behaviour there has been a major discussion at the meeting: on the one hand high accuracy has been suggested by Echtermeier (presented by Kensche at the meeting), on the other hand a total lack of accuracy has been demonstrated by van Delft. The first step in this area should be in the calculation area, maybe followed by tests for verification.

Fatigue tests have been uni-axial until now. In a real structure the stress situation will be multi-axial e.g. normal stress in the spanwise direction combined with shear stress. At the inner blade, the profile changes to a cylindrical shape, multi-axial stresses will occur most heavily. Although theoretical models may be available for multi-axial fatigue, they have to be validated for the typical number of cycles for rotor blades.

The use of carbon fibre reinforced plastics has a large potential for wind turbine rotor blades. Applying these fibres will lead to significantly lighter blades which are less sensitive to fatigue. Structures build up of carbon fibres are known for their flat fatigue slope (1:15 and better). Since the price of raw material is high it is important to optimise the manufacturing system and minimise the thickness. The small thickness increases the importance of (micro-) buckling. The advantage of the high fatigue strength may be counterbalanced by the high price, and a larger sensitivity to lightning strikes.

Other subjects of interest are: properties of sandwich structures, shear properties, bonding, data for roving material at high cycles and the fibre volume fraction.

How can we make a change

The aim of future (materials) fatigue research should be to increase the reliability of the lifetime prediction. Having more knowledge on the material properties and the fatigue loading will improve the design, decrease the conservatism and thereby decrease the risk of premature failure. Since the fatigue loading is not the only loading type for wind turbines it is not possible to state that as a direct consequence the blade costs will decrease.

4 CONCLUSIONS

Fatigue research on wind turbine blade material has been an important issue over the years in many countries and in the E.U. As a result of the effort the knowledge on fatigue properties of fibre reinforced materials has been expanded enormously. Practical fatigue design properties are available for constant amplitude tests at ambient temperatures. A lack of knowledge can be shown in several other fields, such as variable amplitude and multi-axial testing and the influence of the environment and carbon fibres.

Fatigue is seen as dominant for the blade design, improvements in both the load prediction and material fatigue properties should be strove for. In discussions with blade manufacturers and subsidy agencies (E.U. DGXII, NOVEM, ETSU, etc..) on the importance of continuous materials fatigue research the improvement in reliability should be stressed.

5 ACKNOWLEDGEMENT

The writers are grateful for the contribution of the participants of the 4^{th}. IEA expert meeting on fatigue of wind turbines during the plenary discussion and say "Vielen Dank" to Holger Söker for making the minutes of the discussion.

References

[1] Barltrop N.D.P., I.P. Ward, and D.J. Daw. "The implications fo fatigue on the cost of HAWT's". In *Proceedings of the 15^{th} British Wind Energy Association Conference*, 1993.

[2] Van Grol, H.J. and B.H. Bulder. "REFERENCE PROCEDURE TO ESTABLISH FATIGUE STRESSES FOR LARGE SIZE WIND TURBINES –A STATE OF THE ART REPORT ". -C-94–013/14, ECN, March 1994.

4. IEA Symposium - Wind Turbine Fatigue

Name	Address - Phone Fax
Gunner Larson	RisØ 4000 Roskilde Denmark Phone: ..../46 77 50 56
Andreas Röhm	LM Aero Construct 76891 Bundeuthal Germany Phone: 06 39 4/92 15 31
Klaus Schultes	Aero Dynamik Consult Maybachstr. 7 71272 Renningen 1 Germany Phone: 07 15 9/17 07 1 Fax.: 07 15 9/18 93 3
Stefan Kleinhansl	Aero Dynamik Consult Maybachstr. 7 71272 Renningen 1 Germany Phone: 07 15 9/17 07 1
Kimon Argyriodis	Germanischer Lloyd Vorsetzen 32 20459 Hamburg Germany Phone: 04 0/36 14 9 - 138
Markus Rees	Aerodyn Energiesysteme GmbH Provianthausstr. 9 24768 Rendsburg Germany Phone: 04 33 1/12 75 0
Bernard Bulder	The Netherlands Energy Research Foundation ECN P.O. Box, 17 55 26 Petten Netherlands Phone: 00 31/22 45 64 10 2 Fax.: 00 31/22 45 63 21 4

Anthony Riddle	National Wind Power LTD. Riverside House, Meadonbank Furloog Rd. Bourneend Buckinghamshire, SL8 5 AJ Great Britain Phone: 00 44/16 28 53 23 00 Fax: 00 44/16 28 53 19 94
Don van Delft	TU Delft University of Technology Faculty of Civil Engineering P.O. Box 5048 2600 GA Delft Netherlands Phone: 0031/15/78 23 29 Fax.: 0031/15/78 23 08
Peter Josse	Stork Product Engineering b.v. P.O. Box 379 1000 AJ Amsterdam Netherlands Phone: 00 31/20 55 63 40 5 Fax: 00 31/20 55 63 55 6
Herb Sutherland	Sandia National Labs MS 0708 Albuquerque/ NM 87185 USA Phone: 00../50 5 /844-2037 Fax: 00../50 5/845-9500
Neil Bishop	Dept. Mechanical Engineering University Kollege London Tarrington Place London WCIE 15 E Great Britain Phone: 00 44/17 13 80 19 32 Fax: 00 44/17 13 88 01 80
Julian Lowe	Tenax Fibres Kasinostr. 19-21 42103 Wuppertal Germany Phone: 02 02/32 32 69 Fax.: 02 02/32 24 96

Geoff. Lowe

Faculty of Engineering
University of the West of England
Frenchay, Coldharbour Lane
Bristol BS161QY
Great Britain
Phone: 00 44/11 7/96 96 26 1
Fax: 00 44/11 7/91 63 81 3

Holger Söker

Deutsches Windenergie Institut
Ebertstr. 96
26382 Wilhelmshaven
Germany
Phone: 04 42/48 08 25
Fax.: 04 42/48 08 43

Tobias Geiger

DLR - Institute of Structures and Design
German Aerospace Research Establishment
Pfaffenwaldring 38-40
70569 Stuttgart
Germany
Phone: 00 49/(0) 711/68 62 46 5
Fax: 00 49//0) 711/68 62 22 7

Christoph Kensche

DLR - Institute oc Structures and Design
German Aerospace Research Establishment
Pfaffenwaldring 38-40
70569 Stuttgart
Germany
Phone: 00 49/(0) 711/68 62 46 3
Fax: 00 49/(0) 711/68 62 22 7

B.Maribo Pedersen

Technical University of Denmark
Dept. of Fluid Mechanics
Building 404, DK-2800 Lyngby
Denmark
Phone: (+45) 4593 2711
Fax: (+45) 4588 2421